

**Quantum mechanical and experimental Infra-red
studies on stability and structural properties of
substituted acylthiourea compounds**

by

Mengistu Ghebreysus Woldu

Thesis

Submitted in fulfilment of the
requirements for the degree

Magister Scientiae



in the

Faculty of Science

at the

University of Stellenbosch

Supervisor: Prof J.L.M. Dillen

December 2004

Declaration

I, the undersigned, hereby declare that the work contained in this thesis is my own original work and that I have not previously in its entirety or in part submitted it at any university for a degree.

Summary:

A quantum mechanical study, using the 6-31G(d) basis set at the Hartree-Fock level of theory was performed to establish the most stable structures of twelve substituted acylthiourea compounds. The results show that the *trans* orientation of the carbonyl and thio-carbonyl moieties is a common trend in all the compounds studied, and it is concluded that it also is the general trend in all stable structures of substituted acylthioureas.

Experimental IR studies conducted on six substituted acylthioureas showed considerable similarity between the experimental and calculated wavenumbers. Predictions of wavenumbers were made for six more compounds. Based on these results, the effect of substituents on the absorption wavenumber of the chemically active carbonyl and thio-carbonyl groups was analyzed.

X-ray diffraction analysis was carried out on three selected substituted acylthioureas. These and crystal structures obtained from the Cambridge Crystallographic Structural Database (CCSD) and other literature, were compared with the calculated stable structures. The comparisons show that they agree well. This proved the accuracy and reliability of the quantum mechanical calculations.

Analysis of the electron density in terms of the Atoms in Molecules (AIM) theory gives a clear picture of common trends. The analysis shows that an inverse proportional relationship exists between the length of the C-N bonds and the electron density at the bond critical point. Analysis of the Laplacian of the electron density, $\nabla^2\rho(r)$, on the other hand enables the characterization of all bonds in the molecules proving the nucleophilic character of the O and S atoms. Values of the electron density, $\rho(r)$, and its Laplacian, $\nabla^2\rho(r)$, also confirmed the presence of hydrogen bonding in the stable structures of the compounds.

The Natural Bond Orbital (NBO) based population analysis performed on the compounds enables one to assign a charge to their constituent atoms. The second order perturbation theory energy analysis carried out proved that the high energy delocalization of lone pairs of the terminal nitrogen i.e. N(2) to the anti-bonding π -orbital of the thio-carbonyl moiety ($n_{N(2)} \longrightarrow \pi^*_{C(2)-S}$), and to the non-Lewis NBO

lone pair of the thio-carbonyl carbon ($n_{N(2)} \longrightarrow n^*_{C(2)}$) are responsible for shortening of the C(2)-N(2) bond in substituted acylthioureas.

The Natural Resonance Theory (NRT) analysis conducted on acylthioureas allows the quantitative determination of all possible resonance forms that the compounds attain. In all compounds, the two top weighted resonance structures are found to be similar. These top weighted resonance structures are found to have an average weight difference which is not more than 10%. Hence all substituted acylthioureas are believed to exist resonating between these two structures. This resonance gives the C(2)-N(2) bond a partial double bond character and makes it shorter than the other C-N bonds in all substituted acylthioureas. This result is in line with what was found in the perturbation energy analysis.

Opsomming:

Die stabiliteit van twaalf gesubstitueerde asieltio-ureumverbindings is bestudeer met behulp van kwantumeganiese tegnieke deur die Hartree-Fockmetode en die 6-31G(d)-basisstel te gebruik. Die resultate wys dat die *trans* orientasie van die karboniel teenoor die tiokarboniel 'n gemene eienskap is van al die bestudeerde verbindings en die gevolgtrekking word gemaak dat dit inderdaad 'n algemene eienskap is van alle stabiele gesubstitueerde asieltio-ureumverbindings.

Die infrarooispektrum van ses van die twaalf gesubstitueerde asieltio-ureumverbindings is eksperimenteel bepaal en die resultate toon besonder goeie ooreenstemming met die berekende vibrasiegolfgetalle van die onderskeie verbindings. Die oorblywende ses verbindings se berekende vibrasiespektra is gebruik om afleidings te maak rakende die effek van substituenten op die absorpsiegolfgetal van die chemies aktiewe karboniel en tiokarboniel groepe.

Ten einde die akkuraatheid van die berekening verder te toets, is drie van die verbindings se strukture met behulp van X-straaldiffraksie bepaal. Die oorblywende verbindings se strukture is verkry uit die *Cambridge Crystallographic Structural Database* (CCSD) asook die algemene literatuur. Goeie ooreenstemming tussen die eksperimentele en berekende waardes toon weereens die betroubaarheid van die kwantumeganiese berekeninge.

'n Beter bepaling van die algemene eienskappe van asieltio-ureumverbindings is verkry deur die elektrondigtheid te bestudeer in terme van die *Atoms in Molecules*-teorie (AIM). Die ontleding het getoon dat daar 'n inverse verhouding bestaan tussen die lengte van die C-N bindings en die elektrondigtheid by die kritiese punte van die betrokke bindings. Die Laplasiaan van die elektrondigtheid, $\nabla^2\rho(r)$, is gebruik om al die bindings te karakteriseer en die nukleofiliese aard van die O en S atome te bevestig. Die teenwoordigheid van waterstofbindings is ook bevestig met behulp van die berekende elektrondigtheid ($\rho(r)$) en betrokke Laplasiaanwaardes.

Ladings op die onderskeie atome is bereken met behulp van *Natural Bond Orbital*-analise (NBO). Tweede-orde perturbasieteorie is gebruik om alle moontlike elektrondelokalisasies vanaf die optimale Lewis-struktuur te bepaal. Hiermee is aangetoon dat energierike delokalisasie van die alleenpaar op die terminale stikstofatoom na die antibindende π -orbitaal van die tiokarbonielgroepe

$(n_{N(2)} \rightarrow \pi^*_{C(2)-S})$, asook na die nie-Lewis NBO alleenpaar op die tiokarbonielkoolstof $(n_{N(2)} \rightarrow \pi^*_{C(2)})$ verantwoordelik is vir die verkorting van die C(2)-N(2) binding in gesubstitueerde asieltio-ureumverbindings.

Natural Resonance Theory-analise (NRT) is gebruik om alle moontlike resonansiestrukture te bepaal en 'n gewigsfaktor aan elkeen te verskaf. In al die verbindings is die twee resonansstrukture met die grootste gewigsfaktore nie net dieselfde nie, maar hulle gemiddelde gewigsfaktore is ook binne 10% van mekaar. Daar word gevolglik afgelei dat *alle* asieltio-ureumverbindings resoneer tussen hierdie twee elektroniese strukture. Die C(2)-N(2) binding word deur hierdie resonansie gedeeltelike dubbelbindingkarakter gegee wat lei tot 'n korter binding in vergelyking met die ander C-N bindings. Hierdie bevindings bevestig die resultate van die tweede-orde perturbasieteorie analise.

Dedication

To my beloved parent, and all my teachers

Acknowledgements:

- Professor J.L.M. Dillen, my supervisor, for his sincere guidance and supervision, and for his readiness to explain vague concepts.
- Dr C. Esterhuysen, for her help in running X-ray diffraction analysis.
- Dr P. Verhoeven, for his help in running IR spectra.
- Gerhard Venter, my research team mate, for his invaluable assistance in computer manipulation, discussing concepts, and for his encouraging accompany.
- Greta Heydenrych and Gerhard Venter again, for translating summary of my work in to Afrikaans.
- Siraj. M. Abrar, my best friend, for his encouragement personally and through phone calls.
- The state of Eritrea human resource development (EHRD) for funding my study.
- The University of Stellenbosch and my supervisor Professor J.L.M. Dillen for their financial assistance to finalize my thesis.
- My parent and family members for their unrelenting effort, and encouragement throughout my study career.
- I would also like to convey special thanks to the following individuals who encouraged me personally, through e-mails and phone calls.
 - Azieb Araia (University of Asmara)
 - Dr Lula Ghebreysus (Executive director of AIPA)
 - Rezzan Russom (Germany)
- At last but most I would like to thank the almighty God my Kind shepherd in every space and time, who is the cornerstone of all my achievements.

Table of contents:

Declaration	i
Summary	ii
Opsomming	iv
Dedication	vi
Acknowledgements	vii
Table of contents	viii
Acronyms	xi
Chapter 1: Introduction	1
Chapter 2: Basic concepts and background of some computational methods and infrared spectroscopy	4
2.1 Introduction	4
2.2 The quantum mechanical “ <i>ab initio</i> ” method	4
2.2.1 The Hartree-Fock (HF) method	5
2.3 Basis Sets	11
2.3.1 Slater and Gaussian type orbitals	11
2.3.3 Types of basis sets	13
2.3.3.1 Contracted basis sets	14
2.3.3.2 Effective core potential basis sets	16
2.4 Electron correlation methods	16
2.4.1 Configuration Interaction	18
2.4.2 Møller-Plesset Perturbation Theory	19
2.4.3 The Coupled Cluster Method	20
2.5 Semi-empirical methods	21
2.6 Molecular Mechanics Method	22
2.7 Electronic Structure Analysis methods	23
2.7.1 Theory of atoms in molecules (AIM)	23
2.7.1.1 Electron density $\rho(r)$	24
2.7.1.2 Laplacian of the electron density $\nabla^2\rho(r)$	27
2.7.2 Natural Bond Orbital Analysis (NBO)	29
2.7.3 The natural resonance theory analysis (NRT)	32

2.8 Infrared studies	33
2.8.1 Experimental infrared studies	33
2.8.1.1 Requirements for infrared absorption	34
2.8.1.2 Numbers of vibrational modes	35
2.8.1.3 Instrumentation	35
2.8.1.4 Sample preparation	36
2.8.2 Calculated infrared studies	36
Chapter 3: Modelling Substituted Acylthiourea compounds	39
3.1 Introduction	39
3.2 Tautomers of Acylthiourea compounds	40
3.3 Modeling proton and methyl substituted acylthiourea tautomers	40
3.4 Modeling selected substituted acylthiourea compounds	46
3.5 Summary	52
Chapter 4: Infra-red studies of substituted acylthioureas	53
4.1 Introduction	53
4.2 Experimental IR studies on selected substituted acylthioureas	53
4.3 Prediction of experimental IR absorption frequencies of selected Substituted acylthioureas	62
4.4 Effect of substituents on absorption frequencies of the C=O and C=S bonds of substituted acylthioureas	68
4.5 Summary	72
Chapter 5: Electronic structure studies of substituted acylthioureas	73
5.1 Introduction	73
5.2 Single Crystal X-ray diffraction Studies	73
5.3 Cambridge Crystallographic Structural Database (CCSD) and literature search	78
5.4 Atoms in molecules analysis	81
5.5 Natural bond orbital analysis	88
5.5.1 Natural population analysis	88
5.5.2 Second order perturbation theory energy Analysis	91
5.6 Natural resonance theory analysis	93

Chapter 6: Conclusion	107
6.1 Summary	107
6.2 Future work	111
References	112
Addenda	119
Addendum A: Molecular geometries	119
Addendum B: Wavenumber analysis data	120
Addendum C: Crystal structure data	157

Acronyms:

ζ	Signature of a critical point
Ω	Rank of a critical point
ω_α	Resonance weight
$\rho(r_c)$	Electron density at a critical point
$\nabla^2 \rho(r_c)$	Laplacian of electron density at a critical point
5Z	Quintuple zeta
<i>ab initio</i>	Latin term which means “from the beginning” or “from the first principle”
AIM	Atoms in molecules
AM1	Austin Model one
AMBER	Assisted model building with energy refinement
AO	Atomic orbital
CC	Coupled cluster
CCS	Coupled cluster singlet
CCSD	Cambridge Crystallographic Structural Database
CGTO	Contracted Gaussian type orbital
CHARMM	Chemistry at Harvard macromolecular mechanics
CI	Configuration interaction
CIS, CISD, etc.	Configuration interaction at singlet, singlet and doublet, etc. orders
CMO	Canonical molecular orbital
CPU	Central processing unit
DZ	Double zeta
DZP	Double zeta plus polarization
ECP	Effective core potential
FT-IR	Fourier transform infra-red spectrometer
GTO	Gaussian type orbital
GVB	Generalized valence bond
HF	Hartree-Fock
HOMO	Highest occupied molecular orbital
LCAO	Linear combination of atomic orbitals
LUMO	Lowest unoccupied molecular orbital

MCSCF	Multiconfigurational self-consistent field
MMFF	Merck molecular force field
MM_n	Molecular mechanics force field of n th order
MNDO	Modified neglect of diatomic overlap
MP_n	Møller-Plesset theory at n th order
NAO	Natural atomic orbital
NBO	Natural bond orbital
NHO	Natural hybridized orbital
NLMO	Natural localized molecular orbital
NRT	Natural resonance theory
PGTO	Primitive Gaussian type orbital
PM3	Parameterization three
QZ	Quadruple zeta
RECP	Relativistic effective core potential
SAM1	Semi- <i>ab initio</i> method one
SCF	Self-consistent field
SINDO1	Symmetrically orthogonalized intermediate neglect of differential overlap one
STO	Slater type orbital
TZ	Triple zeta
TZ2P	Triple zeta plus double polarization
UFF	Universal force field
VSCC	Valence shell charge concentration
ZINDO	Zerner's intermediate neglect differential overlap

Chapter One

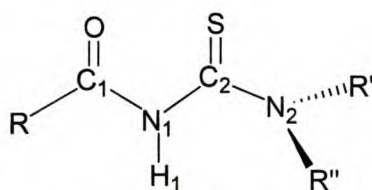
Introduction

The first synthesis of substituted acylthiourea compounds dates back to 1873 by Neucki (Koch et al., 1995). Since then many studies have been conducted on them. One of the early studies conducted on their coordination chemistry was the pioneering work of Beyer and his colleagues, which was mainly focused on the application of these compounds for solvent extraction of transition metal ions (Koch et al., 1998). This work opened up new possibilities for many other further studies.

Later studies made on physical and chemical properties of acylthioureas showed that these compounds are biologically active. Some substituted acylthiourea compounds possess fungicidal and bactericidal properties and display marked anticorrosion properties (Dago et al., 1987), while other compounds serve as chemotherapeutic agents (Yuan et al., 2001).

Some of the recently conducted studies on their coordination chemistry show that substituted acylthiourea compounds in general, and N-acyl-N'-alkyl (H₂L) and N-acyl-N', N'-dialkyl (HL) compounds in particular, have wide applications in solvent extraction of the softer second and third row transition metals. Besides this, these compounds are also widely applicable for selective liquid-liquid extraction, pre-concentration, efficient chromatographic separation and fluorimetric detection of platinum group metals (Koch et al., 1997).

As can be seen from the above much attention has been paid to these compounds. One of the major driving forces for conducting such experimental studies on these compounds is their versatile nature, in that one can readily vary the substitute groups **R**, **R'**, **R''** and get a wide range of different systems with different chemical and physical properties (Sacht et al., 2000).



Where (*R, R', R''* = H, alkyl, aryl, Saturated rings)

Fig. 1.1 General molecular structure of substituted acylthiourea compounds.

Another factor that prompted interest in these compounds is their low cost of preparation (Schuster, M., 1992), due to such valuable properties and many practical applications they have, these compounds are currently being widely used in different areas of agriculture and industry.

Even though many experimental studies have been conducted for many years, an extensive literature survey made on substituted acylthiourea compounds shows that very little theoretical, and

specifically almost no quantum mechanical, studies have been made on them so far. One of the possible reasons for this could be the lack of appropriate tools to conduct such studies on these medium sized compounds, as quantum mechanical studies are usually restricted to small molecules. But the development of sophisticated hardware and program codes with the rapid development of powerful computers in the last decade (Frenking, G., 2000), allows the possibility of conducting such studies.

Therefore the ultimate aim of this project is to conduct quantum mechanical studies on the stability and structural properties of substituted acylthiourea compounds and to fill in the gap in theoretical data that exists for these compounds.

In the general structure in **fig.1.1** the hydrogen atom described as H_1 is a mobile group in the system (Albertus, M.S., Piris, M., 2001). Hence, it is sometimes bonded to the oxygen atom, and other times to the sulphur atom. This mobile nature of H_1 gives rise to the existence of three tautomeric forms of acylthiourea compounds. Therefore, with the aim of starting the stability study at the grass root level, the first task will be detecting the preferential tautomeric form of acylthiourea compounds.

Based on the best preferential tautomeric form, stability studies will be made on a series of acylthiourea compounds, which have substituents of varying degree of complexity. Once the most stable structures of each compound have been identified, the general stable structure of acylthioureas will be defined.

Many experimental studies (Koch et al., 1995, Dago et al., 1989& 1988) have proved that in the stable structures of acylthiourea compounds, the C_1-N_1 bond has an intermediate length, C_2-N_1 the longest and the C_2-N_2 bond is the shortest of the three C-N bonds. Even though the studies show that all the above C-N bonds are shorter than the average single C-N bond length 1.472(5) Å, the C_2-N_2 bond is extremely short, and thus it exhibits a partial double bond character. Despite demonstrating these observations, none of the experimental investigations try to explain it. Therefore confirming the existence of the trends discussed above in the theoretically calculated stable structures, and explaining the factors which are responsible for the partial double bond character observed, are two other important goals of this project.

Due to the versatile nature of acylthiourea compounds cited above, variation of the substituent groups R, R' , and R'' from a simple proton to complex ring systems such as naphthalene gives rise to a significant variation in properties of the compounds. Therefore analyzing such variations and then based on the findings recommending best substituents which enhance the practical applicability of the compounds is also another aim of this project.

So as to supplement this theoretical study, experimental IR and X-ray diffraction studies will also be conducted on the compounds selected for this project. Besides filling the theoretical data

gap mentioned above, this work will also try to explain some experimentally unexplored properties of the compounds.

Relying upon both theoretical and experimental methods of study, this work is expected to show how results of these methods are interrelated. The theoretical and supplementary experimental data which will be gathered are in turn expected to give concrete and tangible information on properties of the compounds that might be helpful to exploit their potential use in different areas.

Having had a brief introduction to the compounds of interest already, in the forthcoming **second chapter** the theoretical background and basic concepts related to the different methods of theoretical studies and infrared spectroscopy will be discussed. The **third chapter** will contain the quantum mechanical studies made on some models and other selected representative compounds. In **chapter four** the experimental IR studies conducted on the selected compounds will be discussed accompanied by the theoretically calculated frequencies. Then the **fifth chapter** will follow containing studies made on the electronic properties of the compounds of interest, which are based on quantum mechanical methods such as Atom in molecule (AIM), Natural Bond Orbital (NBO) and Natural Resonance Theory (NRT), and the X-ray diffraction studies made will also be included there. Finally in the **sixth chapter** a brief summary of the whole work will be given.

Chapter Two

Basic concepts and background of some computational methods and infrared spectroscopy

2.1 Introduction

In this chapter a general discussion will be given on some basic concepts of different computational methods. **Section 2.2** will contain a detailed discussion of the *ab initio* quantum mechanical method, as it is the method of choice for this project. Basis sets will be discussed in **section 2.3**. In **section 2.4** an overview will be given of some electron correlated quantum mechanical methods. Then will follow **sections 2.5** and **2.6**, which contain brief discussions on semi-empirical and molecular mechanics methods, respectively. Finally the **chapter** will be ended with a discussion of different methods of electronic structure analysis in **section 2.7**, and basic concepts of IR spectroscopy in **section 2.8**.

2.2 The quantum mechanical “*ab initio*” method

Ab initio, an expression from the Latin meaning “from the beginning” or “from the first principle”, is one of the most reliable quantum mechanical methods of computation. As its defining term implies, all calculations in this method are based on fundamental physical constants (Planck constant, mass and charge of elementary particles, speed of light etc.) without referring to any experimental data. Being very reliable although slow, it is currently applied to the study of small and medium-sized molecules.

This method is based on the time independent Schrödinger equation:

$$\hat{H} \Psi = E \Psi \quad (2.1)$$

where \hat{H} is the Hamiltonian differential operator representing the total energy. E is the numerical value of the energy of the state, that is, the energy relative to a state in which the constituent particles (nuclei and electrons) are infinitely separated and at rest, and Ψ is the wave function.

Solving this equation exactly is possible for single-electron systems such as the hydrogen atom. However, getting an exact solution is impossible for multi-electron systems, but a highly accurate solution can be obtained by making certain approximations. The approximations made are usually mathematical, such as using a simpler functional form for a function, or finding an approximate solution to a differential equation. In the efforts made to solve this problem, different levels of theories are being used to facilitate the approximations. Among these theories the Hartree-

Fock and the electron correlation methods are the most common ones and will be discussed in the forthcoming sub-sections.

The Hartree-Fock (HF) method

In quantum mechanics, the energy of a molecule is based on the Hamiltonian operator, which in atomic units, is given as:

$$\hat{H} = -\frac{1}{2} \sum_i \nabla^2(\mathbf{r}_i) - \sum_A \sum_i \frac{Z_A}{r_{Ai}} + \frac{1}{2} \sum_{i,j} \frac{1}{r_{ij}} + \frac{1}{2} \sum_{A,B} \frac{Z_A Z_B}{R_{AB}} \quad (2.2)$$

where the prime eliminates $i = j$ and $A = B$ terms. The first term determines the kinetic energy of the electrons, which is obtained by summing up one-particle operators corresponding to r_i . The second is a coulombic electron-nuclear attraction term, with nuclear atomic number Z_A and nuclear-electron distance r_{Ai} . The third term describes the coulombic repulsion between two electrons at separation distance r_{ij} , while the final term describes the nuclear-nuclear repulsion of the nuclei at a separation distance of R_{AB} .

According to the Born-Oppenheimer approximation, the nuclei are considered as rigid entities and this is applicable to almost all molecular calculations. For this reason the nuclear-nuclear repulsion term in Eq. (2.2) is considered as a constant. Therefore the electronic Hamiltonian depends only on the position of the electrons relative to each other as well as their relative positions to the nuclei.

$$\hat{H} = -\frac{1}{2} \sum_i \nabla^2(\mathbf{r}_i) - \sum_A \sum_i \frac{Z_A}{r_{Ai}} + \frac{1}{2} \sum_{i,j} \frac{1}{r_{ij}} \quad (2.3)$$

As it can easily be seen from Eq. (2.3), the first term is a summation of one-electron operators. If one wants to solve the Schrödinger equation exactly, it can be done by assuming that only a single electron exists around a bare nucleus. This assumption gives rise to a one electron Hamiltonian and makes the calculation easy. This is the basic approach used by the Hartree-Fock method and it will be discussed in the forthcoming paragraphs.

In the calculation of molecular energy, because the Hamiltonian operator and the wave function are inseparable physical quantities, once the Hamiltonian operator is well defined as by Eq. (2.3), what should follow is a representation of the respective wave function.

When using a linear combination of atomic orbitals (LCAO) as the wave function, which is applied for solving the Schrödinger equation, consideration is not given to the spin of the electrons in the system. However when the wave function is used for any quantum mechanical calculations, it should be described fully, and this can be done by inclusion of electron spin as an *ad hoc* quantum

effect. Therefore to carry out this task, some modifications should be made to the molecular orbital functions.

Since each electron in any orbital ϕ has a spin quantum number $\frac{1}{2}$, it is obvious that in the presence of an external magnetic field there are two possible states corresponding to an alignment along or against the magnetic field. Hence the corresponding spin states are denoted as α and β . Therefore the total wave function of an electron is obtained as a product of its spatial and spin functions. Hence for an electron i with a spin α and spatial coordinate r_i , the wave function is given as:

$$\phi(r_i, \delta_i) = \phi(r_i) \alpha(i) \quad (2.4)$$

where r_i is the spatial coordinate of electron i , and δ_i is its spin coordinate. A similar expression can also be made for a β spin. Using the shorthand notation \bar{x}_i for the spatial and spin coordinates, the simplified form of the total wave function of electron i is given as:

$$\phi(\bar{x}_i) = \phi(r_i, \delta_i) \quad (2.5)$$

In a multi electron system and assuming that each molecular orbital is fully occupied, i.e. a closed shell system, a specific spatial orbital is expected to have two electrons with opposite spin. On the basis of the Pauli exclusion principle, the total wave function of a system is expected to be antisymmetric with respect to the exchange of two electrons. Beside this, electrons are expected to be indistinguishable from each other in a *linear combination of orbitals*. Therefore, so as to fulfill these fundamental quantum mechanical requirements, the electronic wave function of a system should be expressed in the form of a *Slater determinant*. Hence for a system of N -electrons, the Slater determinant is given as:

$$\Phi = \frac{1}{\sqrt{N!}} \begin{vmatrix} \phi_1(\bar{x}_1) & \phi_2(\bar{x}_2) & \dots & \phi_N(\bar{x}_N) \\ \phi_1(\bar{x}_2) & \phi_2(\bar{x}_2) & \dots & \phi_N(\bar{x}_2) \\ \vdots & \vdots & \ddots & \vdots \\ \phi_1(\bar{x}_N) & \phi_2(\bar{x}_N) & \dots & \phi_N(\bar{x}_N) \end{vmatrix} \quad (2.6)$$

where the constant in front of the determinant, i.e. $\frac{1}{\sqrt{N!}}$, is the normalization factor, converting the Slater determinant into an approximate wave function.

$$\Psi \approx \Phi = \{ \phi_1(\bar{x}_1) \phi_2(\bar{x}_2) \dots \phi_N(\bar{x}_N) \} \quad (2.7)$$

Having determined the electron Hamiltonian and wave function, the major task, which should follow next, is finding the approximate solution to the electronic Schrödinger equation (Eq.2.1). In solving this equation, approximation of the wave function is the primary step. The

Hartree-Fock approximation offers one way of constructing the approximate wave function following some systematic approaches (Springborg, M., 2000). One of the major approaches used in this method is breaking the many-electron Schrödinger equation into simple one-electron equations. Hence this approach greatly simplifies the task of construction of an approximate wave function.

The Hartree-Fock wave function Φ therefore is a single determinant of N one-electron orbitals ϕ_i , and the best set of ϕ_i is determined by searching for the turning point of the Hartree-Fock energy variational function formulated in Eq. (2.8) below. This variational function, since Φ can be completely expressed in terms of ϕ_i components, can be given as:

$$E(\Phi) = E(\phi_i) = \frac{\langle \Phi | \hat{H} | \Phi \rangle}{\langle \Phi | \Phi \rangle} \quad (2.8)$$

In order to solve this variational function, we should either use the fact that the turning point of $E(\phi_i)$ corresponds to a set of optimum orbitals and obtain an equation for ϕ_i , or we should directly minimize the function in some parameterized form. Using the former option and assuming that the selected ϕ_i is an orthonormal set, the numerator and denominator of Eq. (2.8) can be expressed as:

$$\langle \Phi | \hat{H} | \Phi \rangle = \sum_{i=1}^n \langle \phi_i | \hat{h}_1 | \phi_i \rangle + \frac{1}{2} \sum_{i,j=1}^n [\langle \phi_i \phi_j | \hat{h}_2 | \phi_i \phi_j \rangle - \langle \phi_j \phi_i | \hat{h}_2 | \phi_i \phi_j \rangle] \quad (2.9)$$

and

$$\langle \Phi | \Phi \rangle = 1 \quad (2.10)$$

where \hat{h}_1 and \hat{h}_2 are one- and two-electron Hamiltonian operators respectively. Having expressed Eq. (2.8) in terms of integrals of ϕ_i , it is time to investigate the behavior of the resulting energy function $E(\phi_i)$ when ϕ_i is subject to arbitrary variations, e.g.

$$\phi_i \quad \longrightarrow \quad \phi_i + \delta\phi_i \quad (2.11)$$

The aim is to search for the point at which the quotient has a stationary value. However, the variation made in Eq. (2.11) disturbs the orthonormality of ϕ_i and invalidates the energy expression made in terms of the orthonormal orbitals. Hence to overcome this problem, two possible approaches can be followed.

The first approach is the formulation of a general equation for the expression of Eq. (2.8) in terms of a non-orthonormal, un-normalized set of orbitals, so that the variation made does not affect the energy expression. The alternative approach is the use of parameterization, which enables the expansion to be carried out in terms of orthonormal, orbitals without being affected by the variation.

Since the first approach is difficult to apply, it is preferable to use the second alternative approach. This approach not only preserves the orthonormality of the orbitals, but it also makes the derivation easy. The universally used method in this approach is the use of the Lagrange multiplier, Eq. (2.13) below (Cook, D.B., 1998). In applying this variational method, attention is given to the variation of $\langle \Phi | \hat{H} | \Phi \rangle$ under the constraint that all individual orbitals are orthonormal, i.e.

$$\langle \phi_i | \phi_j \rangle = \delta_{ij} \quad (2.12)$$

There are $N(N-1)/2$ constraints in this case, and all of them can be incorporated in the expression:

$$F = \langle \Phi | \hat{H} | \Phi \rangle - \sum_{i,j} \lambda_{i,j} [\langle \phi_i | \phi_j \rangle - \delta_{ij}] \quad (2.13)$$

In the Hartree approximation, a similar approach is followed, but since the wave function is not made to be antisymmetrical, it violates one of the fundamental quantum mechanical principles and fails to be acceptable.

The introduction of a Slater determinant by the Hartree-Fock approximation, however, solves the anti-symmetry problem. Therefore the approximate wave function derived using a Slater determinant in Eq. (2.6) should be inserted into Eq. (2.13). Once this is done, the main requirement is that any of the first order derivatives of the quantity F in Eq. (2.13) with respect to any of the Lagrange multipliers, λ_{ij} , should vanish, i.e.

$$\delta F = 0 \quad (2.14)$$

for small and arbitrary variation of the orbital ϕ_i , as stated in Eq. (2.11). This is the fundamental principle of the Hartree-Fock method, which is used to formulate the Hartree-Fock equation.

Further, considering the single electron in spin orbital ϕ_i in the field of the nuclei and other electrons in spin orbital ϕ_j it is noticed that its Hamiltonian operator contains three terms, which determine the three contributions to its energy. This is written as the integro-differential equation of ϕ_i , as follow:

$$\begin{aligned} & \left[-\frac{1}{2} \nabla_i^2 - \sum_{A=1}^M \frac{Z_A}{r_{iA}} \right] \phi_i(1) + \sum_{j \neq i} \left[\int \phi_j(2) \phi_j(2) \frac{1}{r_{12}} d\tau_2 \right] \phi_i(1) - \\ & \sum_{j \neq i} \left[\int \phi_j(2) \phi_i(2) \frac{1}{r_{12}} d\tau_2 \right] \phi_i(1) = \sum_j \varepsilon_{ij} \phi_j(1) \end{aligned} \quad (2.15)$$

This expression can be written in a simplified form by introducing three operators that represent the contributions to the energy of the spin orbital ϕ_i in the stationary system. These operators are the core Hamiltonian, the coulomb operator, and the exchange operator. The core operator, \hat{H}^{core} , is the only operator that exists in the absence of any interelectronic interactions, and

it describes the motion of a single electron moving in a field of bare nuclei. The coulomb operator, \hat{J} , describes the average potential existing due to the presence of electrons in the ϕ_j orbital, and is the classical analogue of the electrostatic interaction between two charge distributions. Finally, the exchange integral operator \hat{k} has no classical analogue; hence its existence is the direct consequence of the quantum mechanical requirement that the N -electron wave function must be antisymmetric when interchanging any two electrons.

Inserting the operators into Eq. (2.15) gives the following simplified expression:

$$\hat{H}^{core}(1)\phi_i(1) + \sum_{j \neq i}^N \hat{J}_j(1)\phi_i(1) - \sum_{j \neq i}^N \hat{k}_j(1)\phi_i(1) = \sum_j \varepsilon_{ij}\phi_j(1) \quad (2.16)$$

Based on the fact that $\{\hat{J}_i(1) - \hat{k}_i(1)\}\phi_i(1) = 0$, this equation can be modified and written as:

$$[\hat{H}^{core}(1) + \sum_{j=1}^N \{\hat{J}_j(1) - \hat{k}_j(1)\}] \phi_i(1) = \sum_{j=1}^N \varepsilon_{ij}\phi_j(1) \quad (2.17)$$

Further simplification gives the expression:

$$\hat{F}_i \phi_i = \sum_j \varepsilon_{ij}\phi_j \quad (2.18)$$

\hat{F} is called the Fock operator and is an effective one-electron Hamiltonian for an electron in a polyatomic system. This operator describes the kinetic energy of the electron in the ϕ_i orbital, its coulombic attraction to its surrounding nuclei and the average repulsion the electron faces from its surrounding electrons.

The general Hartree-Fock equation described in Eq. (2.18) gives rise to many different solutions, hence it is not reliable to use. So as to avoid this shortcoming, main focus is given to the solution for which the Lagrange multiplier obeys:

$$\lambda_{k,i} = \delta_{k,i}\varepsilon_k \quad (2.19)$$

This value is non-zero only for $k = i$ and in this particular case, $\lambda_{i,i}$ is equal to ε_i . This mathematical manipulation finally gives rise to the standard eigenvalue equation of the Hartree-Fock.

$$\hat{F}_i \phi_i = \varepsilon_i \phi_i \quad (2.20)$$

In deriving this equation, one of the primary approximations made is the central field approximation. According to this approximation, the coulombic electron-electron repulsion is taken into account as an average effect of the repulsion, but not as an explicit one. This is because each electron is assumed to move in a fixed field, which comprises the nuclei and other electrons.

The assumption made above has an important implication for the way in which an attempt is made to solve the Hartree-Fock equation, because any solution found by solving the equation for one electron will naturally affect the solution for the other electrons in the system. Hence the general strategy followed in this case is a self-consistent field (SCF) approach.

According to this approach, starting from a first guess for the initial ϕ_i^0 , an initial set of Fock operators, \hat{F}_i^0 , is created. These are then used to solve the equations:

$$\hat{F}_i^0 \phi_i = \varepsilon_i \phi_i \quad (2.21)$$

This gives rise to a new and improved set of orbitals, ϕ_i^1 , and energies, ε_i^1 . These improved orbitals are then used to construct a new Fock operator, \hat{F}_i^1 , which in turn will give even better orbitals, ϕ_i^2 , and energies, ε_i^2 . This iterative process is repeated many times until Eq. (2.20) achieves self-consistency, i.e. until no further improvement is observed by repeating the iteration process. This results in a set of orbitals, which are called self-consistent field or canonical molecular orbitals.

The Hartree-Fock calculation finally gives a set of orbital energies, ε_i . Hence the energy of an electron in any spin orbital ϕ_i is given as a sum of core, coulombic, and exchange interactions.

$$\varepsilon_i = \hat{H}_{ii}^{core} + \sum_{j=1}^{N/2} (2\hat{J}_{ij} - \hat{k}_{ij}) \quad (2.22)$$

The total electronic energy of the ground state is obtained by a systematic summation of all orbital energies and given as:

$$E = \sum_{i=1}^N \varepsilon_i - \sum_{i=1}^{N/2} \sum_{j=1}^{N/2} (2\hat{J}_{ij} - \hat{k}_{ij}) \quad (2.23)$$

Even though the standard Hartree-Fock equation seems simple, when inserting the precise form of the different operators that enter them, as was done in the derivation process, it is found that they are complicated integro-differential equations.

Taking the difficulty of solving the Hartree-Fock equation into consideration, Roothaan, has proposed an alternative way, which simplifies the calculation process (Springborg, M., 2000). In the same manner as the Hartree-Fock method, Roothaan obtained the approximate wave function, Φ , by solving F in Eq. (2.13). But unlike the Hartree-Fock method, which involves variation of all orbitals in all position-space points where variation of infinitely many parameters is involved, Roothaan makes the variation finite by varying only the expansion coefficients, C_{pi} , of the

orbitals to the basis function. This is made possible by expanding the orbitals in a set of fixed basis functions, X_p :

$$\phi_i(\vec{x}) = \sum_{p=1}^{N_b} X_p(\vec{x}) C_{pi} \quad (2.24)$$

In this method, the basis functions, X_p , as well as their number, N_b , are chosen in advance and only the expansion coefficients, C_{pi} , (coefficient of the i^{th} orbital with the p^{th} basis function), which are finite in number, are allowed to vary.

After inserting Eq. (2.24) into Eq. (2.13) and making many substitutions the Hartree-Fock-Roothaan equation is obtained and by carrying out multi-step simplifications it is expressed in terms of the following matrix eigenvalue equation:

$$\underline{\hat{F}} \cdot \underline{C}_i = \varepsilon_i \cdot \underline{O} \cdot \underline{C}_i \quad (2.25)$$

where $\underline{\hat{F}}$ contains the Fock matrix elements, \underline{O} contains the overlap matrix elements, \underline{C}_i contains the desired (finitely variable) coefficients of different basis functions of the i^{th} orbital, and ε_i is energy of the electron in spin orbital ϕ_i .

As was done in the Hartree-Fock case, the simplified form of the Hartree-Fock-Roothaan equation is solved self-consistently. According to the variational principle, since quality of a given calculation in this case is heavily dependent on the quality of the basis functions, increasing the set of basis functions leads to a better approximation of the total electronic energy. For this reason, with the use of an adequate basis set, the Hartree-Fock-Roothaan equation makes the Hartree-Fock calculations simple and widely used.

2.3 Basis Sets

2.3.1 Slater and Gaussian type orbitals

When a quantum mechanical calculation is carried out on a system, the Hartree-Fock method approximates an N -electron wave function, Ψ , with a single determinant, Φ , containing N single-electron orbitals ϕ_i . With the aim of simplifying the calculation, Roothaan suggested an expansion of the orbitals in a set of pre-defined basis functions, X_p , which can be expressed as stated in Eq.(2.24).

Even though it indeed simplifies the calculation, the main challenge faced in using this equation is the construction of an appropriate basis set. However constructing the basis set using a linear combination of atomic orbitals can solve this problem. Hence, assuming that the basis set function belongs to an atom at the origin, it is given as:

$$X(\vec{r}) = R_{nl}(r) Y_{lm}(\theta, \phi) \quad (2.26)$$

where Y_{lm} is a spherical harmonic function, an angular part which describes the shape of orbitals; r, ϕ , and θ are the spherical coordinates; R_{nl} is the radial part of the basis function; n, l , and m are the principal, angular momentum, and magnetic quantum numbers, respectively. For the sake of simplification, the radial part R_{nl} is given as a product of polynomial and exponentially decaying functions. This gives a basis set of the form:

$$X(\vec{r}) = X_{\bar{R}\zeta nlm}(\vec{r}) = \frac{(2\zeta)^{n+1/2}}{(2n!)^{1/2}} r^{n-1} e^{-\zeta r} Y_{lm}(\theta, \phi) \quad (2.27)$$

where \bar{R} is the radial function expression for a specific atom.

Substituting the first term of the right hand side equation of Eq. (2.27) with N gives:

$$X_S(\vec{r}) = X_{\bar{R}\zeta nlm}(\vec{r}) = N r^{n-1} e^{-\zeta r} Y_{lm}(\theta, \phi) \quad (2.28)$$

where N is normalization constant and ζ is the exponent. S indicates that the orbital is a Slater type orbital.

The functions defined in Eq. (2.28) are the so-called Slater type orbitals (STOs). Since these orbitals have no radial nodes, a node is introduced to their radial part by making linear combinations of STOs. As can easily be seen from Eq. (2.28), the STO functions contain many complex equations, which make calculations prohibitively complicated and very slow. For this reason STOs are mainly used for atomic and diatomic systems where high accuracy is required and in semi-empirical methods where all three and four center integrals are neglected. Most *ab initio* calculations are carried out using Gaussian type orbitals (GTOs). This is made possible because the shape of STOs functions can easily be approximated using a summation of a number of GTOs with different exponents and coefficients.

The Gaussian type orbitals can be written in terms of polar and Cartesian coordinates as follows:

$$X_g(\vec{r}) = X_{\bar{R}\alpha nlm}(\vec{r}) = N r^{n-1} e^{-\alpha r^2} Y_{lm}(\theta, \phi) \quad (2.29)$$

$$X_g(\vec{r}) = X_{\bar{R}\alpha nlm}(\vec{r}) = N e^{-\alpha r^2} x^l y^m z^n \quad (2.30)$$

where α in this case is the exponent, and g indicates that the orbital is a Gaussian type orbital.

Even though the polar and Cartesian representations of GTOs described above seem similar, there is a significant difference between them. For instance, when a d -type GTO is represented in terms of spherical (polar) functions, it gives rise to five components ($Y_{22}, Y_{21}, Y_{20}, Y_{2-1}, Y_{2-2}$). However, in terms of Cartesian coordinates, it has six components ($x^2, y^2, z^2, xy, xz,$

yz). Despite this difference the Cartesian functions can be modified to give five spherical d -functions and one additional s -function which is obtained from the following summations:

$$d_{xx} + d_{yy} + d_{zz} = N(x^2 + y^2 + z^2)e^{-\alpha r^2} = N r^2 e^{-\alpha r^2} = s \quad (2.31)$$

In the same manner, the ten Cartesian functions of the f -orbital can be transformed to seven spherical f -functions and one set of p -functions. Due to the additional functions they have, the Cartesian functions give a slightly lower energy than the polar functions. For this reason, *ab initio* calculations separate the d -orbitals as $5d$, $6d$ or pure- d , Cartesian- d and similarly the f -orbitals are separated as $7f$, $10f$ or pure- f , Cartesian f . Besides lowering the energy, the Cartesian functions also simplify the calculation of integrals.

As can be seen from Eq. (2.29), GTOs differ from STOs only in the value of their exponents, i.e. GTOs depend on r^2 rather than r . Due to this fact, all the Gaussians have a flat tangent at the site of the nucleus, and consequently, GTOs have two limitations. The first one is that since they have zero slopes at the nucleus, they don't have a "cusp" (i.e. discontinuous derivative) as STOs do. For this reason they cannot properly describe behavior of the system near the nucleus and hence nuclear dependent properties such as energy. The second limitation is that since the GTO functions fall off too rapidly far from the nucleus (**fig.2.1**), the tail of the wave function is poorly described. Hence properties that are dependent on the tail of the wave function such as dipole moment and polarization are not being well described.

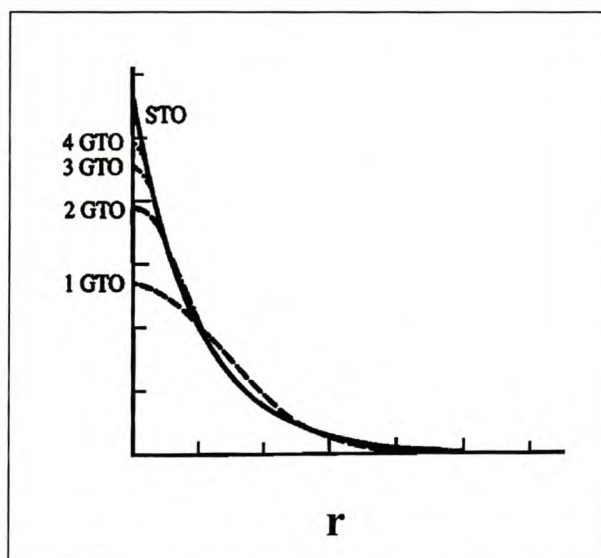


Fig. 2.1: Comparison of 1s Slater type orbital (STO) with its one, two, three and four-termed extended Gaussian type orbital (GTO) counterparts.

Therefore, so as to circumvent this problem, it is common to use multiple GTOs to describe a particular STO. This is clearly demonstrated in **fig.2.1**, where fitting of the GTOs and STOs shows a significant improvement with an increment of the number of GTO functions.

2.3.2 Types of basis sets

There are many types of basis sets being used in the different methods of computation and some of them are discussed in the subsequent subsections.

(A) Contracted Basis Sets:

The two parameters used in a Gaussian expansion are the coefficient and the exponent. The most flexible calculation in which both the two parameters vary uses uncontracted or primitive Gaussians. However, contracted Gaussians, which involve a single expansion at a time, are commonly used.

Most energy optimized basis sets have the limitation that the wave function depends mainly on the inner shell electrons, giving less attention to the chemically important valence electrons. Therefore, the fact that many basis functions go into the description of the energetically important, but chemically unimportant core electrons is the foundation of contracted basis sets (Jensen, F., 1999).

The process of combining the full set of basis functions, which are known as primitive Gaussian type orbitals (PGTOs) into a small set of functions by forming fixed linear combinations is referred to as basis set contraction, and the resulting functions are known as contracted Gaussian type orbitals (CGTOs). This contraction has a general form, which is given as:

$$X(\text{CGTO}) = \sum_i^K a_i X_i(\text{PGTO}) \quad (2.32)$$

where X_i is the orbital contracted, and a_i is the contraction coefficient.

There are two different ways of contracting a set of PGTOs into a set of CGTOs, namely “segmented” and “general” contractions. Among these the “segmented” contraction method is the most widely applicable and hence some examples of it will be discussed here.

There are many basis sets which undergo segmented contractions; among them Pople style, Minimal, Dunning- Huzinaga, and MINI, MIDI&MAXI basis sets are the most common ones. The Pople style basis sets, which are used in this project, and minimal basis sets will now be discussed in some detail.

Pople style basis sets

Pople and coworkers (Hehre, W.J.; Radom, L.; Schleyer, P.R. & Pople, J.A. 1986) proposed these split valence type basis sets. They are generally denoted as $K\text{-}nlG$ or $K\text{-}nlmG$ where K

indicates how many PGTOs are used for representing the core orbitals and the n, l or n, l, m indicate both how many functions the valence orbitals are split into, and how many PGTOs are used for their representation.

In these basis sets generally the s and p contractions belonging to the same “electron shell” (corresponding to the same quantum number n) are folded into an sp -shell. Hence the number of s -type and p -type primitives is the same and they even have identical exponents. However the s and p type contractions have different coefficients.

As the notations above show, functions that describe the valence electrons are either doubled or tripled, but those of the core electrons are kept single. The rationale behind this treatment is that the core orbitals, unlike the valence orbitals, do not affect the chemical properties significantly. The charge distribution around an atom in a molecule is usually perturbed in comparison with the isolated atom. This happens due to mixing of different orbitals in the molecules. So as to solve this problem and to give the wave function more flexibility with change of shape, a polarization function is introduced to the Pople basis sets. Polarization augmented Pople basis sets are denoted as $K-n l G^*$ or $K-n l m G^*$ when only the heavy atoms are augmented with d -type functions. Descriptions such as $K-n l G^{**}$ or $K-n l m G^{**}$ are used when the hydrogens are augmented with p -type functions as well. Augmentation of the hydrogens is optional and mainly depends on their contribution to the property of interest.

In treating anions and molecules containing lone pairs, which have a significant amount of electron density far away from their nuclei, Pople’s basis sets do not perform effectively. This is because their amplitude is low far away from the nucleus. Hence, to remedy this defect, diffuse functions are added. Once they are augmented they have a notation of $K-n l +G$ or $K-n l m + G$ when one diffuse s -type and p -type functions are added to a standard basis set of the heavy atoms only. Notations of $K-n l + + G$ or $K-n l m + +G$ are obtained by adding one diffuse s -type and p -type Gaussian on heavy atoms and one diffuse s -type Gaussian on the hydrogens.

Example:

- 6-31G: In this basis set, the core orbitals are a contraction of six primitive Gaussian orbitals (PGTOs), the inner part of the valence orbitals is a contraction of three PGTOs and the outer part of the valence is represented by one PGTO.

Beside this there are many other types of Pople style basis sets such as 3-21G, 4-31G, 6-311G, etc. These basis sets are very popular and widely used for qualitative calculations made on organic molecules.

Minimal basis sets:

These basis sets contain the smallest number of functions that can be used to describe an electron. Strictly speaking, these basis sets contain just the number of functions that are required to accommodate all filled orbitals in each atom. For example, H and He are described by only a single s function; the first row elements by two s functions ($1s$, $2s$) and one set of p functions (p_x , p_y , p_z); the second row elements by three s functions ($1s$, $2s$, and $3s$) and two sets of p functions ($2p$, and $3p$) etc.

All these basis sets are denoted by STO- n G (STO-3G, STO-4G, etc.); and in each case, n Gaussian functions are used to represent each STO. It was found that at least three Gaussian functions are required to properly describe each STO, for this reason STO-3G is the smallest of all.

These basis sets have certain limitations. One is their equal treatment of elements of the same period despite their difference in number of electrons. The second and major limitation is their possession of only one contraction per atomic orbital, which prevents the variation of the radial function making it inflexible with a change in molecular environment. To overcome these shortcomings, the minimal basis set functions are doubled to get the improved Double-Zeta (DZ), basis set. Compared with the minimal basis sets, the DZ basis set gives a better description of the electron distribution in a system of interest. Similarly, by continuing to increase the number of functions, improved higher level basis sets can be obtained and described as Triple Zeta (TZ), Quadruple Zeta (QZ), Quintuple Zeta (5Z) etc.

The other means of improving the quality of the minimal basis sets is by the introduction of polarization functions, as was done in the Pople type basis sets. Hence, addition of a single set of polarization functions (p -functions on hydrogens and d -functions on heavy atoms) to the DZ basis sets form a double zeta plus polarization (DZP) type basis set. Similarly, addition of two sets of polarization functions to TZ basis give rises to a triple zeta plus double polarization (TZ2P) type basis set.

(B) Effective Core Potential basis sets:

Development of this type of basis set was prompted by the aim of searching for a proper means of description for the inner core electrons, which play a passive role in the determination of chemical bonding. This is particularly needed for elements of the third and higher row of the periodic table.

Even though it is possible to totally ignore the core electrons as semi-empirical methods do, they could affect a proper description of the valence electrons and hence this is not worthwhile. For this reason the *ab initio* method introduces some means of representation of the core electrons. Accordingly the core electrons and their basis functions in the wave function are replaced with

potential terms in the Hamiltonian. These representations are called core potentials (CP), or effective core potentials (ECP). Once these representations are made, it becomes easy to incorporate relativistic effects in the ECP. As all-electron relativistic effect computations are very expensive this approach highly simplifies the task. Hence the basis set in this case is named a relativistic effective core potential (RECP). Therefore the use of ECP basis sets not only reduces the computational cost, but also is also important to address the relativistic effect that is a common problem in elements belonging to the lower half of the periodic table.

The ECP of a system is described in the following Gaussian functions expansion form:

$$ECP(r) = \sum_{i=1}^N a_i r^{n_i} e^{-\alpha_i r^2} \quad (2.35)$$

where N is the number of terms in the expansion, a_i is a coefficient for each term, r denotes the distance from the nucleus, n_i is the power of r for the i^{th} term, and $-\alpha_i$ represents the exponent for the i^{th} term.

So as to describe the system of interest properly, the core potential must be used along with a valence basis set that is created to accompany it. Therefore the introduction of an ECP drastically reduces the number of basis functions needed, because only basis functions of the valence electrons are needed and this significantly simplifies the computational work.

2.4 Electron Correlation Methods.

The Hartree-Fock method can give molecular property calculation results that are accurate enough to be compared with the experimental results for small and medium-sized molecules. However in studies which are sensitive to small energy changes, such as bond dissociation energy, ionization potential, electronic affinities, and electron excitation energies etc, consideration of a method beyond Hartree-Fock is quite crucial. The reason for using an alternative method is the limitation the Hartree-Fock has in not considering electron correlation.

According to the central field approximation, electrons are assumed to be keep on moving in an average potential of the other electrons, hence the instantaneous position of an electron is not influenced by the presence of its neighboring electrons. However, in a real system, the motion of electrons are correlated and they tend to keep far apart from each other, more than the approximation made, hence this allows them to have an energy value that is lower than the one obtained through the Hartree-Fock method of calculations. Therefore consideration of electron correlation is very important to improve the calculated results of molecules both qualitatively and quantitatively.

The energy value obtained by taking electron correlation into account is called correlation energy and is obtained as a difference between the true energy of a molecule and its self-consistently calculated energy value:

$$E_{Corr} = E_{exact} - E_{SCF} \quad (2.36)$$

When electron correlation is introduced into a system, one of the requirements is that the electrons are kept as far apart as possible, so that they can attain their realistic distribution. So as to fulfill this requirement in a one-particle function it is essential to construct a very flexible wave function. When constructing such wave functions based on the Hartree-Fock method, because the Hartree-Fock wave function spans only the occupied orbitals, it is crucial to introduce an additional region of space by admitting “virtual” orbitals. This can be achieved by using different correlation methods.

There are various types of correlation methods, most of them begin with a Hartree-Fock calculation and then correct for correlation. Some of these are: configuration interaction (CI), Møller-Plesset perturbation theory (MPn), coupled cluster theory (CC), multi-configurational self-consistent field theory (MCSCF), generalized valence bond method (GVB) etc. These methods as a group are called correlated calculations and among them the former three will be discussed in brief.

2.4.1 Configuration Interaction (CI)

Configuration interaction is one of the most popular methods of determining electron correlation, in which excited states are introduced into the description of the electronic state of a system. In this method, given a set of $n = n_\alpha + n_\beta$ molecular spin orbitals i, j, k, \dots that are occupied, and a set of $N = N_\alpha + N_\beta$ molecular spin orbitals a, b, c, \dots that are unoccupied, in order to allow electron correlation, the excited state molecular orbitals a, b, c, \dots are introduced into the system wave function to give:

$$\begin{aligned} \Psi_{CI} &= \Phi_0 + \sum_{i,a} C_i^a \Phi_i^a + \sum_{\substack{i<j \\ a<b}} C_{ij}^{ab} \Phi_{ij}^{ab} + \sum_{\substack{i<j<k \\ a<b<c}} C_{ijk}^{abc} \Phi_{ijk}^{abc} + \dots \\ &= C_0 \Psi_0 + C_1 \Psi_1 + C_2 \Psi_2 + C_3 \Psi_3 \dots \end{aligned} \quad (2.37)$$

where Φ_0 is a single determinant wave function which can be obtained by solving the Hartree-Fock equation and the rest are configuration wave functions, which can be derived by replacing one or more of the occupied spin orbitals by virtual spin orbitals. C_0, C_1, C_2 and C_3 are coefficients of the wave functions and they can be obtained by an energy minimization of the system through a variational approach.

In the limit of all possible excitations, the function in Eq. (2.37) gives rise to the full configuration interaction (FCI) solution. A full CI calculation can be made using an infinitely large

basis set and it could give an exact quantum mechanical result, which can be used as reference for other correlated calculations. However, when it is applied to very large systems with K number of basis functions and N number of electrons, the number of Slater determinants required increases exponentially with N as $K^N / N!$, hence it requires an immense amount of computer time. Therefore to avoid the extra time, the number of excitations made should be limited.

Some of the methods used to limit the numbers of excitations are: consideration of only the excitations involved in the HOMO and LUMO orbitals, exclusion of the core electrons (frozen core approximation), etc. Based on the number of excitations used to construct the determinant, the configuration interaction methods are classified into different types. The most common one, which describes the first four excitations are: configuration interaction singlet (CIS), configuration interaction singlet doublet (CISD), configuration interaction singlet doublet triplet (CISDT), and configuration interaction singlet doublet triplet quartet (CISDTQ) respectively.

Even though improvement of the energy value is expected for every advance in the number of excitations, it is not always found to be the case. One of the reasons for this is failure of mixing of some excited states with the ground state. For instance, the single excitation doesn't mix directly with the single determinant ground state wave function and hence it doesn't bring any improvement to the ground state energy value. For this reason, only the double and higher excitations can bring significant improvement to the ground state energy.

As a general property, CI calculations are variational, i.e. the energy value obtained using them is always greater than the true energy value. However, except for the full CI, all the other CI methods have the limitation of being size inconsistent. This means that the energy of an N number of non-interacting atoms or molecule, is not equal to N times the energy of a single component atom or molecule. Hence, as the bond length increases, the energy value of a diatomic molecule fails to be equal to sum of the energy value of its component atoms. Therefore, to overcome such limitations of the CI method, the use of other correlation methods is essential.

2.4.2 Møller-Plesset Perturbation Theory

This is another type of electron correlation method, which was proposed by Møller and Plesset (Leach, A. R. 2001), and, as its name suggests, the correlation is added as a perturbation from the Hartree-Fock equation. Here an attempt is made to solve the correlation problem by introducing a perturbation \hat{V} . Therefore the true Hamiltonian in this method is described as the sum of a zeroth-order Hamiltonian \hat{H}_0 and a perturbation \hat{V} .

$$\hat{H} = \hat{H}_0 + \hat{V} \quad (2.38)$$

In this theory the unperturbed Hamiltonian \hat{H}_0 is obtained by the summation of the one-electron Fock operators for the N electrons and is described as:

$$\hat{H}_0 = \sum_{i=1}^N \hat{F}_i = \sum_{i=1}^N (\hat{H}^{core} + \sum_{j=1}^N (\hat{J}_j + \hat{k}_j)) \quad (2.39)$$

The value of the true Hamiltonian, on the other hand, is described by the sum of the nuclear attraction and electron repulsion terms:

$$\hat{H} = \sum_{i=1}^N (\hat{H}^{core}) + \sum_{i=1}^N \sum_{j=i+1}^N \frac{1}{r_{ij}} \quad (2.40)$$

The eigenfunctions, Ψ_i , and eigenvalues, E_i , of the true Hamiltonian are respectively expressed as:

$$\Psi_i = \Psi_i^{(0)} + \lambda \Psi_i^{(1)} + \lambda^2 \Psi_i^{(2)} + \dots = \sum_{n=0} \Psi_i^{(n)} \quad (2.41)$$

$$E_i = E_i^{(0)} + \lambda E_i^{(1)} + \lambda^2 E_i^{(2)} + \dots = \sum_{n=0} E_i^{(n)} \quad (2.42)$$

where λ is a parameter with value which varies from zero to one.

In order to calculate the high-order wave functions, which are described from the second term onward in Eq. (2.41) above, knowing the perturbation \hat{V} value is essential. It can be obtained from the difference between the true and zeroth-order Hamiltonian values defined in Eq. (2.39) and Eq. (2.40) and given as:

$$\hat{V} = \sum_{i=1}^N \sum_{j=i+1}^N \frac{1}{r_{ij}} - \sum_{j=1}^N (\hat{J}_j + \hat{k}_j) \quad (2.43)$$

Once the high-order wave functions are obtained their energy counterpart can be calculated. As was observed in the CI method, the first-order perturbation does not bring any improvement to the ground state energy. Nevertheless the second and other higher-order perturbation theories such as MP3, MP4, and MP5 etc. give significant enhancement to the energy value, despite the computational difficulties involved.

One advantage of the perturbation theory over CI is its size dependent nature. It maintains this character even when a truncated expansion is considered. However, this correlation method is not variational and hence sometimes gives an energy value that is less than the true energy value.

2.4.3 The Coupled Cluster Method

When considering difficult correlation problems, it may be necessary to search for a better method, and coupled cluster is one of the methods of choice. This method is the ultimate choice

particularly when a single determinant reference function offers a poor approximation to the system of interest.

The coupled cluster method simplifies the whole concept of extensive methods by the theorem, which excludes higher excitation states (linked-diagram theorem) by introducing a very simple exponential wave function (Springborg, M., 2000). Based on this approach the general wave function of a system is written in expanded form as:

$$\Phi = N e^{\hat{T}} \Phi_0 \quad (2.44)$$

$$e^{\hat{T}} = 1 + \hat{T} + \frac{1}{2} \hat{T}^2 + \dots = \sum_{k=0}^{\infty} \frac{1}{k!} \hat{T}^k \quad (2.45)$$

where N is the normalization function, \hat{T} is a cluster operator. In the expansion of $e^{\hat{T}}$, the first term gives the reference Hartree-Fock, the second term the singly excited state, the third term the second excited state and so on.

In this way the correlation correction can be made in an infinite order. Therefore by making the right choice of $e^{\hat{T}}$ value, the size inconsistency problem this method has can be solved. The general exponential wave function expression in Eq. (2.44) restricts the number of configurations that are included, and also establishes a relation between the various parameters for excitation involving fewer and more electrons.

There are various orders of expansion in the CC method, which are named depending on the number of expansions made. For instance, the first order of expansion is called the coupled cluster singlet, and is written as CCS in its abbreviated form. Similarly, the higher order expansions are named CCSD, CCSDT, and CCSDTQ etc. in ascending order, respectively. As the order gets higher, a more improved energy is obtained.

When compared with the configuration interaction and Møller-Plesset perturbation theory methods, the energy value obtained using the CC correlation method is closer to the Full CI results; hence despite its time intensive nature, it is the method of choice to get accurate energies.

2.5 Semi-empirical methods

Being expressed in terms of a Hamiltonian and a wave function, the semi-empirical methods have the same basic structure as *ab initio* methods. Hence they can be analyzed based on the Hartree-Fock-Roothaan equation described in Eq (2.25).

Despite the similarities they have, the semi-empirical methods do not calculate all components of the Fock matrix as the *ab initio* method does. Rather they divide the Fock matrices into parts, which are either completely omitted or approximated.

One of the approximations made in these methods is that for core electrons. With the aim of reducing the large computation time required for many-integral calculations, semi-empirical methods completely ignore the core electrons and explicitly consider only the valence electrons. The rationale behind this is the fact that most chemical reactions and properties are governed by the valence electrons.

Another important approximation made in the semi-empirical method involves the overlap matrix. According to this approximation, all diagonal elements of the overlap matrix are set equal to one, whereas all off-diagonal elements become zero. This leads to simplification of the Hartree Fock-Roothaan equation to $\underline{\hat{F}} \cdot \underline{C}_i = \varepsilon_i \cdot \underline{C}_i$, which is in a standard matrix form. So as to remedy the calculation errors that occur due to the omissions and approximations made, semi-empirical equations are parameterized based on *ab initio* calculation and experimental results.

As compared with the *ab initio* method, semi-empirical calculations are very fast, which is advantageous. However, they encounter the limitation that the results obtained are not accurate enough. This worsens when the molecule under consideration does not exist in the parameterization database. Therefore the different sets of properties such as geometry, energy, dipole moment, heat of reaction, ionization potential etc. are parameterized with the aim of reproducing the various results obtained.

There are many types of semi-empirical methods, among them those contributed by Dewar and his colleagues such as MNDO (Dewar and Thie, 1977), AM1 (Dewar et al 1985), PM3 (Stewart 1989 a, b), and SAM1 (Dewar et al 1993) are the most popular ones. Beside these SINDO1, of Jug (Jug, K.; Neumann, F. 1998) and ZINDO of Zerner (Zerner, M.C.; 1991) are also well known. In particular the ZINDO program is very useful for calculation of transition metal and lanthanide compounds; it is also used for the prediction of molecular electronic spectra.

In general even though they are not as accurate as the *ab initio* methods, Semi-empirical methods play a significant role in the description of different properties of many organic and some inorganic compounds. Sometimes even they excel over *ab initio* when applied to large molecules, which are difficult to handle using the *ab initio* method.

2.6 Molecular Mechanics methods

The molecular mechanics method, which is alternatively called the force field method, is another important computational tool. *Ab initio* and semi-empirical methods need very long CPU times, and hence are not economical to use for large molecules such as proteins, nucleic acids (DNA and others), polymers etc. Therefore the molecular mechanics method is a common choice to handle such tasks.

Unlike *ab initio* and semi-empirical methods, the molecular mechanics method does not use a wave function or total electron density, but, rather it considers the energy of a system as a function of nuclear position. Hence it uses terms of simple algebraic equations to describe the energy. The terms used for the energy expression are accompanied by constants, which are derived from either spectroscopic data or *ab initio* calculations. Therefore these sets of equations, with their associated constants, are called force fields.

The molecular mechanics energy is written as a sum of terms each describing the energy required for distorting a molecule in a specific manner.

$$E_{MM} = \sum_{bond} \frac{k_i}{2} (l_i - l_{i,0})^2 + \sum_{angle} \frac{k_i}{2} (\theta_i - \theta_{i,0})^2 + \sum_{torsion} \frac{v_n}{2} (1 + \cos(n\omega - \gamma)) + \sum_{i=1}^N \sum_{j=i+1}^N \left(4\epsilon_{ij} \left[\left(\frac{\delta_{ij}}{r_{ij}} \right)^{12} - \left(\frac{\delta_{ij}}{r_{ij}} \right)^6 \right] + \frac{q_i q_j}{4\pi\epsilon_0 r_{ij}} \right) \quad (2.46)$$

Here the first term is the energy function of a bond stretching between two atoms. The second term represents the energy required for bending an angle. The third term is the torsional energy for rotation around a bond, while the fourth term describes the non-bonded atomic interactions.

Depending on the need, cross terms may be added to describe the coupling between the first three terms. However, this is optional because some force fields completely ignore these terms and compensate for them by using sophisticated electrostatic functions.

Due to its transferability and fast computing ability, the molecular mechanics method is a valuable tool for predicting geometries and heats of formation of molecules for which a force field is available. It is also useful to compare different conformations of the same molecules. However, this method has two limitations. First, force fields are based on the properties of known, similar molecules. Hence if one is interested in the properties of a new type of molecule, an appropriate force field probably will not be available for that molecule. The second limitation is that since the molecular mechanics method is based on a classical mechanics model, it describes a molecule as a group of atoms held together by elastic bonds, and hence it can't be used to predict electronic properties of molecules. Therefore when one is interested in electronic properties, the quantum method is the best choice.

Today there are many commonly used molecular mechanics force fields (Young, D., 2001); MM2 (Allinger, 1977), MM3 (Allinger et al., 1989), MM4 (Allinger et al., 1996), and the Merck Molecular Force Field (MMFF) perform well for many organic molecules, the Universal Force Field (UFF) (Rappé et al., 1992) works well for many inorganic molecules, while the Assisted Model Building with Energy Refinement (AMBER) (Cornell et al., 1995), and the Chemistry at

Harvard Macromolecular Mechanics (CHARMM) (Brooks et al., 1983) force fields are used for proteins and nucleic acids.

2.7 Electronic Structure Analysis methods

2.7.1 Theory of atoms in molecules (AIM)

AIM is a powerful and novel theory, which is based on the electron density, $\rho(r)$, of molecules to explain fundamental chemical concepts such as atomic properties, bonds, and molecular structures based on quantum mechanical principles (Popelier, P., 2000). Being such an important tool it will be discussed in detail below.

(i) Electron density [$\rho(r)$]

Schrödinger's stationary state equation (Eq.2.1) is an eigenvalue equation which yields eigenvalues E and eigenfunctions Ψ as a solution. From these variables the theory of AIM uses the wave function, Ψ , to derive the electron density, $\rho(r)$, in a system.

Even though the wave function is expected to yield all the information about a quantum system, this situation is not simple because Ψ cannot be directly observed. The two main reasons for this are on one hand that the values of Ψ are complex numbers, and on the other the Ψ is difficult to determine in real 3D space. To overcome the first problem, Ψ is changed to a real number by multiplying it with its complex conjugate, Ψ^* . The product of the operation $\Psi\Psi^*$, which can be written as $|\Psi|^2$, is a real number and defines the probability of charge distribution of an electron.

The second problem arises due to the multi-dimensional nature of Ψ . As discussed earlier, four coordinates describe an electron: three spatial coordinates denoted by $r_i = (x_i, y_i, z_i)$ for electron i and one spin coordinate denoted as $\delta_i = (\alpha / \beta)$ (Eq.2.4). In a molecule of N electrons the electronic wave function contains $4N$ coordinates and this makes the function more complicated. In this system the probability of finding each one of N electrons in an infinitesimal volume element is given as:

$$\Psi^*(X)\Psi(X)d\bar{x}_1 d\bar{x}_2 \dots d\bar{x}_K \dots d\bar{x}_N \quad (2.47)$$

where \bar{x}_i is the set of four coordinates describing the i^{th} electron, which is given as $\bar{x}_i = (r_i, \delta_i)$, and X is the set of $4N$ coordinates described as: $X = (\bar{x}_1, \bar{x}_2, \dots, \bar{x}_N)$. The above lengthy equation can be simplified by integrating Ψ over all the spatial coordinates, with the resulting function giving the probability per unit volume of finding one electron, regardless of its spin and the instantaneous positions of the remaining electrons.

Expressing the volume element as $dr_i = dx_i dy_i dz_i$, the probability of finding one of the electrons (electron 1) in the volume element dr_1 , independent of the instantaneous positions or spins of the other electrons, is given by:

$$\sum_{spins} [\int dr_2 \int dr_3 \dots \int dr_N \Psi^*(X) \Psi(X)] dr_1 \quad (2.48)$$

where \sum_{spins} is the summation of spins of all the electrons. After multiplying the above equation by N and mathematically normalizing the probability to unity the equation of electron density obtained is described as:

$$\rho(r_1) = N \sum_{spins} [\int dr_2 \int dr_3 \dots \int dr_N \Psi^*(X) \Psi(X)] \quad (2.49)$$

When written in a more general form it becomes:

$$\rho(r) = N \int \Psi^*(X) \Psi(X) dr' \quad (2.50)$$

where $\int dr'$ stands for integration over all the spin coordinates of all electrons except the one under consideration. This electron density equation is the cornerstone of the AIM theory and the electron density, ρ , value, which is the main source of information for this theory, can be obtained either from *ab initio* calculations that are made at higher level or DFT (Dillen, J.L., 2003); or it can be obtained experimentally by carrying out an X-ray diffraction analysis on the molecule of interest.

In the study of AIM the electron density encountered can be represented either numerically or pictorially. The numerical representation can be done by selectively listing the ρ values of interest from the bulk ρ data. In case of the pictorial representation, different types of pictures such as two or three-dimensional contour maps, relief maps, or others can be used. The following contour map representations of proton substituted acylthiourea are typical examples, (**fig. 2.2**).

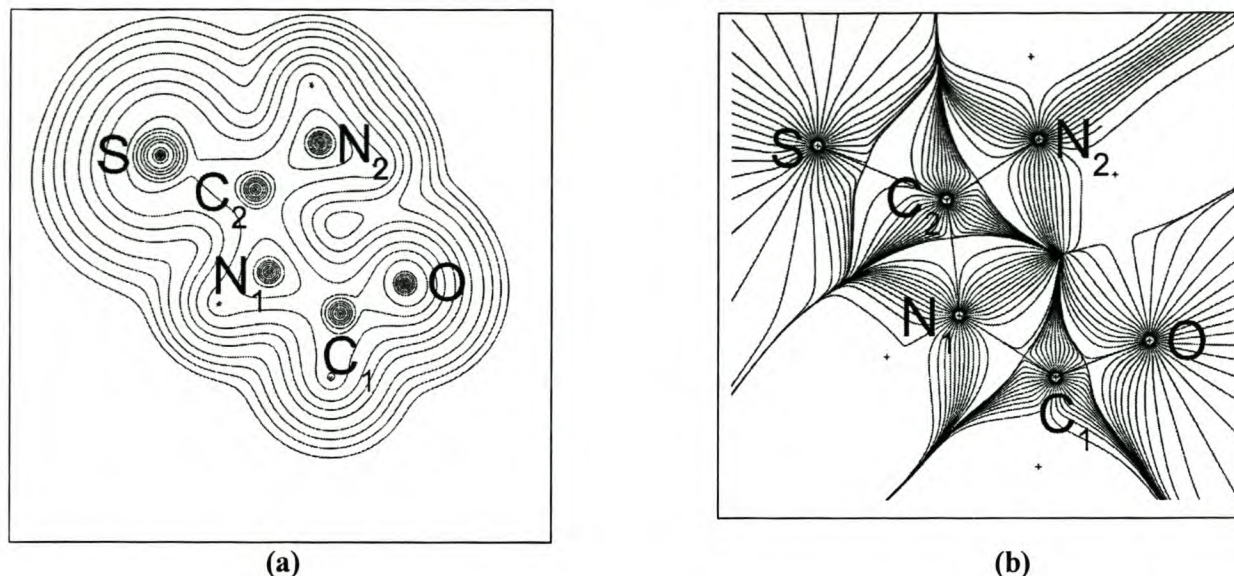


Fig.2.2: (a) Contour map of the electron density distribution for the molecular plane of a proton substituted acylthiourea compound. The contour values increase and decrease from a zero contour in steps $\pm 2 \times 10^{-3}$, $\pm 4 \times 10^{-3}$, $\pm 8 \times 10^{-3}$, $\pm 2 \times 10^{-2}$ up to $\pm 8 \times 10^{-2}$ au. (b) The corresponding gradient vector field of the electron density in the same plane. As the graph shows, all the gradient paths originate at infinity and terminate on one of the nuclei. The open crosses indicate the projected position of out of plane proton nuclei.

The first derivatives of the electron density of every topological feature such as maxima, minima, or saddle points have a value of zero ($\nabla\rho = 0$), the point where this density is located is called a *critical point* (r_c). The Hessian matrix of ρ , which is composed of nine second derivatives of $\rho(r)$, is real and symmetrical, and upon diagonalization it gives a set of eigenvalues and eigenvectors. The eigenvalues correspond to the three principal curvatures of ρ at the critical point; while the eigenvectors correspond to orientations of the curvatures in space i.e. they are the principal axes of curvature.

Every critical point in a molecule is described in terms of a rank (Ω) and its signature (ζ). The rank (Ω) stands for the number of non-zero curvatures on the specific critical point whereas the signature (ζ) is the sum of the algebraic signs of the non-zero curvatures. With few exceptions, most molecules at or in the neighborhood of an energetically stable geometrical configuration of the nuclei are of rank three. Hence there are four well-known critical points of this rank:

Nuclear Attractor: This critical point has a rank and signature representation of (3, -3). Here all curvatures of the electron density at the critical point are negative and $\rho(r)$ is a local maximum at r_c . This corresponds to the position of an atom.

Bond Critical Point: The rank and signature representation of this critical point is (3, -1). In this case two of the curvatures, which are located in the interatomic surface, are negative and the electron density is a maximum at r_c in the plane defined by the two associated principal axes of curvature. The third curvature, which is located along the atomic interaction line, is positive and $\rho(r)$ is a minimum at r_c along the axis perpendicular to this plane. This indicates the presence of a bond between two atoms.

Ring Critical Point: This has a rank and signature representation of (3, +1). At this critical point two of the curvatures are positive and the electron density is a minimum at r_c in the plane defined by the two associated axes. The third curvature is negative and $\rho(r)$ is a maximum at r_c along the axis perpendicular to this plan. Presence of this critical point verifies the presences of a ring of atoms.

Cage Critical Point: The rank and signature representation of this point is given as (3, -3). In this case all curvatures are positive and the electron density is a local minimum at r_c .

(ii) Laplacian of the electron density

Another useful scalar function in AIM is the Laplacian of the electron density. This function is the scalar derivative of the gradient vector field of the electron density, and is defined as:

$$\nabla^2 \rho(r) = \frac{\partial^2 \rho(r)}{\partial x^2} + \frac{\partial^2 \rho(r)}{\partial y^2} + \frac{\partial^2 \rho(r)}{\partial z^2} \quad (2.51)$$

Besides complementing the topology of the electron density $\rho(r)$, the Laplacian contains a lot of valuable chemical information. To mention some: the Laplacian supports the valence shell electron pair model, it redefines acidity in terms of the balance between kinetic and potential energy densities, it leads to the complementary principle useful in the study of nucleophilic and electrophilic attack, it predicts Van der Waals complexes and also predicts the preferred site of protonation. (Popelier, P. 2000).

The Laplacian determines where electronic charge is locally concentrated ($\nabla^2 \rho(r) < 0$) and where it is depleted ($\nabla^2 \rho(r) > 0$). Hence for convenience the topology of the Laplacian, $L(r)$, is by convention designated as the negative of the Laplacian. i.e. $L(r) = -\nabla^2 \rho(r)$. The topology of the Laplacian shows that the inner charge concentration of an atom in a molecule remains spherical, but that the valence shell charge concentration (VSCC) is always distorted from a spherical shape,

because it is the interactive part of the atom. The extent of distortion depends on the nature of the molecules. In polar molecules, for instance, it could disappear completely; hence it could give some clue about the polarity of molecules.

$L(r)$ exhibits a shell structure within each quantum shell. For elements with an atomic number less than forty, a quantum shell of high concentration is followed by one with depleted concentration and so on. Hence $L(r)$ can be used to differentiate atoms based on their shell sequence. A typical example that can demonstrate this observation is the contour map of the Laplacian of methyl substituted acylthiourea in **fig. 2.3**. Besides showing the pattern of electron localization on the bonding and non-bonding charge concentration (CC) regions, it also shows regions of the entire quantum shells of the sulphur and other atoms very clearly.

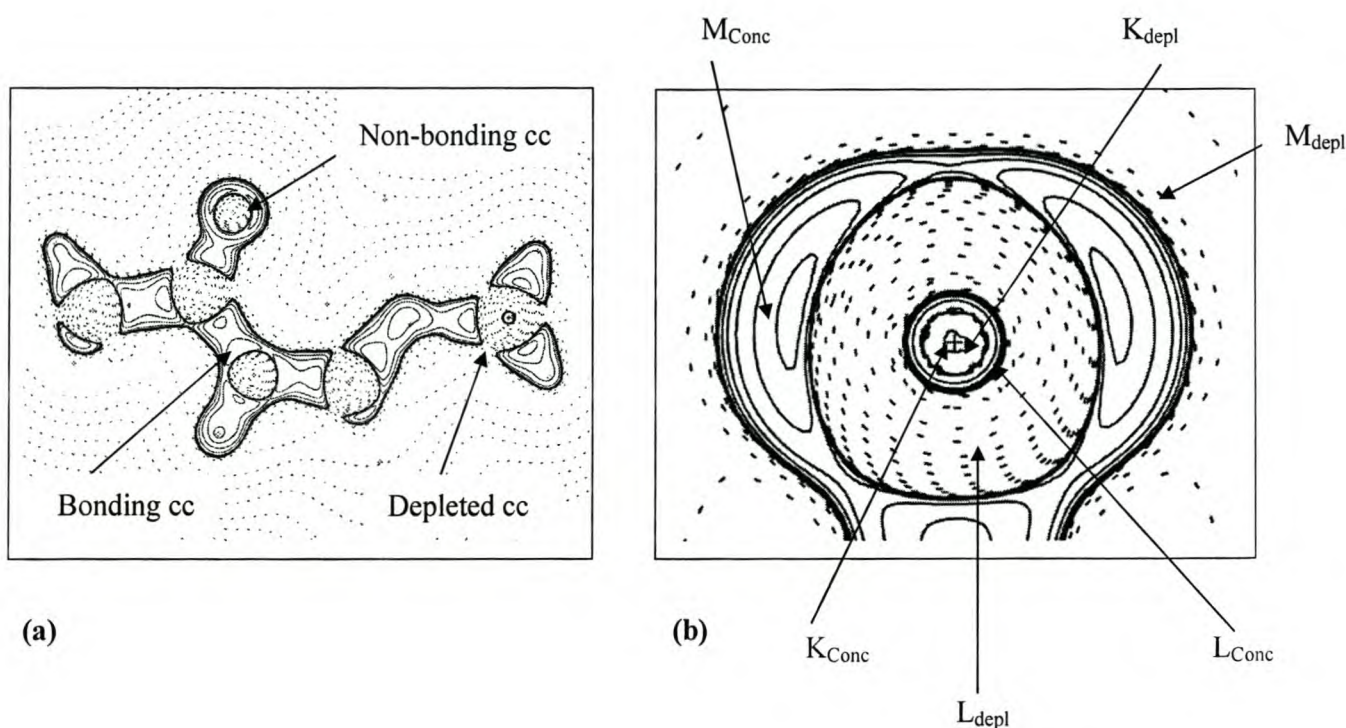


Fig. 2.3 Contour map of the Laplacian of electron density of methyl substituted acylthiourea. Solid lines indicate positive $L(r)$ values and dashed lines indicate negative values. (a) Demonstration of the electron localization on the bonding, non-bonding and depleted regions. (b) Nature of charge concentration on the K , L , and M shells of the sulphur atom in the molecule.

When applied analogously to other molecules the contour map of the Laplacian can give a similar wealth of information. Hence it is reasonable to say that the Laplacian is a magnifying glass for the electron density in the study of atoms in molecules (Dillen, J.L., 2003).

2.7.2 Natural Bond Orbital Analysis (NBO)

NBO is one of the most well-known quantum mechanical methods used for the analysis of chemical bonds (Frenking, G., Fröhlich, N., 2000). It contains many sets of analysis techniques to describe the N -electron wave function, $\Psi(1, 2, N)$, in terms of localized orbitals or configurations that are closely related to the chemical bonding concept. One of the techniques used in this method is natural population analysis (NPA), which is mainly used to determine the occupancy (number of electrons in an atom) and charge distribution in molecules.

In conducting a population analysis, the NBO method does not use molecular orbitals directly. Instead, it uses natural orbitals, which are the eigenfunctions of the first-order density matrix. When conducting the analysis the NBO method performs a sequence of transformations, \hat{T} , from a one-center input basis, i.e. Atomic orbitals (AOs), to various localized sets such as Natural Atomic Orbitals (NAOs), Natural Hybridized Orbitals (NHOs), Natural Bond Orbitals (NBOs), and Natural Localized Molecular Orbitals (NLMOs). The localized sets may be subsequently transformed to delocalized Natural Orbitals (NOs) or Canonical Molecular Orbitals (CMOs).



In this transformation sequence the first one ($\hat{T}_{AOs \longrightarrow NAOs}$) is a non-unitary transformation, because the input basis is nonorthogonal, but the other transformation steps ($\hat{T}_{NAOs \longrightarrow NHOs} \dots \hat{T}_{NLMOs \longrightarrow CMOs}$) are unitary. Once the input basis is orthogonalized, each step involves an orthonormal set that spans the full space of the input basis and can be used as an exact representation of the calculated wave function allowing the series of transformations to take place.

The NBO method follows three major steps to carry out the analysis task. The first step is diagonalization of the one electron density matrix to get the natural orbital. The second step is orthogonalization of pre-NAOs; while the last one involves occupancy and charge assignment, and occupancy based classification of the orbitals (core, bonding, anti-bonding, Rydberg etc.).

(i) Diagonalization of the one center (atomic) block

As already mentioned, the NBO method is based on natural orbitals. According to the classical Löwdin sense “Natural” orbitals are derived from properties of the one-particle density operator (Reed A.E., Curtiss, L.A., & Weinhold, F., 1988).

$$\hat{I}(1/1') = N \int \Psi(1,2,\dots,N) \Psi^*(1',2',\dots,N) d\tau_2 \dots d_N \quad (2.53)$$

This equation of \hat{I} can be represented in matrix form based on the AO basis $\{\phi(x_i)\}$ as:

$$\left(\hat{\Gamma}\right)_{i,j} = \int \phi(x_i)^* (l) \Gamma(l/l') \phi(x_j)(l') d\tau_1 d\tau_{l'} \quad (2.54)$$

Therefore, by definition the natural orbitals $\{\phi_i\}$ are the eigenfunctions of the first-order reduced density matrix operator $\hat{\Gamma}$ and expressed as:

$$\hat{\Gamma} \phi_i = \gamma_i \phi_i \quad (2.55)$$

where the eigenvalue γ_i is the occupancy number.

Diagonalization of the above one-center blocks within a molecule leads to a set of “pre-NAOs”, an orthonormal set of orbitals for each atom that are optimal for the atom in its molecular binding environment. As in the pure atomic case, pre-NAOs can be divided into two sets on the basis of their occupancy. The first set is the “minimal” set and corresponds to all atomic (n, l) sub shells of non-zero occupancy in the atomic ground state electronic configuration. The second is the “Rydberg” set which constitutes the remaining (formally unoccupied) orbitals; this set includes all the pre-NAOs whose overlap with adjacent centers increases without limit as the basis set is enlarged.

(ii) Orthogonalization of the pre-NAOs

This step involves orthogonalization of the pre-NAOs in different atoms of a molecule and their conversion to natural atomic orbitals (NAOs). Symmetric orthogonalization of all pre-NAOs would not lead to the desired set, because this would treat the strongly occupied minimal set and the weakly occupied Rydberg set equally. Hence the orthogonalization should be carried out based on the occupancy weight of each set. With the aim of separating the treatment of the two sets of orbitals, a method known as “occupancy weighted symmetric orthogonalization” (OWSO) is introduced. Once the non-orthogonal orbitals are transformed into an orthonormal set, the “OWSO” of the “minimal” set (ϕ_{im}) is carried out as follows:

$$\{\phi_{im}^{(w)}\} = \hat{W} \{\phi_{im}\} \quad (2.56)$$

where \hat{W} is the diagonal weight matrix operator.

Similarly OWSO orthogonalization of the Rydberg set function $\{\phi_{ir}\}$ is performed with the Schmidt orthogonalization step:

$$\{\phi_{ir}^{(s)}\} = \hat{S} \{\phi_{ir}\} \quad (2.57)$$

$$\{\phi_{ir}^{(w)}\} = \hat{W} \{\phi_{ir}^{(s)}\} \quad (2.58)$$

where \hat{S} is the Schmidt operator and the aim of its introduction in this case is to avoid over-counting of electrons which are already accommodated in the minimal set function.

Introduction of the occupancy weighted symmetric orthogonalization treatment plays two major roles. On one hand it preserves the resemblance of the NAOs to their pre-NAO counterparts, and on the other hand, it ensures the stability of the orthogonalization process toward basis set enlargement. The latter role is the secret of NBO's robust nature against any change in basis set, in comparison to the Mulliken and other population analysis methods.

(iii) Occupancy and charge assignment

Once the orthogonalization process of the pre-NAOs is over, the resulting NAOs, $\{\phi_i^N\}$, are obtained as the eigenfunctions of the one-center angular symmetry density matrix blocks on this basis, with the NAO population as their eigenvalues. Accordingly, for a given set of NAOs in atom A (ϕ_i^A), their occupancies (q_i^A), which are diagonal elements of the reduced density operator in the NAO basis, are given as:

$$q_i^A = \langle \phi_i^{(A)} | \hat{\Gamma} | \phi_i^{(A)} \rangle \quad (2.59)$$

This value is non-negative and obeys the Pauli exclusion principle:

$$0 \leq q_i^A \leq 2 \quad (2.60)$$

Summation of the occupancies q_i^A gives the total number of electrons N_A :

$$N_A = \sum_i q_i^A \quad (2.61)$$

Based on the total number of electrons N_A and the atomic number of atom A (Z_A), the 'natural' charge on atom A is given as:

$$Q_A = Z_A - N_A \quad (2.62)$$

In a similar way, calculations of occupancy and charge can be carried out for all atoms in a given molecule. Then, based on the occupancy weighted values, a classification of the orbitals can be made. Therefore, one-centered NAOs of high occupancy, i.e. near to 2 ($>1.99e$), are referred to unhybridized core orbitals K_A , and orbitals with occupancy values that exceed the paired electron threshold ($\rho_{\text{thresh}} = 1.90$) are referred as lone pairs, n_A , in the case of one-centered blocks and bond pairs, δ_{AB} , in the case of two-centered blocks.

Each bond pair (δ_{AB}) is decomposed into its normalized hybrid contributions, h_A and h_B , in each atom and hybrids from each center participating in different bonds are symmetrically orthogonalized to remove intra-atomic overlap during the orthogonalization process. This gives rise to a bond (δ_{AB}) and anti-bond (δ_{AB}^*) in the NBO basis:

$$\delta_{AB} = c_A h_A + c_B h_B$$

$$\delta^*_{AB} = c_B h_A - c_A h_B \quad (2.63)$$

The set of localized electron pairs $(K_A)^2 (n_A)^2 (\delta_{AB})^2 \dots$, found in this way constitutes a “natural Lewis structure”, which describes the system. The accuracy of the Lewis structure obtained may be assessed by the total occupancy ρ_{Lewis} of its occupied NBOs, which is commonly found to exceed 99.9% of the total electron density for ordinary molecules. The best NBO structure is that corresponding to the largest overall ρ_{thresh} value and is generally found to agree with the pattern of bond and lone pairs of the standard Lewis structural formula.

Since application of the NBO method of analysis makes no special reference to the form of the wave function or density, it can be used to compare results from arbitrary levels of semi-empirical, *ab initio* and DFT methods. For this reason, the NBO method is user friendly for many chemical systems.

2.7.3 The Natural Resonance theory analysis (NRT)

Natural resonance theory is a new quantum mechanical technique which is mainly used to quantitatively determine the possible resonance forms molecules attain. This method is based on the first-order reduced density matrix (Eq. 2.53). Since this method gathers its information from the reduced density matrix, it is applicable to any *ab initio* or semi-empirical wave functions, density functional, or perturbation method for which a density matrix is available. When the reduced density matrix approximated in resonance-average form it is described as:

$$\hat{\Gamma} = \sum_{\alpha} \omega_{\alpha} \hat{\Gamma}_{\alpha} \quad (2.64)$$

$$\omega_{\alpha} \geq 0, \quad \sum_{\alpha} \omega_{\alpha} = 1 \quad (2.65)$$

where Γ_{α} is an idealized first-order density matrix of resonance structure α ; and ω_{α} is its resonance weight value.

Since it can determine resonance qualitatively, the NRT method is comparatively superior to the Pauling-Wheland (PW) classical resonance theory, which is limited to qualitative resonance representation. Therefore NRT gives results, which are in qualitative accord with conventional resonance theory and chemical intuition.

The resonance weights in NRT are obtained by solving the non-linear least squares optimization of the weak and strong delocalizations that are respectively described as:

$$d(W) = \min \{ \omega_{\alpha} \} \left[\frac{1}{n_{\text{bas}}} \sum_K (q_K - \bar{q}_K)^2 \right]^{1/2} \quad (2.66)$$

and

$$D(W) = \min \{ W^{(r)} \} \left\| \hat{r} - \sum_r W^{(r)} \hat{r}^{(r)} \right\| \quad (2.67)$$

where in the first equation q_K describes the NBO occupancies of the one-particle wave function, and \bar{q}_K is the corresponding resonance weight density operator. In Eq. (2.67), $r^{(r)}$ describes a selected reference structure and $W^{(r)}$ is the resonance weight of the selected structure.

After both optimizations are made, the composite resonance weight is obtained as:

$$\omega_\alpha = \sum_r^{n_{ref}} W^{(r)} \omega_\alpha^{(r)} \quad (2.68)$$

Once obtained, the resonance weight (ω_α) can be used to calculate natural bond order, natural atomic valence, and other atomic and bond indices, which reflect the resonance composition of the wave function.

Besides offering quantitative resonance results and putting resonance theory into the mainstream of *ab initio* studies, the NRT method also plays a great role in the systematic treatment of bond order and atomic valency terms. In this treatment both the bond order and atomic valency are expressed in terms of electrovalent and covalent contributions. This allows NRT to be uniformly applicable to a wide variety of organic and inorganic molecules. Therefore such systematic treatment of NRT is helpful to analyse bond order and atomic valency terms of diverse system based on the comparisons made on their electrovalent and covalent contributions.

2.8) IR studies

2.8.1) Experimental IR studies

Infrared spectroscopy is one of the commonly used spectrometric methods of analysis. It deals with the interaction of infrared radiation with matter. Since covalently bonded organic or inorganic compounds absorb various frequencies of electromagnetic radiation, which lie in the infrared region, infrared spectroscopy is a very important tool for the study of chemical nature and structural elucidation of many compounds.

In the electromagnetic spectrum, the IR region lies in the wave number range of 12,900 to 10 cm^{-1} . This region is further divided into three sub-regions namely, the near-infrared region (12,900-4000 cm^{-1}), the mid-infrared region (4000-200 cm^{-1}) and the far-infrared region (200-10 cm^{-1}). Among these sub-regions more attention is given for the mid-infrared region in the study of acylthiourea compounds in this project.

Effect of the IR radiant energy is on the order of vibration transition. Hence when atoms and molecules absorb such radiation, they get excited from a lower vibrational state, which is the ground state to higher states. However such vibrational transitions are not take place randomly, but they are governed by some quantum mechanical restrictions.

2.8.1.1) Requirements for IR absorption

The selection rule for IR frequency absorption can be determined by evaluating the transition moment, R . This moment refers to the electric dipole transitions involving the first-order interaction of the oscillating electric vector of the radiation field with the electric dipole moment of an atom or molecule. Beside this, radiative transition can also arise due to the interaction of the radiation field with electric quadrupole moment or magnetic dipole moment. However these second order effects are extremely weak compared with the first order electric dipole transition.

Transition moment R is calculated from wave function as,

$$R = \int \psi_i^* \mu \psi_j d\tau \quad (2.69)$$

for a transition between states i and j where μ is the electric dipole moment operator and $d\tau$ indicates the integration over all space.

As mentioned earlier the transition between certain energy levels are not done at random, however it depends on some selection rules. In Eq. (2.69) above, if the wave functions have symmetry it lead to zero R value and the vibrational transitions in this case are forbidden. On the other hand if R is finite the transitions involved are allowed transitions.

For vibrational motion, the electric dipole moment μ can be expressed as,

$$\mu = \mu_0 + (r - r_e) \left(\frac{\partial \mu}{\partial r} \right)_0 + \frac{1}{2} (r - r_e)^2 \left(\frac{\partial^2 \mu}{\partial r^2} \right)_0 + \dots \quad (2.70)$$

where μ_0 is the permanent dipole moment, r is the internuclear distance, and r_e is the equilibrium bond distance. Neglecting all but the first two terms of Eq. (2.70) and substituting it in Eq. (2.69) after simplification gives.

$$R = \int \psi_i^* [(r - r_e) \left(\frac{\partial \mu}{\partial r} \right)_0] \psi_j d\tau \quad (2.71)$$

As Eq. (2.71) show there must be a change in dipole moment during the vibration in order for a molecule to absorb infrared radiation.

When bonds of a molecule undergo displacement from their equilibrium bond distance, r_e , these motions are considered as harmonic oscillation. Due to quantum mechanical restrictions such molecule can assume only certain value of vibrational energy. From the Schrödinger equation for a harmonic oscillator, the allowed energy levels are given by,

$$E(V) = h\nu \left(V + \frac{1}{2} \right) \quad (2.72)$$

where V is the vibrational quantum number, whose value may be $V = 0, 1, 2, \dots, v$, ν is the vibrational frequency in Hertz, and h is Planck's constant.

Expressing the energy value in Eq. (2.72) in terms of wave number unit, which is called term values, T , gives:

$$T(V) = \acute{\nu} \left(V + \frac{1}{2} \right) \quad (2.73)$$

where ν , is vibrational frequency in terms of wave number (cm^{-1}). That is $\nu = 1/\lambda$, where λ is wavelength in cm.

Eq. (2.73) gives many equally spaced energy levels (**fig. 2.4**). Therefore the basic quantum mechanical selection rule for a harmonic oscillator limits vibrational energy transition between adjacent states only, that is $\Delta V = \pm 1$. The transition from the ground state to the next quantum number i.e. $V = 0$ to $V=1$ is called fundamental absorption, while much weaker overtone absorptions correspond to $V = \pm 2$ and so on.

The transition moment R is very useful not only to determine the selection rule, but also peak intensity. Therefore the intensity of a vibrational band in the infrared spectrum depend on square of the transition moment, R , and as Eq. (2.71) show also on that of dipole moment.

2.8.1.2) Numbers of vibrational modes

As stated earlier effect of the IR radiant energy is on the order of vibrational transition. Hence the IR is part of the vibrational spectroscopy. Therefore even though all molecules undergoes three kind of motions, namely translation, rotation and vibration over the entire range of real temperature above absolute zero, here more attention is given to the vibrational modes.

Any molecule composed of N atoms possesses $3N$ numbers of degree of freedom of motion. Where 3 stands for the three Cartesian coordinates (x, y, z), along which an atom undergoes its motion. These degree of freedom are sum of the translational, rotational, and vibrational motions. Therefore the total numbers of normal modes of vibrations of a molecule are obtained by subtracting the non-vibrational motions from the total numbers of degree of freedom ($3N$). According to this fact, linear polyatomic molecules undergo three translational and two rotational motions; therefore they possess $3N-5$ vibrational modes. Non-linear molecules on the other hand undergo three translational and three rotational motions, therefore these molecules possesses $3N-6$ normal vibrational modes.

The predictions made on the numbers of vibrational modes above however didn't always hold true. This is because some transitions are forbidden, or two or more modes may be degenerate and thus have the same vibrational frequency, causing decrease in the numbers of expected normal modes of vibrations. On the other hand even additional bands can occur due to overtones.

2.8.1.3) Instrumentation

Currently three different instruments are being used for IR analysis namely, dispersive IR spectrometers, Fourier transform IR (FTIR) spectrometers, and nondispersive IR spectrometers. Dispersive spectrometers are used for the mid-IR region for spectral scanning and qualitative analysis. FTIR spectrometers are widely applied in the far-IR as well as in the mid-IR regions. Non-

dispersive spectrometers are often used for gas analysis at specific wavelengths. Among these instruments the modern and fast FTIR spectrometer is used for this project.

2.8.1.4) Sample preparation

Since almost all substances at certain wavelength absorb the IR radiation, when preparing samples for IR analysis, cell window materials, cell pathlengths, and solvents must be carefully chosen for the wavelength and sample of interest. As outcomes of many studies made, today there are a number of techniques of preparation for a wide variety of samples such as gases, pure liquids, solutions, films as well as solids.

In this project a solid sample is being analysed. There are three well-known methods of preparation of solid samples. The first one is by mixing some grounded grains of the compound of interest with KBr powder and preparing KBr pellet. The second is by dissolving the solid sample in mineral oil (nujol), and the third by dissolving the solid sample in carbon tetrachloride (CCl₄). The last two methods have limitations because the solvents absorb some of the IR radiation and obscure some bands of the sample under analysis. However the first method have no such interference problem. For this reason samples of this project are prepared as KBr pellets.

2.8.2) Calculated IR studies

In the study of vibrational state of a compound experimentally, assignment of each vibrational motion to their respective peaks is quite difficult. This happens due to the existence of large numbers of closely spaced peaks even in a very simple molecule. However currently such problems are being tackled by the introduction of computer simulations to calculate vibrational frequencies of molecules. These calculated frequencies are accompanied with animation of each vibrational motions, this therefore considerably simplify the peak assignment task.

Computation of vibrational frequencies can be carried out using two methods of approximations, namely harmonic and anharmonic oscillator approximations. The harmonic oscillator approximation considers the displacement bonded atoms undergo away from their equilibrium distance (r_e) as a harmonic motion (periodic motion of a point mass m connected to a mass less spring, or that of a pendulum with small amplitude.). This approximation is based on the Hook's law, and the potential energy curve in this approximation varies parabolically as a function of displacement. After treated based on quantum mechanical restriction this approximation gives equally spaced energy separation (**fig. 2.4**). This treatment works fairly well only near the internuclear distance (r_e). The anharmonic oscillator approximation on the other hand states that the variation of potential energy of a system with internuclear distance usually is not a symmetric

parabola, but it rather has an appearance of a Morse curve. The energy separation in this case is progressively decline as the quantum number rise (**fig. 2.4**).

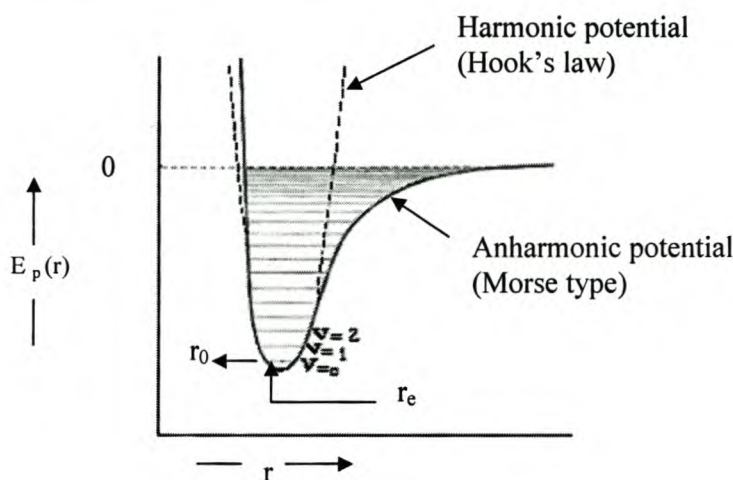


Fig. 2.4 The harmonic and anharmonic potential energy versus displacement curves for a diatomic molecule. As the curves show in the harmonic approximation the energy separation gap is equal in each successive quantum numbers, however in case of the anharmonic approximation the energy gap declines progressively as the quantum number ascend.

Unlike the harmonic one, the Morse potential works very well for all internuclear distance. Therefore the anharmonic oscillator approximation is more realistic than the harmonic approximation. However since the anharmonic oscillator approximation require large amount of CPU time, it is seldom used. For this reason the harmonic oscillator approximation is widely used.

Due to the abovementioned approximations made, calculated frequency values are always deviated from the experimentally obtained frequency values. For example a frequency calculation carried out using the HF level of theory and a quantum harmonic oscillator approximation shows a 10% higher frequency value than experimentally obtained frequency value (James, D. I. Jr.; Stanley, R.C. 1988). This deviation is aroused due to the harmonic approximation made and due to failure of the HF level of theory to consider the electron correlation. Therefore to remedy this deviation, the calculated frequency values should be multiplied by a scaling factor. In this project a 6-31G(d) basis set at HF level of theory is used for the frequency calculations, hence to convert them to their respective experimental frequency values, the calculated frequencies are multiplied with a scaling factor of 0.8929.

Therefore in carrying out frequency calculations using different level of theories, and approximations, different scaling factors are used to convert these frequency values to their experimentally obtained frequency counterparts. Currently many researches are being made to introduce scaling factors even to the different vibrational modes of molecules (stretching, bending, etc...); these efforts are expected to narrow the gap that exists between the scaled calculated and experimentally obtained frequency values.

Chapter Three

Modelling Substituted Acylthiourea Compounds

3.1 Introduction

As already stated in **chapter one**, substituted acylthiourea compounds have a wide range of applications. For this reasons many experimental studies have been conducted on them. However from a theoretical aspect, sufficient studies were not performed until very recently, when some progress was made. One of the theoretical studies of these compounds was on the alkylation of 3, 3-disubstituted benzoyl thiourea (Plutin, A.M., et al., 2000). As many experimental studies show these compounds form polydentate ligands which are endowed with three different nucleophilic centers sited at the S, O and N atoms (Rodríguez, Y., et al., 1988). These studies also prove that the alkylation preferentially takes place at the sulphur atom, however they do not explain why. The main purpose of the theoretical study of Plutin et al. was thus to explain this observation. The work was based on calculations using *AMI* and *PM3* semi-empirical methods, and proved that the S atom has a high contribution to the HOMO energy of the compound studied, hence this result was able to quantitatively explain the reason behind the preferential alkylation of sulphur.

The optimum energy structures of the compounds obtained using the above mentioned computational methods, were called '*quasi-S*' conformers, i.e. conformers with *trans* oriented carbonyl and thio-carbonyl groups (Plutin, A.M. et al., 2000). In the calculated structures the S atom was found to be less hindered than the O and N atoms and more exposed to alkyl attack, hence even the geometries obtained qualitatively explain the reason behind the preferential alkylation of the S atom.

Another computational study using the 6-31G (d) basis set at the Hartree-Fock level of theory involved the conformational analysis of 3, 3-disubstituted benzoyl thiourea (Albertus, M.S. & Piri, M., 2001). This study was carried out on compounds with substituent groups that are different to the previous study. This study further confirms that the '*quasi-S*' conformation is the most stable one.

Even though the abovementioned studies are good news as a starting point for theoretical studies on substituted acylthiourea compounds, because they were restricted to only benzoyl thiourea compounds, they were not comprehensive enough. Hence with the aim of expanding the study to a wider range of substituted acylthiourea compounds and then analyzing different properties of them, such as the nature of their C-N bonds, the current project involved carrying out quantum mechanical studies on a wider range of compounds. Therefore this chapter comprises extensive quantum mechanical calculations of substituted acylthioureas with different levels of complexity. **Section 3.2** contains a brief discussion of tautomers of acylthiourea compounds. The modelling of proton and methyl substituted compounds is discussed in **section 3.3**. Then follows an

molecule, the conformational energy can be calculated using *ab initio*, semi-empirical or molecular mechanics methods. Selection of the appropriate method primarily depends on the size of the system, and the required accuracy of the calculated energies. Tautomers of proton and methyl substituted acylthioureas, which are the topic of interest, are not very complex. Taking this fact into consideration an *ab initio* method of calculation, which is the most accurate of the methods, was chosen for their analysis.

3.3.1 Computational Procedure

In modelling proton and methyl substituted tautomers, as in the case of the other substituted acylthioureas under study, all the calculations were made using a 6-31G (d) basis set (Ditchfield, Hehre and Pople, 1971; Hehre, Ditchfield and Pople, 1972; Hariharan and Pople, 1973; Gordon, 1980; Hariharan and Pople, 1974) at the Hartree-Fock level of theory. As was discussed earlier, the Hartree-Fock level of theory is accurate enough for calculations of medium sized molecules (**section 2.2**); hence since substituted acylthioureas are in this size range it was the optimal choice. The Pople type basis set was chosen because this split valence basis set is very effective for qualitative calculations on medium sized molecules (**section 2.3.2**).

During the search for the global minimum energy conformer, a random starting geometry was taken for a specific tautomer. To get as many conformers as possible, rotations around some selected bonds of the starting geometry were carried out. The rotations were made in the range of 0° to 360° ; and once all the possible conformers were obtained and their energy minimized, frequency calculations were also performed.

Finally, based on their energy and frequency values, the various energy optimized conformers were categorized into different stationary points. According to this categorization, stationary points with no imaginary frequencies are minimum energy conformers, stationary points with only one imaginary frequency are real transition state conformers, and those with more than one imaginary frequency are maximum energy conformers (Foresman, J.B., & Frisch, A.E., 1996).

3.3.2 Results and discussion

As already discussed earlier, a search for the global minimum energy conformer is a multi-step process. For this reason a thorough analysis of all possible conformers of the molecules of interest is essential. Therefore, to simplify the search, drawing a full conformational map of the compound under consideration is an important step. Once the map is drawn, it is relatively easy to pick up the global minimum energy structure. A typical example of such a map is that for the proton substituted tautomer (**i**) given in **fig. 3.2** below.

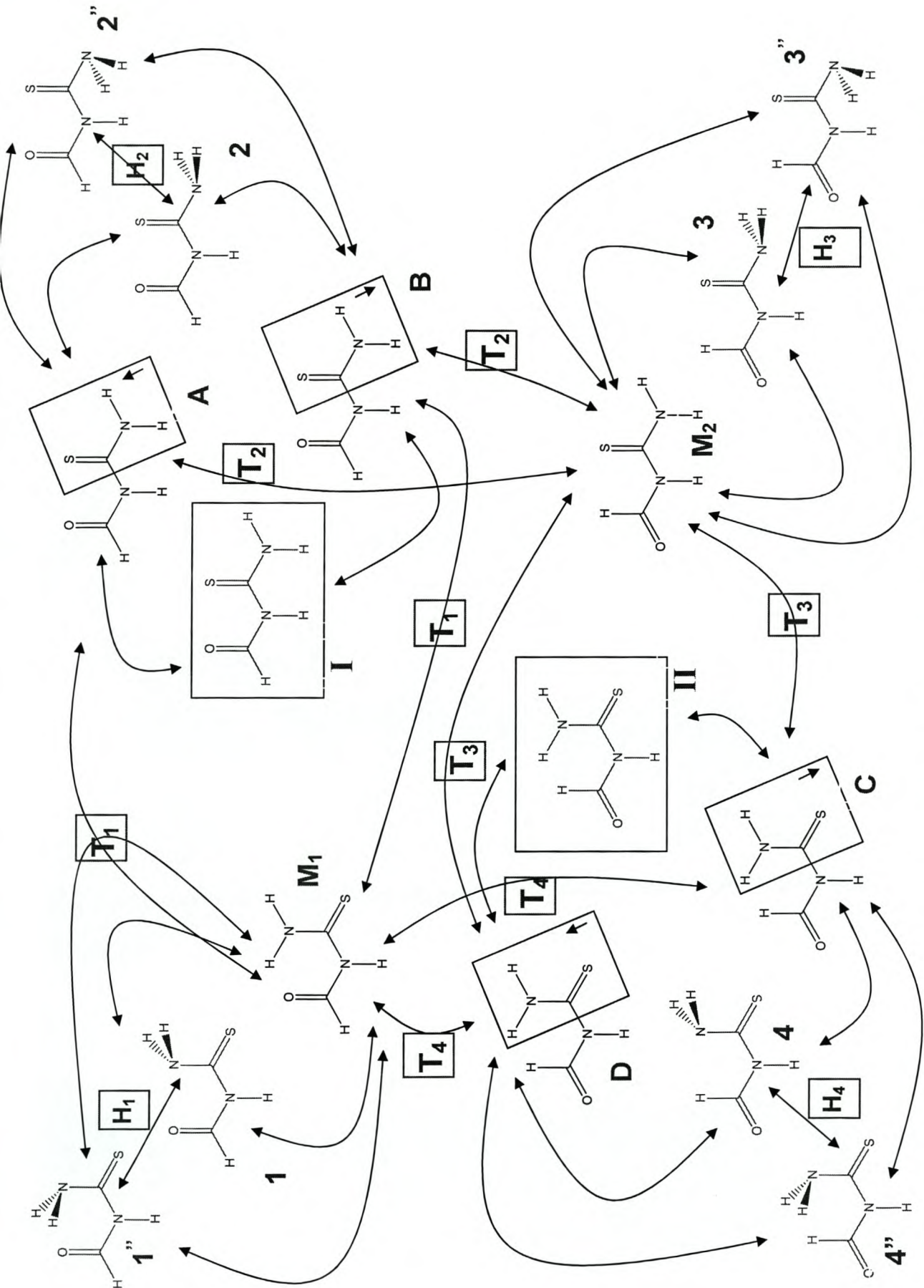


Fig 3.2 Conformation map of proton substituted acylthiourea compound, where T_n are transition states and H_n are hill top (saddle point) conformers.

The conformational map of a proton substituted acylthiourea tautomer (**i**) described in **fig. 3.2** above comprises many conformers. Due to the limitation in space and for clarity some of the conformers are represented using either numbers or letters, with the 3D pictures of these conformers available in **addendum A**. The energies, lowest frequencies, and a description of each conformer are given in table 3.1 below.

Table 3.1 Energy, lowest frequency values and stationary point descriptions of conformers of proton substituted acylthiourea tautomer - (i). (1 Hartree = 627.51Kcal/mol = 2226 KJ/mol)

Conformer	Optimum energy (Hartree)	Lowest wavenumber (cm ⁻¹)	Stationary point assignment
M₁	-659.3605	105.4	GM
M₂	-659.3531	142	LM
I	-659.3358	-137.4	TS
II	-659.3488	-119.5	TS
A	-659.3361	62.7	LM
B	-659.3361	62.1	LM
C	-659.3492	104.4	LM
D	-659.3492	104.6	LM
T₁	-659.3313	-131.3	TS
T₂	-659.3261	-245.5	TS
T₃	-659.3344	-184.3	TS
T₄	-659.3288	-264.4	TS
1	-659.3194	-520.0	TS
2	-659.3210	-364.8	TS
3	-659.3329	-391.3	TS
4	-659.3327	-382	TS
1''	-659.3216	-433.4	TS
2''	-659.3069	-407.9	TS
3''	-659.3206	-438.3	TS
4''	-659.3186	-409.2	TS
H₁	-659.3107	-791.7, -721.4	SP
H₂	-659.3052	-781.3, -567.7	SP
H₃	-659.3181	-780.0, -610.3	SP
H₄	-659.3175	-759.8, -585.7	SP

* GM = Global minimum; LM = Local minimum; TS = Transition state; SP = Saddle point (Hill top)

The above conformational map not only helps in detecting the global minimum energy structure, but also provides a lot of other valuable information. For instance, it can be used to calculate the energy barrier between two conformers; it can also give the experimentally unexplored transition state structures of the molecules etc. Therefore it is very informative to use these maps when conformational studies are done.

Once conformational analysis of all proton substituted tautomers had been carried out, comparisons were made between energy values of all minimum energy conformers of each tautomer, which was obtained through energy minimization of a variety of starting geometries. From this the following structures were found to be global minimum energy conformers of the three proton substituted acylthiourea tautomers.

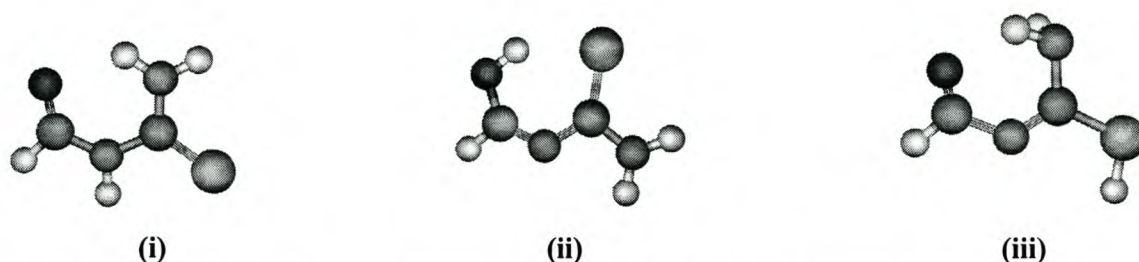


Fig. 3.3 Minimum energy conformers of proton-substituted acylthiourea tautomers. Oxygen indicated with red, sulphur with yellow, nitrogen with blue, carbon with grey and hydrogen with white.

Energy values of the global minimum energy structures of each tautomer shown in **fig. 3.3** above are recorded in table 3.2 below.

Table 3.2 Energy values of the global minimum energy structures of proton substituted acylthiourea tautomers.

Tautomer	Energy (Hartree)	Lowest wavenumber (cm ⁻¹)
(i)	-659.3605	105
(ii)	-659.3367	66.9
(iii)	-659.3326	115.2

1 Hartree = 627.51 Kcal/mol = 2226 KJ/mol

A comparison of the global minimum energy values of the three proton substituted tautomers listed in Table 3.2 shows that the tautomer with an energy value of -659.3605 Hartree has the lowest energy value and hence is the most stable one.

After a similar conformational analysis was conducted on each methyl substituted acylthiourea tautomer, the following three global minimum energy conformers for the three tautomers were obtained.

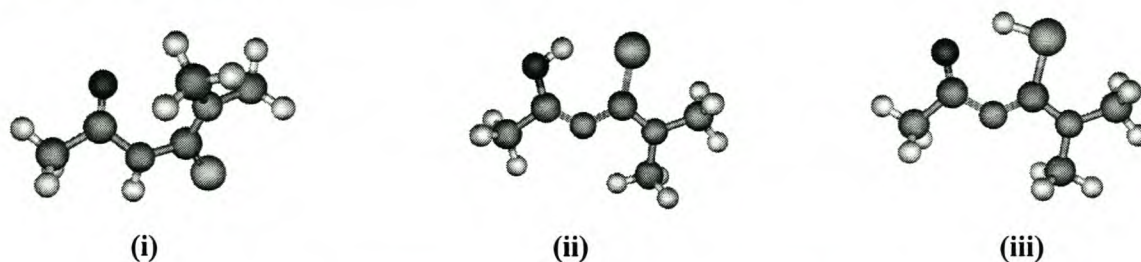


Fig. 3.4 Minimum energy conformers of methyl-substituted acylthiourea tautomers. Oxygen indicated with red, sulphur with yellow, nitrogen with blue, carbon with grey and hydrogen with white.

Table 3.3 Energy values of global minimum energy structures of methyl substituted acylthiourea tautomer.

Tautomer	Energy (Hartree)	Lowest wavenumber (cm ⁻¹)
(i)	-776.4472	78
(ii)	-776.4360	31.2
(iii)	-776.4257	18.6

1 Hartree = 627.51Kcal/mol = 2226 KJ/mol

Comparison of the global minimum energy values of the three methyl substituted acylthiourea tautomers listed in Table 3.3 shows that the conformer with an energy value of -776.4472 Hartree is the most stable.

As can easily be seen from the comparisons made above, the most stable tautomer in both proton and methyl substituted compounds is the trans oriented carbonyl and thio-carbonyl moieties bearing tautomer (i). To confirm this observation, further comparisons of the energies of transition states, saddle points, and other corresponding conformers of the three tautomers in both proton and methyl substituted compounds, verify that tautomer (i) is the most stable form. In the intensive literature search made for substituted acylthiourea compounds, no compound was found in the form of tautomers (ii) and (iii). Therefore based on these observations, it is assumed that the most stable of all tautomers of acylthiourea compounds is tautomer (i), and hence they all exist preferentially in this form.

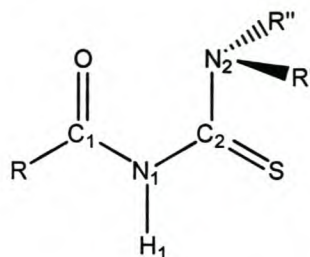


Fig. 3.5: General structure of the most stable acylthiourea tautomer.

Having identified the most stable acylthiourea tautomer, all the further computational and infra-red, studies, in plan to be made will be conducted based on this tautomer.

3.4 Modeling selected substituted acylthiourea compounds

3.4.1 Introduction

One of the primary tasks for this project was the establishment of the general structure of the most stable conformations of various acylthioureas. Having started with the simple proton and methyl substituted compounds, the study was broadened by further considering compounds bearing substituents of relatively high complexity; in order to have a reasonable number of representative compounds. For this purpose twelve compounds, namely N-pivaloyl-N'-pyrrolidine thiourea (**A**), N-(2,6-dimethylpiperidine)-N'-(3,4,5-methoxy) benzoyl thiourea (**B**), N-diethyl-N'-pivaloyl thiourea (**C**), N,N-dibutyl-N'-pivaloyl thiourea (**D**), N,N-diethyl-N'-benzoyl thiourea (**E**), N,N-dibutyl-N'-benzoyl thiourea (**F**), N-(n-butyl)-N'-benzoyl thiourea (**G**), N-(n-Propyl)-N'-benzoyl thiourea (**H**), N-(p-hexoxy)aniline-N'-(p-ethoxy)benzoyl thiourea (**I**), N-di(n-butyl)-N'-naphthoyl thiourea (**J**), N,N-di(2-hydroxyethyl)-N'-benzoyl thiourea (**K**), and N,N-diethyl-N'-4-nitrobenzoylthiourea (**L**) were selected.

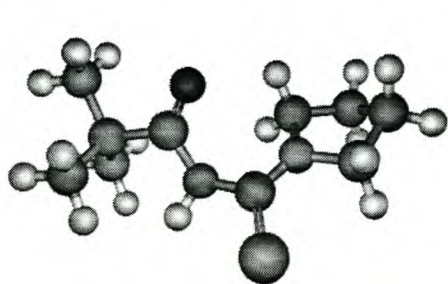
The other important objective of this project is the verification of the experimentally observed shortening of one of the C-N bonds of acylthiourea compounds (Dago, A., et al., 1989; Fajardo, F., et al., 1990). Before making any generalizations regarding these observations it is necessary to make a broad and careful study, on a reasonable number of representative compounds. Even though conducting the study with such a wide range of representative compounds is tedious, it is rewarding as it helps to make reasonable deductions regarding the properties of substituted acylthiourea compounds.

3.4.2 Computational procedure

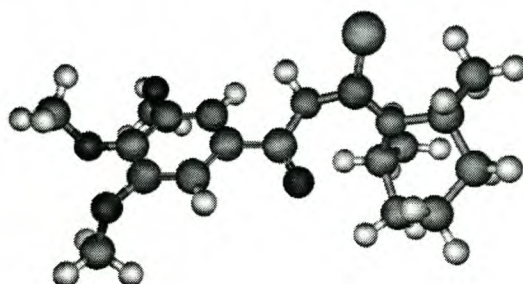
Conformational analysis of the selected compounds was carried out using the same basis set and level of theory as used for the proton and methyl substituted acylthioureas. Following the same procedure discussed in **section 3.3.1**, rotations were carried out along selected torsion angles such as, C'-C₃-C₁-O, O-C₁-N₁-C₂, C₁-N₁-C₂-S, and S-C₂-N₂-C''. In order to find all possible starting geometry conformers in some cases the rotations around two bonds were carried out simultaneously. These rotations, which were carried out in the range 0⁰-360⁰, at intervals of 45⁰, yielded a large number of starting geometries. After energy minimizations were carried out on all of them, many starting geometries were found to give the same minimum energy conformer. Therefore the final comparison made between the different minimum energy conformers enabled the selection of the global minimum energy conformer of each compound.

Result and discussion

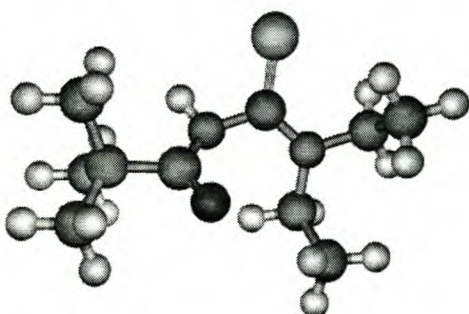
Once the lengthy conformational analyses of all the selected compounds had been completed, the global minimum energy structures of each compound were found as shown below.



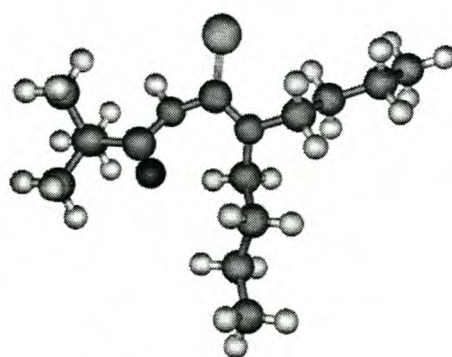
(A)



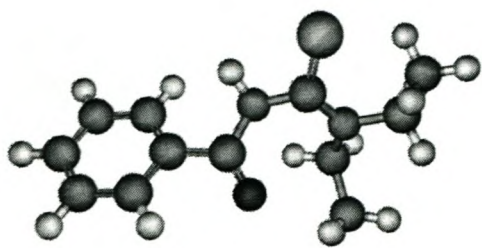
(B)



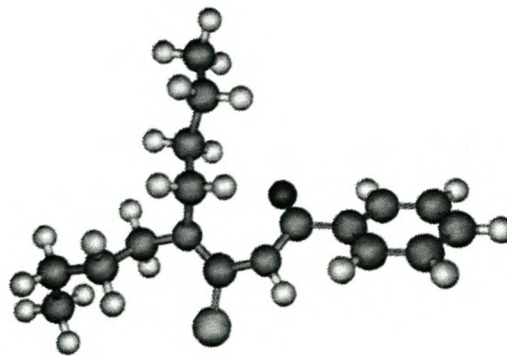
(C)



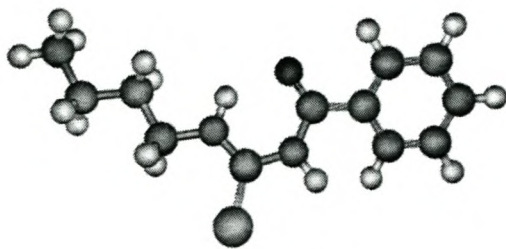
(D)



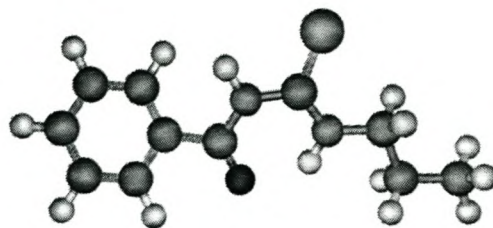
(E)



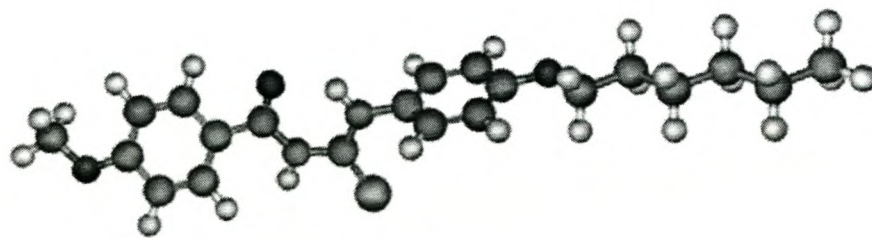
(F)



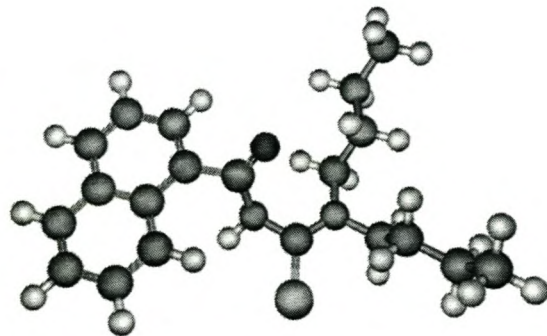
(G)



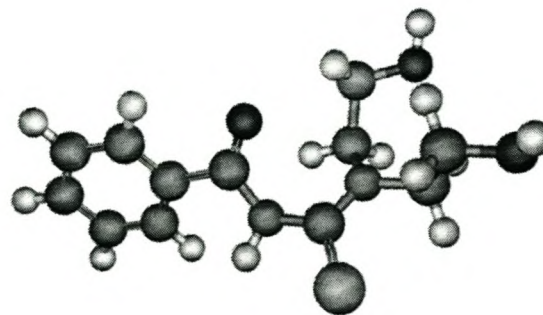
(H)



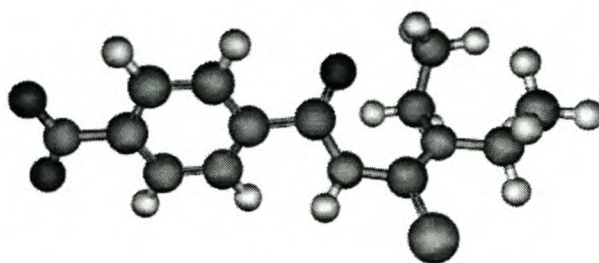
(I)



(J)



(K)



(L)

Fig. 3.6 The most stable (global minimum energy) structures of: (A) *N*-pivaloyl-*N'*-pyrrolidine thiourea, (B) *N*-(2,6-dimethyl-piperidine)-*N'*-(3,4,5-methoxy)benzoyl- thiourea, (C) *N,N*-diethyl-*N'*-pivaloyl thiourea, (D) *N,N*-dibutyl-*N'*-pivaloyl thiourea, (E) *N,N*-diethyl-*N'*-benzoyl thiourea, (F) *N,N*-dibutyl-*N'*-benzoyl thiourea (G) *N*-(*n*-butyl)-*N'*-benzoyl-thiourea, (H) *N*-(*n*-propyl)-*N'*-benzoyl-thiourea, (I) *N*-(*p*-hexoxy)aniline-*N'*-(*p*-ethoxy)benzoyl-thiourea, (J) *N,N*-di-(*n*-butyl)-*N'*-naphthoyl-thiourea, (K) *N,N*-di(2-hydroxyethyl)-*N'*-benzoyl-thiourea, and (L) *N,N*-diethyl-*N'*-4-nitrobenzoyl-thiourea, molecules. In all structures, oxygen indicated with red, sulphur with yellow, nitrogen with blue, carbon with grey and hydrogen with white.

The optimum energy and lowest frequency values of the global minimum energy structures of the acylthioureas shown above are listed in table 3.4 below.

Table 3.4 Optimum energy and lowest frequency values of the most stable calculated structures of the substituted acylthiourea compounds under investigation. (1 Hartree = 627.51Kcal/mol = 2226 KJ/mol)

Compound	Optimum energy (Hartree)	Lowest Wavenumber (cm ⁻¹)	Compound	Optimum energy (Hartree)	Lowest wavenumber (cm ⁻¹)
A	-970.4696	25.8	G	-1045.0554	24.6
B	-1502.5970	20.5	H	-1006.0207	29.5
C	-971.6180	26.2	I	-1541.3974	4.6
D	-1127.7567	24	J	-1353.8121	19
E	-1045.0284	36.3	K	-1194.7220	32.8
F	-1201.1656	26.9	L	-1248.4956	28.4

The above energies were found to be the lowest among those of many other possible conformers of each compound. For instance in compound **A**, twenty-one starting geometries were initially obtained by rotations around selected torsion angles; upon energy minimization five minimum energy structures were obtained, while the remaining structures were either transition states or maximum energy conformers. Finally, comparison of the five minimum energy structures gives rise to the global minimum energy structure of compound **A** listed above, which has an energy value of -970.4696 Hartree. Global minimum energy values of the other compounds were also obtained in the same way.

An interesting point to note about the data in the above table is that the lowest frequency values of the compound are all non negative and hence the molecules have no imaginary frequency values; this is a clear indication of being at an energy minimum. A detailed discussion of the vibrational spectra will be made in the next chapter.

Having obtained the most stable structures it is time to look for trends in the molecular geometry. As can be seen from **fig. 3.5**, the compounds attain their most stable energy structures through avoidance of steric hindrance. Since the compounds have substituents of different complexity, the manner in which they reduce steric hindrance in their stable structure differs accordingly. For instance the most stable structure of proton substituted compound is planar, however when the substituents get larger the stable structures spread in 3D space with various torsion angle values. Despite such differences, the compounds have one common trend in the orientation of their carbonyl and thio-carbonyl groups. As the calculated optimum energy structures of each show the carbonyl and thio-carbonyl moieties are always oriented *trans* to each other. Since this trend is observed in both mono-alkyl (G, H, I), and di-alkyl (A, B, C, D, E, F, J, k, & L) substituted compounds it is fair to generalize saying that all optimum energy structures of substituted acylthiourea compounds have *trans* oriented carbonyl and thio-carbonyl moieties. One early theoretical work (Albertus, M.S., & Piris, M., 2001) also reported a similar result; therefore the generalization made here is reasonable.

Having successfully answered the stability question, the next task is analysis of the internal coordinates of the calculated optimum energy structures. The main purpose of this analysis is to confirm whether the experimentally reported shortening of one of the C-N bonds of substituted acylthiourea compounds (Koch et al., 1995) holds true in the calculated structures as well. Therefore bond lengths, valence angles, and dihedral angles of the calculated structures are recorded in table 3.5 below.

Table 3.5 Some selected internal coordinates of the calculated minimum energy structures of substituted acylthioureas (A-L).

<i>Internal coordinate</i>	Compound					
	A	B	C	D	E	F
Bond (Å)						
C(3)-C(1)	1.536	1.497	1.536	1.536	1.497	1.497
C(1)=O	1.193	1.195	1.193	1.193	1.194	1.194
C(1)-N(1)	1.388	1.386	1.387	1.387	1.387	1.386
N(1)-C(2)	1.401	1.412	1.406	1.407	1.406	1.407
C(2)-S	1.682	1.682	1.684	1.686	1.683	1.684
C(2)-N(2)	1.314	1.322	1.320	1.320	1.321	1.320
Valence angle (°)						
C(3)C(1)O	122.8	122.1	122.9	122.8	122.1	122.1
C(1)N(1)H	114.8	113.3	114.3	114.2	113.5	113.5
C(1)N(1)C(2)	125.4	122.6	125	125.4	124.6	125
SC(2)N(2)	125	126.2	125.6	125.6	125.6	125.7
Dihedral angle (°)						
C'C(3)C(1)O	9.7	22.4	-10.1	-10.4	21.7	-22
OC(1)N(1)C(2)	15.6	-14.8	-20.3	-20	-12	12.1
C(1)N(1)C(2)S	124.5	-115.1	-121.5	-120.6	-121.3	121.5
SC(2)N(2)C''	-5	10.8	6.2	5.1	4.9	-4.7

Bond (Å)	Compound					
	G	H	I	J	K	L
C(3)-C(1)	1.496	1.496	1.489	1.504	1.497	1.504
C(1)=O	1.202	1.202	1.203	1.194	1.195	1.192
C(1)-N(1)	1.374	1.374	1.377	1.382	1.384	1.381
N(1)-C(2)	1.388	1.387	1.386	1.407	1.407	1.410
C(2)-S	1.681	1.680	1.676	1.685	1.681	1.680
C(2)-N(2)	1.314	1.314	1.323	1.319	1.324	1.320
Valence angle						

(^o)						
C(3)C(1)O	121.6	121.6	121.7	122.2	122	121.4
C(1)N(1)H	118.2	118.2	118.1	114.8	113.8	114
C(1)N(1)C(2)	129.6	129.6	130	125.8	125	124
SC(2)N(2)	125.3	125.3	126.2	125.6	125.8	126
Dihedral angle (^o)						
C'C(3)C(1)O	24.2	24.2	19.2	51.4	-22	-24.1
OC(1)N(1)C(2)	4.2	4.2	4.3	22.3	12.8	13.4
C(1)N(1)C(2)S	180	180	-179.5	122.4	123	121.9
SC(2)N(2)C''	-0.2	-0.2	-0.0	-6	-5	-6

* N.B: C(3) is the carbon atom of the substituent **R** attached to C(1); C' is the carbon atom of **R**, that forms the smallest C'-C(3)-C(1)-O dihedral angle; C'' is the carbon atom of either **R'** or **R''**, that is attached to N(2) and forms the smallest C''-N(2)-C(2)-S dihedral angle. Labelling of the other atoms is available in **fig. 1.1**.

As can be seen from the internal coordinate data above, all the C(1)-N(1) bonds of the optimum energy structures are of intermediate length; the C(2)-N(1) bonds are the longest while the C(2)-N(2) bonds have the shortest lengths of all. This finding confirms that one C-N bond in acylthioureas bond C(2)-N(2), is shorter than the others. Therefore, the calculated results are in good agreement with earlier experimental findings (Koch et al., 1995, Dago et al., 1989& 1988), confirming the reliability of the quantum mechanical calculations made.

3.5 Summary

The modelling of a number of substituted acylthioureas has answered some important questions. Comparison of the three tautomeric forms proved that the tautomeric form that has the mobile proton H(1) bonded to the central nitrogen atom, i.e. N(1), is the most stable one. Hence this is the preferential tautomeric form of acylthioureas.

Analysis of the calculated optimum energy structures of all compounds shows that a *trans* orientation of the carbonyl and thio-carbonyl moieties is the common trend, in agreement with what has been found in previously conducted experimental studies.

The internal coordinate analysis of the calculated stable structures proved that the C(2)-N(2) bond is the shortest relative to the two other C-N bonds. This finding is again in agreement with what has been observed experimentally.

Chapter Four

Infra-red studies of substituted acylthioureas

4.1 Introduction

As a continuation of the investigation into the structural properties of substituted acylthioureas, the IR absorption analysis of these compounds is discussed in this chapter. In **section 4.2** experimental IR studies carried out on six substituted acylthiourea compounds are discussed. Within this section, interpretation of the experimentally obtained frequencies, which was based on literature and calculated values, is also discussed. Due to the close similarities found between the calculated and experimentally determined frequencies, predictions of experimental IR absorptions are made for six additional substituted acylthiourea compounds and are discussed in **section 4.3**. Once assignment of frequencies of all the compounds under consideration had been accomplished, a study of the effect of substituents on the IR absorption frequencies of the chemically active C=S and C=O bonds is discussed in **section 4.4**. Finally a brief summary of the chapter is given in **section 4.5**.

4.2 Experimental IR studies on selected substituted acylthioureas

Having determined the most stable structures of a number of substituted acylthioureas in the previous chapter the next step is the analysis of their structural properties. One of the properties of interest is their IR absorption spectrum. Hence experimental IR studies were conducted on six substituted acylthiourea compounds namely N-pivaloyl-N'-pyrrolidine thiourea (A); N-(2,6-dimethyl-piperidine)-N'-(3,4,5-methoxybenzoyl)thiourea (B); N,N-diethyl-N'-pivaloyl thiourea (C); N,N-dibutyl-N'-pivaloyl thiourea (D); N,N-diethyl-N'-benzoyl thiourea (E); and N,N-dibutyl-N'-benzoyl thiourea (F).

4.2.1 Basic procedure

The experimental IR analysis was carried out on a NEXUS-TM FTIR spectrometer. The sample was prepared as a KBr pellet, in a dry-air glove box that was continually purged with dry nitrogen gas, so as to keep the sample and the KBr powder free from moisture and interfering gases. Silica gel and anhydrous P₂O₅ were used as moisture indicator and moisture absorbing agent respectively. A few milligrams of the sample was added to KBr powder and ground to a homogenous mixture. A 13 mm diameter pellet was obtained using a hydraulic press.

The mid range (4000-400 cm⁻¹) IR spectra of the samples were recorded with the FT-IR spectrometer, operating at a resolution of 4cm⁻¹ and a scan rate of 32. The spectrometer was also purged with dry nitrogen gas at a flow rate of 30 cubic feet per hour (850L/hour).

4.2.2 Results and discussion

Following the procedure given above, experimental IR spectra of good quality were obtained for the six compounds analyzed, as shown in **fig. 4.1-4.6** below.

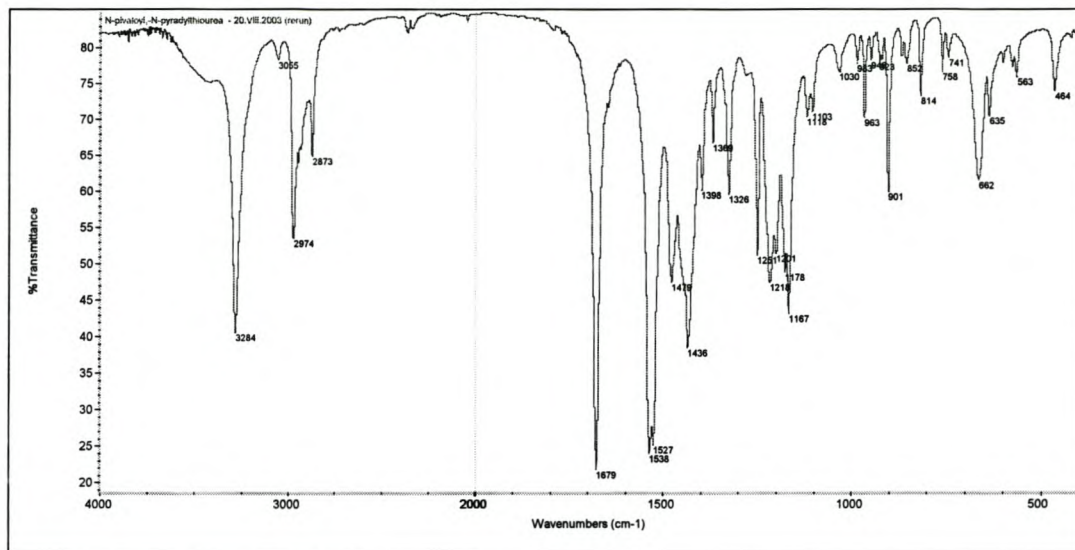


Fig. 4.1 IR spectrum of crystalline *N*-pivaloyl, -*N'*-pyrrolidine thiourea in a KBr pellet at 4cm^{-1} resolution.

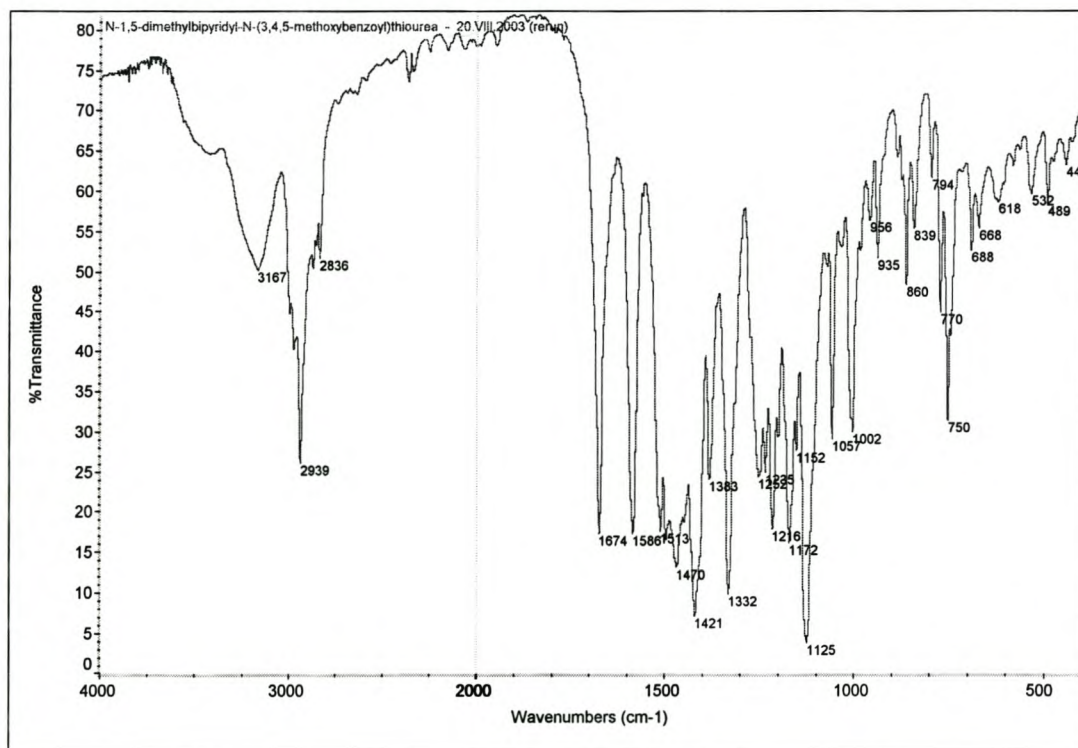


Fig. 4.2 IR spectrum of crystalline *N*-(2, 6-dimethyl piperidine)-*N'*-(3, 4, 5-methoxy benzoyl) thiourea in a KBr pellet at 4cm^{-1} resolution.

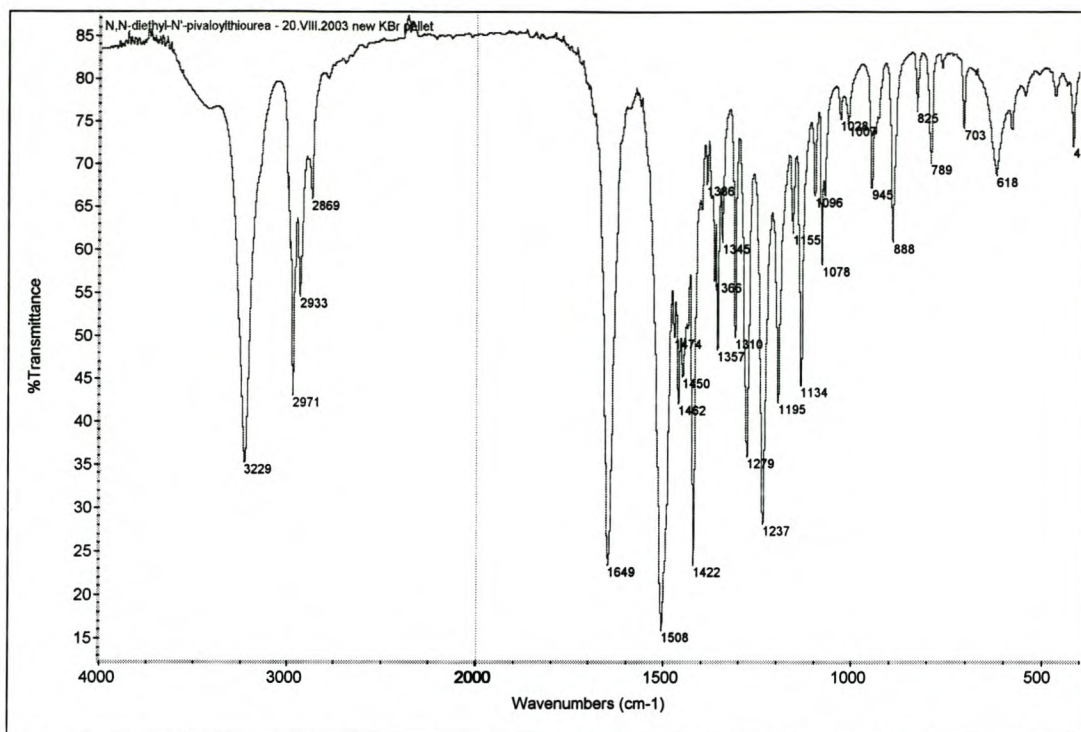


Fig. 4.3 IR spectrum of crystalline *N, N*-diethyl-*N'*-pivaloyl thiourea in a KBr pellet at 4 cm^{-1} resolution.

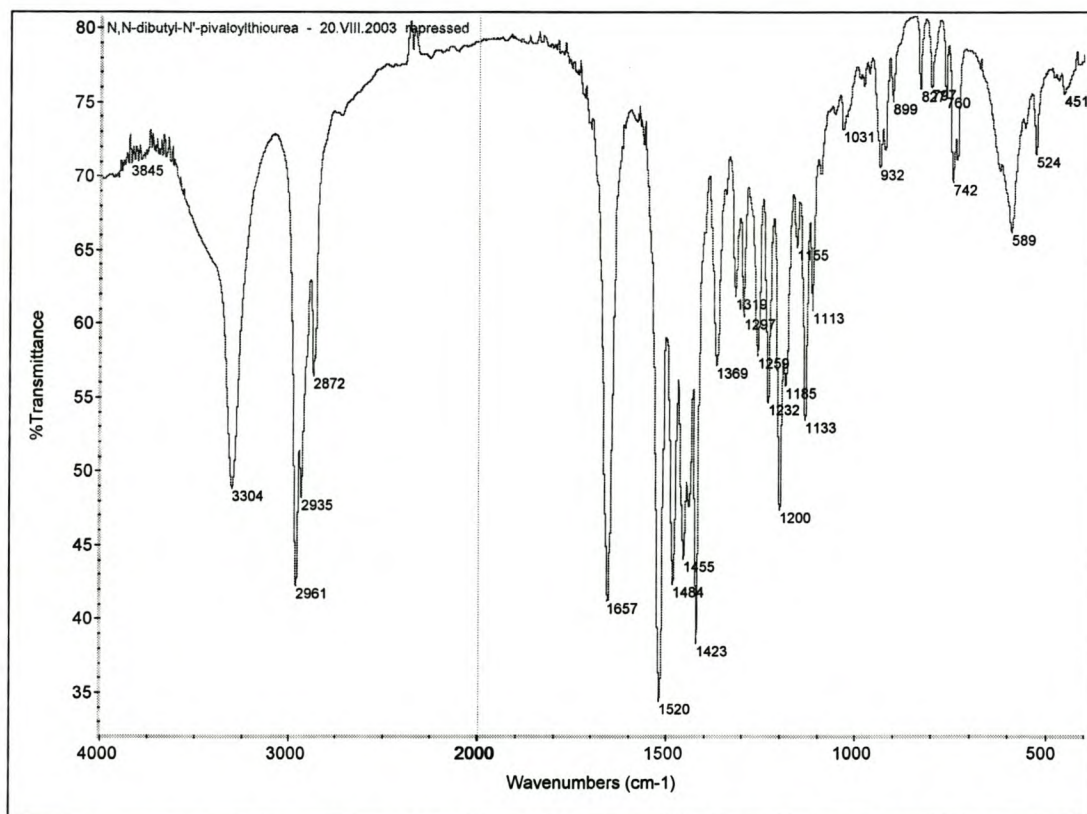


Fig. 4.4 IR spectrum of crystalline *N, N*-dibutyl-*N'*-pivaloyl thiourea in a KBr pellet at 4 cm^{-1} resolution.

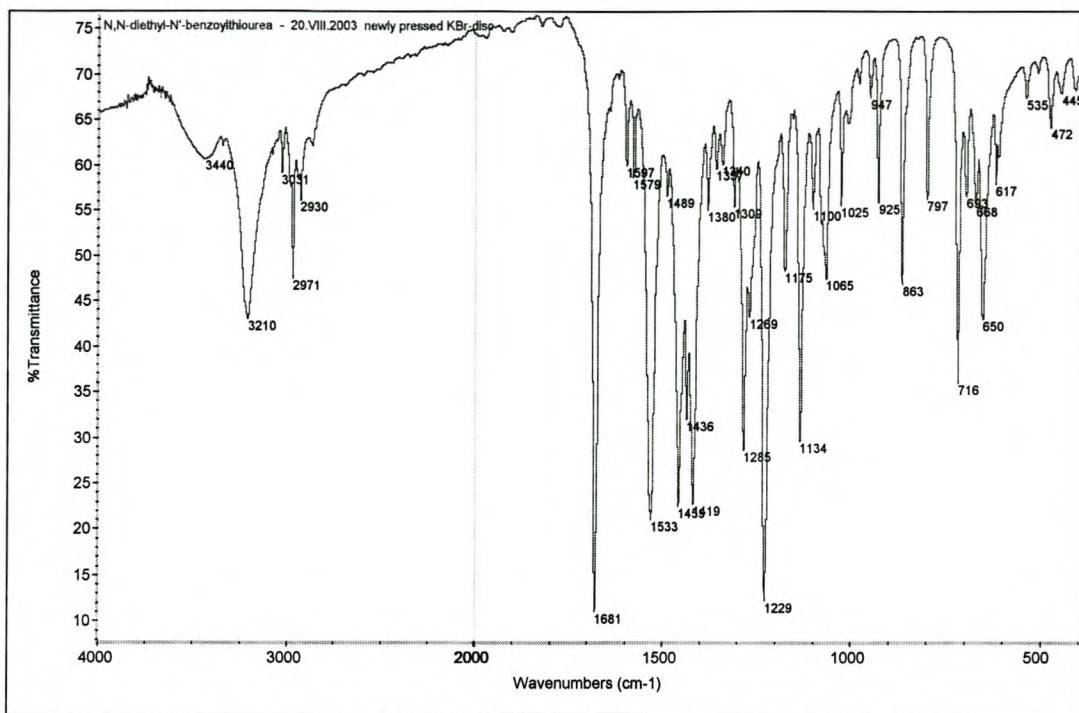


Fig. 4.5 IR spectrum of crystalline *N, N*-diethyl-*N'*-benzoyl thiourea in a KBr pellet at 4 cm⁻¹ resolution.

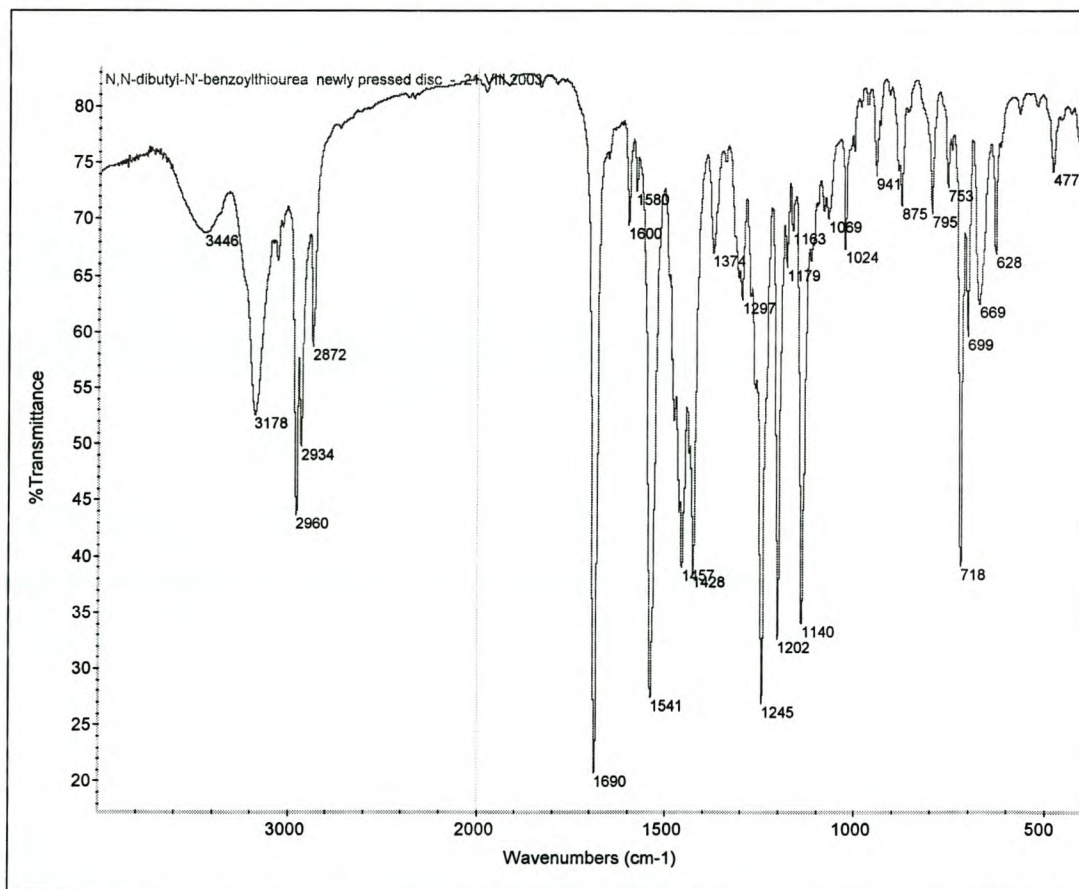


Fig. 4.6 IR spectrum of crystalline *N, N*-dibutyl-*N'*-benzoyl thiourea in a KBr pellet at 4 cm⁻¹ resolution.

Once the IR spectrum of each compound had been obtained, they were interpreted based on the literature and by comparing the experimental absorption frequencies with their calculated counterparts. The assignment of normal modes of vibrations was greatly simplified by animating the calculated molecular vibrations using the *Gaussview2* programme.

The calculation of frequencies was performed in parallel with the energy optimization during the search for the most stable structures of substituted acylthiourea compounds. Hence all the theoretical frequencies were calculated using the 6-31G (d) basis set at the Hartree-Fock level of theory. As discussed earlier the Hartree-Fock level of theory does not take electron correlation into consideration. For this reason, the frequencies obtained are always larger than the experimentally obtained values and there is an overestimation of about 10-12% of the frequency (Dubis, A.T. & Grabowski, S.J., 2003). To correct for this systematic error, it is essential to multiply the Hartree-Fock frequencies with a standard scaling factor of 0.8929 (Scott, A.P., & Radom, L., 1996). Based on this, all the calculated frequencies were scaled before comparison with their experimental counterparts.

In table 4.1 below only bands that have corresponding experimental peaks are considered, but full descriptions of all vibration modes of the calculated wavenumber of each compound are available in **addendum B**.

Table 4.1 Calculated and experimentally obtained wavenumbers (cm^{-1}) of substituted acylthioureas.

Compound	Description	Calculated value (cm^{-1})	Scaled* value (cm^{-1})	Experimental value (cm^{-1})	Difference (cm^{-1})
A	N ₁ -H stretching	3869	3454	3284	170
	CH ₃ symm. stretching	3222	2877	2873	4
	CH ₃ assym. stretching	3309	2955	2974	-19
	C ₁ =O stretching	1988	1775	1679	96
	C ₂ -N ₂ stretching	1605	1433	1436	-3
	C ₂ -N ₁ stretching	1361	1215	1218	-3
	C ₁ -N ₁ stretching	1290	1152	1167	-15
	C ₂ =S stretching	977	872	852	20
	N ₁ -H oop. bending	1734	1548	1538	10
	N ₁ -H in-plane bending	751	671	662	9
	CH ₃ scissoring	1562	1394	1398	-4
			1560	1393	1369

	CH ₃ twisting	1654	1477	1479	-2
B	N ₁ -H stretching	3842	3430	3167	263
	Pipe.ring CH ₃ symm. str.	3220	2875	2871	4
	Pipe. ring CH ₃ assym. str.	3331	2974	2973	1
	Pipe. ring CH ₂ symm. str.	3205	2862	2856	6
	Pipe. ring CH ₂ assym. str.	3294	2942	2939	3
	Methoxy CH ₃ assym. str.	3332	2975	2998	-23
	C = O stretching	1975	1763	1674	11
	C ₂ -N ₂ stretching	1597	1426	1421	5
	C ₂ -N ₁ stretching	1259	1124	1125	-1
	C ₁ -N ₁ stretching	1359	1213	1216	-3
	C ₂ =S stretching	858	766	770	-4
	N ₁ -H in-plane bending	1716	1532	1586	-54
	N ₁ -H out-of-plane bending	765	683	688	-5
	Pipe. ring CH ₃ scissoring	1638	1463	1469	-6
	Pipe. ring CH ₂ wagging	1554	1388	1383	5
	Pipe. ring CH ₂ twisting	1420	1268	1252	16
	Phe. ring C-H in-plane bend.	1398	1248	1235	13
Phe. ring C-H oop. bending	1032	922	935	-13	
C	N ₁ -H stretching	3870	3455	3229	226
	CH ₂ symm. stretching	3211	2867	2869	-2
	CH ₂ assym. stretching	3332	2976	2971	5
	CH ₃ assym. stretching	3312	2958	2933	25
	C ₁ =O stretching	1990	1777	1649	128
	C ₂ -N ₂ stretching	1609	1437	1422	15
	C ₂ -N ₁ stretching	1315	1174	1155	18
	C ₁ -N ₁ stretching	1273	1137	1134	3
	C ₂ =S stretching	953	851	825	26
	CH ₂ -N (2)-CH ₂ symm.str.	1115	996	1007	-11
	CH ₂ -N (2)-CH ₂ assym.str.	1380	1232	1237	-5
	N ₁ -H out-of-plane bending	1740	1554	1508	46
	N ₁ -H in-plane bending	703	628	618	10

	CH ₂ scissoring	1674	1495	1462	33
	CH ₂ twisting	1433	1279	1279	0
	CH ₃ scissoring	1560	1393	1386	7
	CH ₃ twisting	1633	1458	1450	8
D	N ₁ -H stretching	3872	3457	3304	153
	CH ₂ assym. stretching	3310	2955	2935	20
	CH ₃ symm. stretching	3222	2877	2872	5
	CH ₃ assym. stretching	3310	2955	2961	-6
	C ₁ =O stretching	1989	1776	1657	19
	C ₂ -N ₂ stretching	1615	1442	1423	19
	C ₂ -N ₁ stretching	1310	1170	1155	15
	C ₁ -N ₁ stretching	1279	1142	1133	9
	C ₂ =S stretching	971	867	899	-32
	C ₃ -C ₁ stretching	1378	1231	1232	-1
	N ₁ -H oop bending	1740	1554	1520	34
	CH ₂ scissoring	1663	1485	1484	1
	CH ₂ twisting	1406	1256	1259	-3
	CH ₃ scissoring	1560	1393	1369	24
	CH ₃ twisting	1644	1468	1455	13
	Isobutyl group wagging	1369	1222	1200	22
Butyl groups wagging	630	563	589	-26	
E	N ₁ -H stretching	3847	3435	3210	225
	Ring C-H symm. stretching	3395	3031	3031	0
	CH ₂ assym. stretching	3290	2938	2930	8
	CH ₃ assym. stretching	3315	2960	2971	-11
	C ₁ =O stretching	1983	1770	1681	89
	C ₂ -N ₂ stretching	1619	1445	1419	26
	C ₂ -N ₁ stretching	1306	1167	1134	33
	C ₁ -N ₁ stretching	1399	1249	1269	-20
	C ₂ =S stretching	925	826	797	29
	CH ₂ -N (2)-CH ₂ assym.str.	1374	1227	1229	-2
	N ₁ -H in-plane bending	1736	1550	1533	17

	CH ₂ scissoring	1661	1484	1459	25
	CH ₂ twisting	1463	1306	1309	-3
	CH ₃ scissoring	1572	1403	1380	23
	CH ₃ twisting	1636	1461	1436	25
F	N ₁ -H stretching	3848	3435	3178	257
	CH ₂ assym. stretching	3311	2957	2934	23
	CH ₃ symm. stretching	3204	2861	2872	-11
	CH ₃ assym. stretching	3265	2915	2960	-45
	C ₁ =O stretching	1980	1768	1690	78
	C ₂ -N ₂ stretching	1618	1445	1428	17
	C ₂ -N ₁ stretching	1302	1162	1163	-1
	C ₁ -N ₁ stretching	1393	1244	1245	-1
	C ₂ =S stretching	953	851	875	-24
	N ₁ -H in plane bending	1738	1551	1541	10
	N ₁ -H oop. bending	746	666	669	-3
	CH ₂ scissoring	1645	1469	1457	12
	CH ₂ twisting	1448	1293	1297	-4
	CH ₃ scissoring	1564	1396	1374	22
	CH ₃ assym. bending	1644	1468	1457	11

*Scaling factor 0.8929, assym. = antisymmetric, bend = bending, oop. = out of plane, Pipe. = piperidine, Phe. = phenyl

str. = stretching symm. = symmetric

As can be seen from the data tabulated above, the experimental IR absorption frequencies of the C=O bonds of the six substituted acylthioureas are found to be in the range of 1649 cm⁻¹ to 1690 cm⁻¹ for all compounds. All these values are within the expected range obtained from the literature of 1630-1690 cm⁻¹ (Pavia, D.L. et al., 2001). This is a clear indication of the accuracy of the experimentally conducted IR studies. When the experimentally obtained frequencies are compared with their calculated counterparts, they show differences of 78 cm⁻¹ to 128 cm⁻¹. These differences are relatively large next to those observed in the N-H bonds. The main reason for the large difference between the calculated and experimentally obtained vibrational modes of the C=O and N-H bonds can be attributed to the existence of strong intermolecular hydrogen bonding in the crystals of substituted acylthioureas. In the calculations however, isolated molecules are considered.

Thus the effect of intermolecular hydrogen bonding, which weakens the C=O and N-H bonds, is not taken in to account. This in turn leads to the value of the calculated frequency being too high.

The next vibrational mode to be analyzed is that of the C=S bond. As proved by many experimental studies it is difficult to assign the vibrational mode of the C=S bond in substituted acylthioureas without ambiguity due to its coupling with other vibrational modes (Sacht, C.; Datt, M.S. 2000, Mohamadou, et al., 1993). One experimental investigation reported the C=S vibrational mode of N-ferrocenylcarbonyl-N'-(2-pyridyl) thiourea to be 1300cm^{-1} (Che, D.-J. et al., 1999). Another study made on N, N-diethyl-N-(2-chlorobenzoyl) thiourea reported that its C=S vibrational mode is 730 cm^{-1} . This indicates the absence of any general trend for the C=S vibrational mode of substituted acylthioureas, hence this study focused on clarifying the situation.

In this work experimental wavenumbers of the C=S bonds in the six compounds found to be in the range of 770 cm^{-1} to 899 cm^{-1} . All these values differ from the absorption band of a carbon-sulphur single bond, which is $705\text{-}570\text{ cm}^{-1}$, as well as that of a carbon-sulphur double bond, $1430\text{-}1130\text{ cm}^{-1}$ (Cross, A.D., 1960). Thus the experimental values lie in between the single and double bond values similar to what was observed for the carbon-sulphur double bonds of some thiourea compounds experimentally studied by Gambino and his co-workers (Gambino, D. et al., 2002). This finding can be explained by the delocalization that exists in the thio-carbonyl region of the compounds, causing the C=S bond to lose its double bond character (see **fig. 3.1**).

When the above experimental C=S IR absorption bands are compared with their calculated equivalents, they show differences which lie in the range 4cm^{-1} to 32cm^{-1} . These values are smaller than those observed for N-H and C=O vibrations. This may be because the C=S is not strongly involved in interatomic hydrogen bonding due to the delocalization. The close similarity between the scaled calculated and experimental vibrational modes suggest that the C=S absorption band for substituted acylthioureas can be assigned with relative certainty as being in the range of $728\text{-}872\text{ cm}^{-1}$.

Other vibrations that attract attention for analysis are those of the C-N bonds. Absorption bands for the C(1)-N(1) bonds of the six compounds are within the 1133 cm^{-1} to 1269 cm^{-1} range, while those for the C(2)-N(1) bonds are between 1125cm^{-1} and 1218 cm^{-1} . All these values are within the normal carbon nitrogen single bond range of $1350\text{cm}^{-1}\text{-}1000\text{ cm}^{-1}$ (Pavia, D.L., et al., 2001). Absorption bands for the C(2)-N(2) bonds of the six compounds however, were found to be between 1419cm^{-1} to 1436 cm^{-1} , which lies neither in the abovementioned range for a single bond, nor in the carbon-nitrogen double bond region of $1660\text{-}1480\text{ cm}^{-1}$. This indicates that the C(2)-N(2) bonds are not simple single bonds, but exhibit a partial double bond character. This character has been proved experimentally (Morales, A.D. et al., 2000) and also computationally as indicated by the structural results discussed in the previous chapter.

The comparison between the experimentally obtained and theoretically calculated absorption frequencies of all the C-N bonds shows that the differences are all less than 33cm^{-1} . This observation further verifies the accuracy of the theoretically calculated frequencies.

Besides the bonds discussed above comparisons were made between the experimentally obtained and scaled calculated frequencies of stretching vibration modes of other bonds in the compounds studied. No significant differences were found for these or for the various bending modes studied. This verifies the accuracy of the frequency calculations.

4.3 Prediction of experimental IR absorption frequencies of selected substituted acylthioureas.

As stated above, there is a considerable similarity between the scaled calculated and experimental IR absorption frequencies. This finding enables the prediction of the vibrational modes of a further six substituted acylthioureas with some confidence. These compounds are N-(n-butyl)-N'-benzoyl thiourea (G), N-(n-propyl) N'-benzoyl thiourea (H), N-(p-hexoxy) aniline-N'-(p-Methoxy) benzoyl-thiourea (I), N,N-di(n-butyl)-N'-naphthoyl-thiourea (J), N,N-di(2-hydroxyethyl)-N'-benzoyl thiourea (K) and N,N-diethyl-N'-4-nitrobenzoylthiourea (L).

As before only selected frequencies will be discussed here, with the full assignment of each vibrational mode, except those of zero intensity, available in **addendum B**.

Table 4.2 Predicted wavenumbers (cm^{-1}) for substituted acylthioureas (G-L).

Ligand	Description	Calculated wavenumber (cm^{-1})	Predicted* wavenumber (cm^{-1})	Intensity
G	N(1)-H stretching	3893	3476	0.08
	N(2)-H stretching	3813	3404	0.24
	Ring C-H stretching	3385	3022	0.03
	CH ₂ assym. stretching	3291	2938	0.05
	CH ₃ assym. stretching	3264	2914	0.09
	CH ₂ symm. stretching	3197	2855	0.07
	CH ₃ symm. stretching	3201	2858	0.04
	C(1)=O stretching	1948	1740	0.45
	C(2)-N(2) stretching	1539	1374	0.20
	N(1)-C(2) stretching	1303	1163	0.32
	C(1)-N(1) stretching	1398	1248	0.26
	C(2)=S stretching	846	755	0.05
	N(2)-H in-plane bending	1759	1570	0.65
	N(1)-H in-plane bending & C(2)-N(2) stretching	1731	1546	1.00
	Ring C-H in-plane bending	1670	1491	0.01
	CH ₂ scissoring	1666	1488	0.03
	CH ₃ twisting	1644	1468	0.01
	CH ₂ wagging	1580	1410	0.05
Ring C-H rocking	1613	1441	0.02	
H	N(1)-H stretching	3893	3476	0.08
	N(2)-H stretching	3812	3404	0.25
	Ring C-H stretching	3395	3032	0.02
	CH ₂ assym. stretching	3291	2939	0.06
	CH ₃ assym. stretching	3275	2924	0.06
	CH ₂ symm. stretching	3199	2856	0.04
	CH ₃ symm. stretching	3206	2862	0.03
	C(1)=O stretching	1948	1740	0.45

H	C(2)-N(2) stretching	1517	1354	0.32
	N(1)-C(2) stretching	1309	1169	0.28
	C(1)-N(1) stretching	1399	1249	0.25
	C(2)=S stretching	848	757	0.05
	N(2)-H in-plane bending	1759	1571	0.63
	N(1)-H in-plane bending & C(2)-N(2) stretching	1731	1546	1.00
	Ring C-H in-plane bending	1670	1491	0.01
	CH ₂ scissoring	1666	1488	0.03
	CH ₃ assym. bending	1644	1468	0.01
	Ring C-H rocking	1613	1441	0.02
	CH ₂ & CH ₃ wagging	1576	1408	0.08
	CH ₃ symm. bending	15667	1399	0.03
	N (2)-H oop. bending	752	672	0.05
	N (1)-H oop. bending	730	652	0.07
I	N(1)-H stretching	3900	3482	0.06
	N(2)-H stretching	3787	3382	0.30
	Ring-1 C-H stretching	3419	3053	0.01
	Ring-2 C-H stretching	3413	3047	0.01
	Methoxy CH ₃ assym. stretching	3284	2932	0.05
	Hexoxy CH ₂ assym. stretching	3264	2914	0.17
	Hexoxy CH ₃ assym. stretching	3262	2913	0.06
	Methoxy CH ₃ symm. stretching	3217	2872	0.05
	Hexoxy CH ₂ symm. stretching	3191	2849	0.06
	Hexoxy CH ₃ symm. stretching	3198	2856	0.04
	C(1)=O stretching	1940	1732	0.38
	C(2)-N(2) stretching	1505	1344	0.49
	N(1)-C(2) stretching	1299	1160	0.57
C(1)-N(1) stretching	1406	1256	0.13	

I	C(2)=S stretching	815	728	0.06
	N(2)-H in-plane bending	1750	1563	0.73
	N(1)-H in-plane bending & C(2)-N(2) stretching	1731	1546	0.56
	Ring-2 C-H in-plane bending	1697	1516	0.15
	Ring-1 C-H in-plane bending	1695	1514	0.20
	Hexoxy CH ₂ scissoring	1676	1496	0.06
	Hexoxy CH ₂ wagging	1592	1421	0.04
	Methoxy CH ₃ wagging	1337	1193	0.06
	C (3)-C (1)-N (1) oop. bending	859	767	0.09
	N (2)-H oop. bending	793	708	0.04
	N1-H oop. bending	729	651	0.05
J	N(1)-H stretching	3858	3444	0.16
	Naphthalene C-H stretching	3388	3025	0.07
	CH ₂ assym. stretching	3206	2862	0.90
	CH ₃ assym. stretching	3266	2916	0.14
	CH ₂ symm. stretching	3184	2843	0.09
	CH ₃ symm. stretching	3200	2857	0.1
	C(1)=O stretching	1981	1768	1.00
	C(2)-N(2) stretching	1610	1438	0.84
	N(1)-C(2) stretching	1195	1067	0.10
	C(1)-N(1) stretching	1322	1181	0.21
	C(2)=S stretching	959	856	0.05
	N(1)-H in-plane bending & C(2)-N(2) stretching	1733	1547	0.88
	Naphthalene C-H in-plane bending	1684	1504	0.06
	CH ₂ scissoring	1670	1491	0.34
	CH ₃ assym. bending	1644	1468	0.02
	CH ₂ wagging	1572	1404	0.24
Naphthalene C-H rocking	1548	1382	0.01	

	CH ₂ twisting	1446	1291	0.25
	N (1)-H oop. bending	773	690	0.24
	C(2)-N(2)-C''bending	597	533	0.04
K	O(2)-H stretching	4125	3684	0.14
	O(3)-H stretching	4120	3679	0.15
	N(1)-H stretching	3847	3435	0.12
	Ring C-H stretching	3385	3023	0.07
	CH ₂ assym. stretching	3196	2854	0.17
	CH ₂ symm. stretching	3221	2876	0.11
	C(1)=O stretching	1974	1763	0.81
	C(2)-N(2) stretching	1598	1427	0.81
	N(1)-C(2) stretching	1255	1121	0.06
	C(1)-N(1) stretching	1397	1248	0.76
	C(2)=S stretching	917	818	0.06
	N(1)-H in-plane bending & C(2)-N(2) stretching	1734	1548	1.00
	N (1)-H oop. bending	732	653	0.12
	CH ₂ scissoring	1679	1500	0.30
	CH ₂ wagging	1536	1372	0.10
	Ring C-H rocking	1614	1441	0.12
	C-O-H bending	1354	1209	0.32
	CH ₂ rocking	1245	1112	0.34
	C-O(2) stretching	1212	1082	0.25
	C-O(3) stretching	1194	1066	0.19
O (2)-H oop. bending	211	189	0.26	
	N(1)-H stretching	3841	3429	0.11
	Ring C-H stretching	3395	3031	0.01
	CH ₂ assym. stretching	3382	3019	0.05
	CH ₃ assym. stretching	3338	2980	0.02
	CH ₃ symm. stretching	3219	2875	0.08
	C(1)=O stretching	1989	1776	0.65
	C(2)-N(2) stretching	1611	1439	1

L	C(2)-N(1) stretching	1374	1227	0.65
	C(1)-N(1) stretching	1402	1252	0.41
	C(2)=S stretching	925	826	0.12
	O (2)-N (3)-O (3) assym. Str.	1873	1673	0.87
	N (1)-H in-plane bending & C (2)-N (2) str.	1739	1553	0.88
	N (1)-H oop. bending	779	696	0.12
	CH ₂ scissoring	1663	1485	0.12
	CH ₃ assym. bending	1637	1462	0.09
	CH ₃ scissoring	1633	1458	0.09
	CH ₂ wagging	1535	1370	0.13
	CH ₂ twisting	1430	1277	0.4
	Ring C-H oop. bending	993	887	0.04
	O(2)-N(3)-O(3) bending	967	863	0.12

* Scaling factor 0.8929, assym. = asymmetric, oop. = out of plane, Ring-1 = Methoxy bearing phenyl ring,

Ring-2 = hexoxy bearing phenyl ring, str. = stretching, symm. = symmetric,

As the data for the predicted IR frequencies show, the values for the stretching mode of the C=O bonds of the new compounds (G to L) are found to be in the range of 1732cm⁻¹ to 1776 cm⁻¹. These values are equivalent to the scaled values of the former six compounds. Values of the C=S stretching frequencies of the new compounds are found to be in the range of 728 cm⁻¹ to 826 cm⁻¹. These values are also equivalent to their counterparts in the six previously studied compounds.

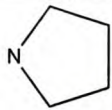
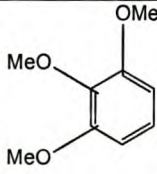
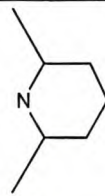
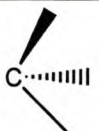
Further analysis of the predicted IR stretching frequencies of the C-N bonds of the new compounds show that the C(1)-N(1) and C(2)-N(1) stretching frequencies are found to be within the range of single C-N bond frequencies. However, stretching frequencies for the C(2)-N(2) bonds of each new compound lie between the single and double C-N frequency bands, indicating their partial double bond character. These findings are in agreement with what was observed in the previous six compounds. Since the scaled calculated and experimental frequencies correspond so well, the studies planned on some structural properties of substituted acylthioureas will be based on the scaled calculated values.

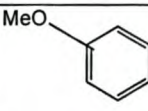
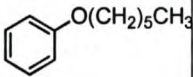
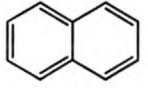
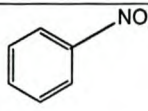
4.4 Effect of substituents on absorption frequencies of the C=O and C=S bonds of substituted acylthioureas.

As discussed at the very beginning, the versatility and interesting nature of substituted acylthioureas when used as ligands is a result of their flexible coordinating potential. As proved in many studies, these ligands can act as monodentate sulphur donors, bidentate sulphur and oxygen donors, or bidentate oxygen and nitrogen donors. They can even coordinate through the keto- or enol-thione form depending on the nature of the ligand and the coordinating substrate (Yuan, Y.F., et al., 2001). Being two of the major coordinating sites, the C=O and C=S bonds play a vital role in the application of these compounds; this is one of the reasons why more attention is given to these bonds relative to other bonds in the molecules.

Remembering the general structure of substituted acylthioureas (**fig. 3.5**) it is important to see what effect variation of the **R**, **R'**, and **R''** substituents has on the absorption frequencies of the C=O and C=S bonds. The variation of the frequencies is directly related to the properties and to the reactivity of the compounds at large hence it is worth studying it.

Table 4.3 Calculated wavenumbers (cm^{-1}) for the C=O and C=S bonds of substituted acylthioureas in the presence of different substituents.

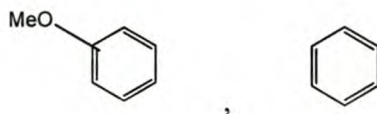
Compound	Substituent	C=O stretching (cm^{-1})	Substituent(s)		C=S stretching (cm^{-1})
	R		R'	R''	
A		1775			872
B		1763			766
C		1777	CH ₂ CH ₃	CH ₂ CH ₃	851
D		1776	(CH ₂) ₃ CH ₃	(CH ₂) ₃ CH ₃	867

E		1770	CH ₂ CH ₃	CH ₂ CH ₃	826
F		1768	(CH ₂) ₃ CH ₃	(CH ₂) ₃ CH ₃	851
G		1740	(CH ₂) ₃ CH ₃	H	755
H		1740	(CH ₂) ₂ CH ₃	H	757
I		1732		H	728
J		1768	(CH ₂) ₃ CH ₃	(CH ₂) ₃ CH ₃	856
K		1763	CH ₂ CH ₂ OH	CH ₂ CH ₂ OH	818
L		1775.9	CH ₂ CH ₃	CH ₂ CH ₃	826.3

During the analysis of the effect of the substituents on the absorption frequencies of the C=O and C=S bonds it is essential to treat the mono-alkyl and di-alkyl substituted compounds separately in order to compare equivalent systems.

When analysing the effect of each substituent, the proton substituted acylthiourea was used as standard i.e. $R=R'=R''=H$. In this reference compound, the C=O absorption band is at 1780 cm^{-1} and that of C=S is at 665 cm^{-1} . The entire set of C=O and C=S frequencies obtained through variation of substituents were then compared with these standard values.

The first set of molecules investigated was the mono-alkyl substituted compounds such as G, H, and I. Comparison between the C=O absorption frequencies of these compounds and the standard value mentioned above shows that the frequencies of all compounds are lower than the standard value. This indicates that all the R substituents of the mono-alkyl substituted compounds have the effect of lowering the C=O stretching frequency. The extent of the effect, however, differs from one substituent to another. The substituents can be written in descending order of decreasing the C=O frequencies as:

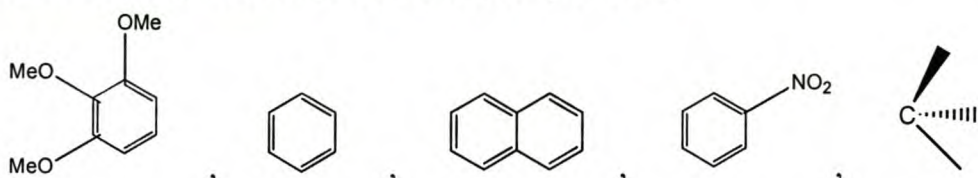


As the above sequence shows, substitution of the **R** group by a methoxy phenyl ring severely lowers the absorption frequency of the carbonyl group. On the other extreme, substitution of the **R** group with a phenyl group has little effect on the absorption frequency of the carbonyl group.

The reduction in C=O absorption frequency observed for the methoxy phenyl, group in the above sequence can be attributed to the relatively strong conjugation effect it has. As this group is unsaturated ring, when it is bonded to the carbonyl group is cause delocalization of the π electrons in the carbonyl bond. This conjugation enhances the single bond character of the C=O bond, and consequently the absorption frequency of this bond is lowered.

The relatively lower effect on the absorption frequency of C=O observed in the phenyl group, on the other hand, is due to the absence of any substituent group attached to the ring which enhance its conjugation potential. For this reason the phenyl ring has relatively lower C=O absorption frequency lowering effect.

The effect of substituents in the di-alkyl substituted acylthioureas was also studied. As before, the carbonyl frequencies are found to be lower than the standard value. Hence substituents of these compounds also have the effect of lowering the frequency. The substituents could again be sorted into the following descending order of frequency lowering:

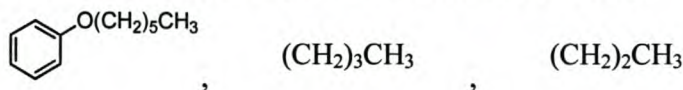


In this sequence the tri-methoxy phenyl ring has the greatest effect on the C=O frequency and this decreases in moving toward the tertiary-butyl group. The cause of the strong frequency lowering effect observed in tri-methoxy phenyl group is the conjugation effect discussed above. On the other extreme the weak frequency lowering effect observed in the tertiary-butyl group is due to inductive effect. The tertiary-butyl group has a greater electron donating nature than the standard hydrogen atom, hence this group through donation of electrons it weaken bond of the carbonyl group; consequently absorption frequency of this group is lowered.

The next effect of the **R'** and **R''** groups to be examined was on the C=S absorption frequencies. Comparison between the C=S absorption frequencies of both the mono-alkyl and di-alkyl substituted compounds and that of the standard C=S absorption frequency shows that the

frequencies in all the compounds are higher than the standard value. This indicates that all the **R'** and **R''** substituents have the effect of raising the C=S stretching frequency.

Analysis of mono-alkyl substituted compounds enables one to sort the substituents into the following ascending order of increasing the C=S stretching frequency.

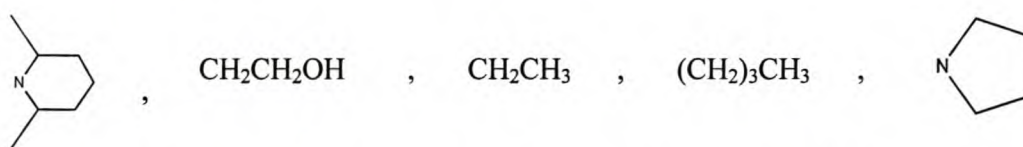


In this sequence the hexoxy phenyl ring has the least effect, while the n-propyl has the greatest effect.

The hexoxy phenyl group, attached as an α -substituent to the thio-carbonyl group, does not undergo conjugation, even though it is an unsaturated ring. This is because the parent thio-amide group is highly stabilized through resonance. Hence the hexoxy phenyl ring rather removes electrons from the C=S bond. This removal of electrons is compensated by tightening of the π bond of the C=S group; this leads to a rise in absorption frequency of the C=S bond.

In case of the n-propyl and n-butyl substituent groups, their frequency raising effect is due to their electron withdrawing nature. Even though alkyl groups are in general known for their electron donating nature, many studies show that they can even act as electron withdrawing groups especially when bonded to saturated groups (March, J., 1992; Sebastian, J.F., 1971; Perry, W.O., et al.; 1970). Hence the n-propyl and n-butyl groups withdraw electrons from the C=S bond causing its stretching frequency to rise.

Finally, the effect of substituents on the C=S absorption frequencies of the di-alkyl substituted compounds was studied. Again, substituents of these compounds increase the C=S absorption frequency as mentioned earlier. Hence the ascending orders of frequency rising is given as:



The above substituents also increase the absorption frequencies of the thio-carbonyl group by their electron withdrawing nature.

As discussed at the very beginning, the O and S atoms are nucleophilic centres. Substitution of the **R**, **R'**, **R''** groups by electron donating groups enhance the nucleophilic character of the O and S atoms. Therefore, as the current analysis shows substitution of the **R'** and **R''** groups by the weakest electron withdrawing groups such as hexoxy phenyl in the mono-alkyl substituted compounds and piperidine ring in the di-alkyl substituted compounds enhance the nucleophilic character of the S atom. On the other hand, substitution of the **R** group with strong conjugating

groups such as methoxy phenyl and tri-methoxy phenyl in the mono and di-alkyl substituted compounds enhance the nucleophilic character of the O atom. Even though reactivity of substituted acylthioureas during their coordination depends on steric and other factors, enhancement of the nucleophilic character of the O and S atoms via the variation of substituents as discussed above can also have a significant contribution.

Summary:

An experimental IR study was carried out with the aim of analyzing the structural properties of six substituted acylthioureas. Once spectra of good quality were obtained, they were interpreted based on literature values and by comparing them to theoretical frequencies calculated using the 6-31G (d) basis set at the Hartree-Fock level of theory and scaled using a factor of 0.8929.

The sound agreement between the experimentally obtained and theoretically calculated frequencies enabled the prediction of IR spectra for six more substituted acylthioureas with a high degree of confidence. Once IR frequencies had been calculated for the twelve compounds, the effect of the substituents on the absorption frequencies of the chemically active C=S and C=O bonds was analyzed.

According to this analysis the weakest electron withdrawing groups, hexoxy phenyl for the mono-alkyl substituted compounds and piperidine ring for the di-alkyl substituted compounds are found to have the smallest effect in increasing the stretching frequency of the C=S bond. On the other hand, the strongly conjugating methoxy phenyl ring for mono alkyl substituted compounds and the tri-methoxy phenyl ring for di-alkyl substituted compounds are found to lower the C=O stretching frequency the most. By the relative electron enriching effect they have, these substituents enhance the nucleophilic character of the S and O atoms, and the compounds' coordination potential. The general trend of the C=O frequency lowering and C=S frequency raising effects of the remaining substituents was also established.

Chapter Five

Electronic structure studies of substituted acylthioureas

5.1 Introduction

This chapter describes the electronic structure studies of a number of substituted acylthioureas. In **section 5.2**, the X-ray diffraction analysis of three substituted acylthioureas is discussed. A search of the Cambridge Crystallographic Structural Database (CCSD) (Allen, H.H. & Kennard, O. 1993) as well as in literature for compounds whose crystal structures had already been determined is discussed in **section 5.3**. An Atoms in Molecules (AIM) study that was undertaken to get a clearer picture of the electron density in the molecules is discussed in **section 5.4**. A Natural Bond Orbital (NBO) analysis, performed to investigate charge distribution and electron occupancies, is discussed in **section 5.5**. Finally a Natural Resonance Theory (NRT) analysis carried out to quantitatively determine the possible resonance forms attained by substituted acylthioureas is discussed in **section 5.6**.

5.2 Single crystal X-ray diffraction studies

The theoretical calculations described in **chapter three** identified the most stable (global minimum energy) structures of all the substituted acylthiourea compounds under investigation. The main purpose of the experimental crystal structure studies was to compare the computationally obtained structures with their experimental counterparts, and hence to confirm that they are indeed the stable structures.

The single crystal X-ray diffraction studies were performed on compounds whose crystal structures were not previously known. The compounds studied are N-pivaloyl-N'-pyrrolidine thiourea (A), N-(2, 6-dimethyl piperidine)-N'-(3, 4, 5-methoxy)-benzoyl thiourea (B), and N, N-dibutyl-N'-pivaloyl thiourea (D). Details are discussed below.

5.2.1 Experimental procedure

Single crystals of the substituted acylthioureas were grown from a solution in acetone by slow evaporation at room temperature. The X-ray diffraction data were collected on a Bruker AXS single crystal X-ray diffractometer using a SMART APEX CCD detector (Siemens, 1996b). The X-ray generator was operated at 40KV and 30mA using MoK α radiation ($\lambda = 0.71073\text{\AA}$). All the structures were solved and refined using X-Seed (Barbour, L. J. 2001). Molecular and packing diagrams were generated using ORTEP32 (Farrugia, L. J. 1997).

5.2.2 Result and discussion

Crystallographic data of N-pivaloyl-N'-pyrrolidine thiourea (A), N-(2, 6-dimethyl piperidine)-N'-(3, 4, 5-methoxy)-benzoyl thiourea (B), and N, N-dibutyl-N'-pivaloyl thiourea (D) are given in table 5.1.

Table 5.1 Crystallographic data for N-pivaloyl-N'-pyrrolidine thiourea, N-(2, 6-dimethyl piperidine)-N'-(3, 4, 5-methoxy)-benzoyl thiourea, and N, N-dibutyl-N'-Pivaloyl thiourea.

Compound name	A	B	D
Formula	C ₁₀ H ₁₈ N ₂ OS	C ₁₈ H ₂₆ N ₂ O ₄ S	C ₁₄ H ₂₈ N ₂ OS
Formula weight/g mol ⁻¹	214.32	366.47	272.44
Temperature/K ⁰	173(2)	173(2)	103(2)
Wavelength	0.71073	0.71073	0.71073
Crystal system	Orthorhombic	Triclinic	Orthorhombic
Space group	Pca2 ₁	P $\bar{1}$	Pna2 ₁
a/ Å	12.243(4)	12.427(2)	10.0259(8)
b/ Å	9.924(3)	12.666(2)	13.2126(10)
c/ Å	10.002(3)	13.894(2)	12.1805(10)
α /°	90	96.486(2)	90
β /°	90	91.758(3)	90
γ /°	90	118.402(2)	90
Volume/Å ³	1215.1(7)	1902.5(5)	1613.5(2)
Z	4	4	4
Density /g cm ⁻³	1.172	1.279	1.122
Abs.coef/mm ⁻¹	0.240	0.194	0.194
F(000)	464	784	600
θ min, max	2.05, 28.31	1.85, 25.00	2.27, 28.29
h min,max ; k min,max ; l min,max	-16, 15; -12, 13; -13, 12	-14, 14; -15, 15; -16, 16	-13, 12; -17, 16; -16, 8
No. refl. measured	13163	18232	9342
No. unique refl.	2882	6672	2926
No. parameters	130	444	168
Refinement method	Full-matrix least squares on F ²	Full-matrix least squares on F ²	Full-matrix least squares on F ²

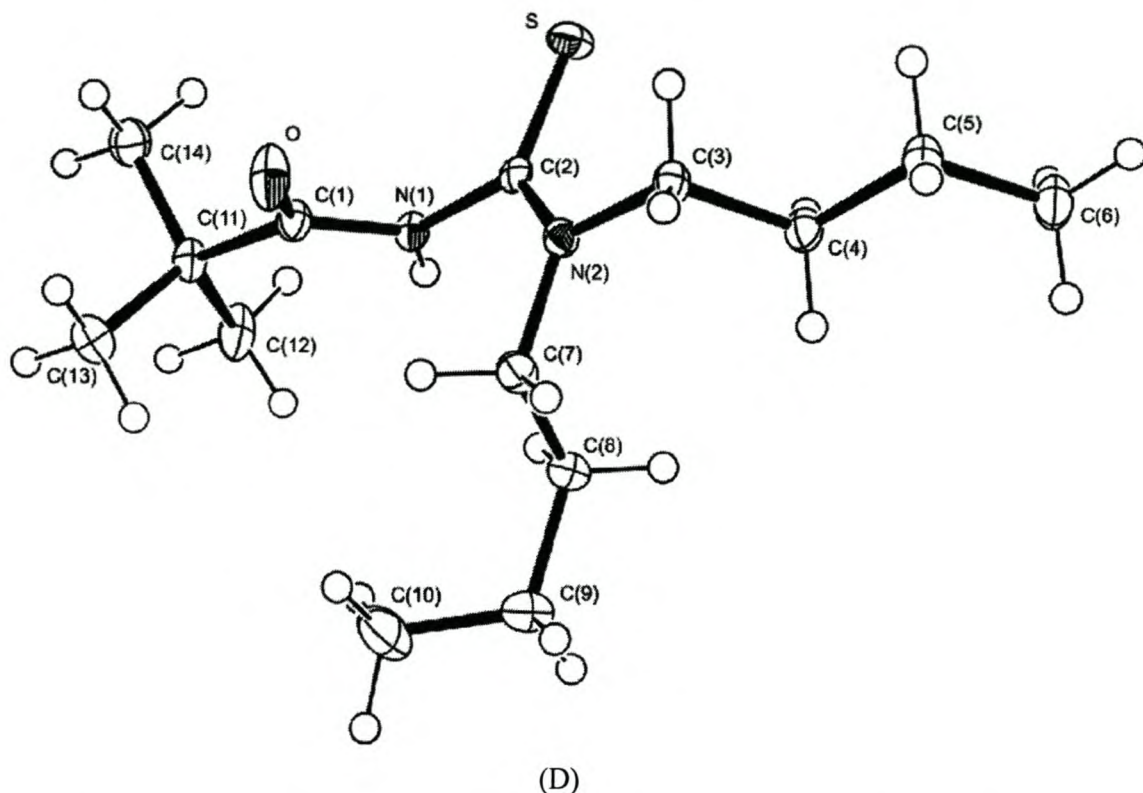


Fig. 5.1 Molecular structures of (A) *N*-pivaloyl-*N'*-pyrrolidine thiourea, (B) *N*-(2, 6-dimethyl piperidine)-*N'*-(3, 4, 5- methoxy)-benzoyl thiourea, and (D) *N, N*-dibutyl-*N'*-pivaloyl thiourea. Ellipsoids are shown at the 50% probability level.

The experimental geometries of the molecules above match very well with the minimum energy structures obtained through the quantum mechanical calculations described in **chapter three** (see **fig.3.6**). Selected values of experimental structural features are tabulated in table 5.2 below, with full crystal data of each molecule available in **addendum B**.

Table 5.2 Selected experimental internal coordinates of *N*-pivaloyl-*N'*-pyrrolidine thiourea (A), *N*-(2, 6-dimethyl piperidine)-*N'*-(3, 4, 5- methoxy)-benzoyl thiourea (B), and *N, N*-dibutyl-*N'*-pivaloyl thiourea (D).

Internal coordinate	Compound			
	A	B		D
		B-1	B-2	
Bond length (Å)				
C(3)-C(1)	1.523(3)	1.495(3)	1.491(3)	1.540(2)
C(1)-O	1.220(2)	1.215(3)	1.220(3)	1.222(2)
C(1)-N(1)	1.377(2)	1.386(3)	1.372(3)	1.355(2)

N(1)-C(2)	1.405(2)	1.412(3)	1.418(3)	1.431(2)
C(2)-S	1.6763(19)	1.679(2)	1.676(2)	1.668(2)
C(2)-N(2)	1.321(2)	1.325(3)	1.329(3)	1.321(3)
Valence angle (°)				
C(3)-C(1)-O	122.97(16)	122.3(2)	122.0(2)	121.03(16)
O-C(1)-N(1)	121.42(16)	121.8(2)	120.6(2)	121.07(17)
C(1)-N(1)-C(2)	122.33(14)	121.36(18)	121.58(19)	120.84(14)
S-C(2)-N(2)	124.33(13)	124.80(17)	126.71(17)	126.07(14)
Dihedral Angle (°)				
C'-C(3)-C(1)-O	7.1(3)	12.5(3)	4.5(3)	-45.23(0.28)
O-C(1)-N(1)-C(2)	0.8(3)	-10.6(3)	-7.3(3)	-10.67(0.33)
C(1)-N(1)-C(2)-S	122.49(15)	-115.45(19)	-103.2(2)	-101.41(0.20)
S-C(2)-N(2)-C''	-5.7(2)	6.8(3)	-1.5(3)	3.52(0.24)

NB - In compound A: C''=C(7), C'=C(4); in compound B: C''=C(12), C'=C(4); and in compound D: C(3)=C(11), C'=C(13), & C''=C(3); in the main crystal structure as tabulated in **addendum C**, (i.e. the labelling in **fig. 5.1** is made to suit the calculated structures labelling).

- Compound B- has two molecules called B-1 & B-2 within the asymmetric unit.

When compared the coordinates of the crystal structures tabulated above and their calculated counterparts in **chapter three** (table 3.5) show marked similarities. The comparison shows that the bond lengths and valence angles of the crystal and calculated structures are very similar. Minor differences are observed in some of the dihedral angle values; however, this is expected as the calculations were performed on isolated molecules, which are free from any external pressure, which might affect their dihedral angle through steric hindrance.

All the important structural trends of the calculated structures are also manifested in the experimental crystal structures. For instance, the crystals' C(2)-N(2) bond lengths which lie in the range of 1.321(2)-1.329(3)Å are found to be shorter than the C(1)-N(1) and N(1)-C(2) bond lengths, which are 1.355(2)-1.386(3)Å and 1.405(2)-1.431(2) Å respectively. Besides this, the *trans* orientation of the carbonyl and thio-carbonyl moieties is also a common characteristic in the crystal structures. These observations confirm the close agreement between the theoretically calculated and experimentally determined molecular structures of the three compounds discussed so far, thus proving the accuracy of the quantum mechanical calculations performed.

5.3 Cambridge crystallographic Structural database (CCSD) and literature searches

As an extension of the structural comparison, a general search was made for all possible substituted acylthioureas in the Cambridge Crystallographic Structural Database (CCSD) (Allen, H. H. & Kennard, O. 1993). A number of crystal structures with reference codes BUTQEM, BUTQIQ, BUTCOW, BZATSC, DIFRIT EGOSEV, FEMQUE, HIJMOC, IDOJOA, JABCIY, KIYHUV, KOYCIK, ROLCAW, ROLCAW01, and SETKOR, were identified in the CSD. Since the majority of these exist in coordinated form additional screening showed that only three of the above fit in with the scope of the current work. These three substituted acylthioureas are given by the CCSD reference codes: JABCIY, KIYHUV, and ROLCAW01 (see **fig. 5.4**). JABCIY represents N'-(2-chlorobenzoyl)-N, N-diethylthiourea (Bailey, R.A. et al., 1988), KIYHUV represents N'-(3-Methoxybenzoyl)-N, N-diethylthiourea (Morales, A.D. et al., 2000) and ROLCAW01 represents N'-(4-methylbenzoyl)-N, N-diethylthiourea (Plutin, A.M. et al., 2000).

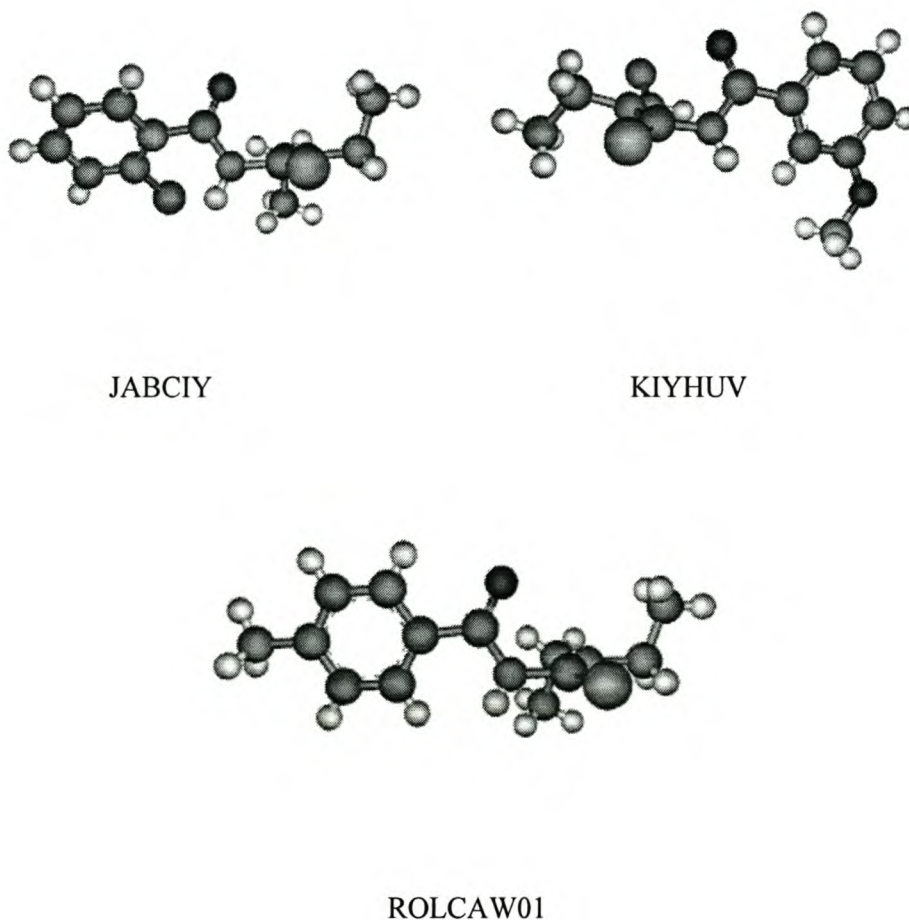


Fig. 5.4 Crystal structures of the three substituted acylthioureas obtained from the CCSD search. Oxygen indicated with red, sulphur with yellow, nitrogen with blue, carbon with grey and hydrogen with white.

Because the CCSD search did not yield enough crystal structures to be compared with all the theoretically calculated structures, a further literature search was made, which gave crystal structure data from compounds which were experimentally studied by Prof Koch, K.R. and his co-workers but not yet listed in CCSD. These compounds are N-(n-butyl)-N'-benzoyl thiourea(G) (Koch, K.R. et al., 1994), N-(n-propyl)-N'-benzoyl thiourea(H) (Koch, K.R.; Wang, Y.; Coetzee, A. 1999), N-(p-hexoxy)aniline-N'-(p-Methoxy)benzoyl-thiourea(I) (unpublished), N,N-di(n-butyl)-N'-naphthoyl thiourea (J) (Koch, K.R. et al., 1995), N,N-di(2-hydroxyethyl)-N'-benzoyl-thiourea(K) (Koch, K.R.; Sacht, C.; Bourne, S. 1995), and N,N-diethyl-N'-4-nitrobenzoyl thiourea(L) (Koch, K.R.; Matoetoe, M.; Mangaka, C. 1991).

5.3.1 Results and discussions

Despite the presence of small groups such as Cl, OCH₃, and CH₃ attached to the phenyl rings in JABCIY, KIYHUV, and ROLCAW01 respectively, the calculated structures of benzoyl thiourea compounds such as N, N-diethyl-N'-benzoyl thiourea (E), and N, N-dibutyl-N'-benzoyl thiourea (F) are considered to be similar enough to these molecules. In order to assess how close the structural similarity is comparisons were made between some internal coordinates of the comparable compounds.

Table 5.4 Selected internal coordinates of calculated structures E and F and experimental structures obtained from the CSD search.

Internal coordinate	Calculated Structures		Experimental crystal structures		
	E	F	JABCIY	KIYHUV	ROLCAW01
Bond length (Å)					
C(3)-C(1)	1.497	1.497	1.496	1.487	1.488
C(1)-O	1.193	1.193	1.217	1.212	1.223
C(1)-N(1)	1.386	1.385	1.360	1.388	1.349
N(1)-C(2)	1.405	1.406	1.428	1.403	1.432
C(2)-S	1.682	1.684	1.657	1.676	1.656
C(2)-N(2)	1.321	1.320	1.327	1.327	1.326
Valence angle(°)					
C(3)-C(1)-O	122.11	122.05	121.95	121.59	122.08
C(1)-N(1)-H	113.50	113.48	118.96	118.81	118.48

C(1)-N(1)-C(2)	124.64	124.98	122.02	122.34	121.59
S-C(2)-N(2)	125.63	125.66	126.13	124.18	126.36
Dihedral angle(°)					
C'-C(3)-C(1)-O	21.66	-21.96	-54.21	20.86	-8.75
O-C(1)-N(1)-C(2)	-11.95	12.05	6.53	0.78	5.36
C(1)-N(1)-C(2)-S	-121.32	121.52	103.95	-123.59	95.74
S-C(2)-N(2)-C''	4.87	-4.70	-3.90	12.09	-0.68

As **table 5.4** shows, both the calculated and experimental structures have similar values for bond lengths and valence angles. Minor differences are observed in the torsion angles, as was observed previously but as before these are expected. Therefore the calculated structures again correspond reasonably well to the crystal structures; hence the calculations made were accurate enough.

So as to assess all the molecules under study, further comparisons were made between the remaining six structures calculated in **chapter three**, and their crystal structures as found through the literature survey. Again there are close similarities between the calculated structures and their respective crystal structures, as can be seen from Table 5.5 below.

Table 5.5 Selected bond lengths (Å) of some experimental crystal structures of substituted acylthioureas G-L with their calculated counter parts in parenthesis.

Internal coordinate	Compound					
	G	H	I	J	K	L
C(1)-O	1.226(6) (1.202)	1.226(5) (1.202)	1.229(9) (1.203)	1.215(3) (1.194)	1.213(2) (1.195)	1.230(2) (1.192)
C(1)-N(1)	1.368(6) (1.374)	1.383(4) (1.374)	1.376(3) (1.377)	1.376(4) (1.382)	1.371(2) (1.384)	1.344(2) (1.381)
N(1)-C(2)	1.386(6) (1.388)	1.393(5) (1.387)	1.389(3) (1.386)	1.420(6) (1.407)	1.391(2) (1.407)	1.430(3) (1.410)
C(2)-S	1.676(5) (1.681)	1.678(4) (1.680)	1.661(2) (1.676)	1.662(2) (1.685)	1.672(2) (1.681)	1.663(2) (1.680)
C(2)-N(2)	1.317(6) (1.314)	1.332(7) (1.314)	1.332(3) (1.323)	1.320(3) (1.319)	1.335(3) (1.324)	1.324(3) (1.320)

In general, comparing the calculated structures with their respective experimental crystal structures obtained from single crystal x-ray diffraction analysis and the literature show that there is considerable agreement between the structures. Therefore, all the global minimum energy structures obtained in **chapter three** correspond to stable structures of the substituted acylthioureas under study. Hence these findings are tangible evidence for the accuracy of the quantum mechanical structural calculations made.

5.4 Atoms in Molecules analysis

In order to analyse the nature of the electron distribution in substituted acylthiourea compounds, AIM studies were conducted on the twelve compounds of interest. In the analysis calculations of the electron density, $\rho(r)$, and the Laplacian of electron density, $\nabla^2 \rho(r)$, and generation of the electron density diagrams were carried out using the **AIMPAC-95** suite of programs (Biegler-König, F.W.; Bader, R.F.W.; & Ting-Hau, T.J. 1982).

5.4.1 Results and discussions

Selected results of the AIM analysis carried out on the twelve (A-L) substituted acylthioureas are given in table 5.6 below.

Table 5.6 Electron density, $\rho(r)$, and Laplacian of the electron density, $\nabla^2 \rho(r)$, calculated at the bond critical point for selected bonds in acylthioureas (A-L).

Property	Bond	Compound					
		A	B	C	D	E	F
$\rho(r)$ (au)	C(1)-N(1)	0.308	0.313	0.309	0.309	0.312	0.312
	C(2)-N(1)	0.309	0.304	0.307	0.307	0.307	0.306
	C(2)-N(2)	0.359	0.355	0.356	0.356	0.355	0.356
	C(1)=O	0.432	0.432	0.432	0.432	0.433	0.432
	C(2)=S	0.207	0.207	0.207	0.206	0.207	0.206
	N-H	0.348	0.346	0.349	0.349	-	0.347
	O.....H	-	-	0.010	-	-	-
	N.....H	-	-	0.016	0.016	0.016	-
	S.....H	-	-	-	-	-	-
	C(1)-N(1)	-0.858	-0.959	-0.865	-0.864	-0.932	-0.930

$\nabla^2\rho(r)$ (au)	C(2)-N(1)	-1.080	-1.110	-1.109	-1.108	-1.101	-0.097
	C(2)-N(2)	-0.776	-0.841	-0.834	-0.825	-8.331	-0.829
	C(1)=O	0.456	0.405	0.454	0.452	0.412	0.406
	C(2)=S	0.264	0.260	0.253	0.248	0.262	0.258
	N-H	-1.826	-1.815	-1.831	-1.833	-	-1.819
	O.....H	-	-	0.041	-	-	-
	N.....H	-	-	0.069	0.069	0.069	-
	S.....H	-	-	-	-	-	-
$\rho(r)$ (au)		G	H	I	J	K	L
	C(1)-N(1)	0.318	0.318	0.316	0.312	0.314	0.317
	C(2)-N(1)	0.311	0.311	0.312	0.306	0.306	0.303
	C(2)-N(2)	0.363	0.363	0.357	0.357	0.355	0.357
	C(1)=O	0.426	0.426	0.425	0.433	0.431	0.434
	C(2)=S	0.206	0.206	0.207	0.207	0.208	0.207
	N-H	0.347	0.347	0.348	0.347	0.347	0.346
	O.....H	-	-	-	0.011	-	0.009
	N.....H	-	-	-	0.011	0.017	0.016
	S.....H	-	-	-	0.016	0.011	-
$\nabla^2\rho(r)$ (au)	C(1)-N(1)	-0.854	-0.854	-0.856	-0.884	-0.928	-0.949
	C(2)-N(1)	-0.918	-0.918	-0.928	-1.100	-1.085	-1.065
	C(2)-N(2)	-0.905	-0.905	-0.956	-0.833	-0.869	-0.840
	C(1)=O	0.317	0.317	0.294	0.403	0.392	0.425
	C(2)=S	0.296	0.296	0.325	0.251	0.274	0.278
	N-H	-1.832	-1.832	-1.837	-1.823	-1.819	-1.814
	O.....H	-	-	-	0.042	-	0.039
	N.....H	-	-	-	0.042	0.071	0.069
	S.....H	-	-	-	0.066	0.042	-

Comparison of the electron density, $\rho(r)$, of the three C-N bonds shows that in every case bond C(2)-N(2) has the highest value, bond N(1)-C(1) has an intermediate value and bond N(1)-C(2) has the lowest value of the three. As electron density is the ratio of number of electrons per unit volume, this means that the C(2)-N(2) bond which was computationally and experimentally

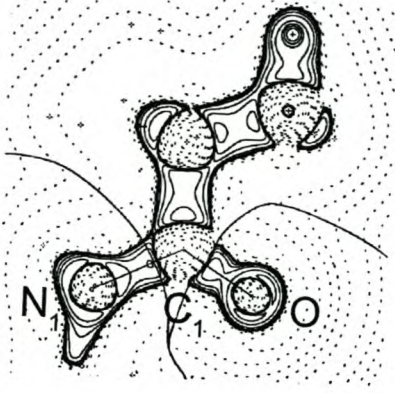
found to be the shortest has the highest electron density, as expected. Likewise, the N(1)-C(1) bond is found to have intermediate electron density, while the N(1)-C(2) bond, which is relatively the longest bond, is found to have the least electron density. This trend shows the inverse relationship that exists between bond length and electron density at the bond critical point, for a specific bond.

For all the C-N bonds, the N(1)-H bond, and all the hydrogen bonds, the Laplacian has negative values ($\nabla^2\rho(r) < 0$). Hence, according to the general definition (**section 2.7.1**), the bond critical points of these bonds have a high electron charge concentration. On the other hand, the C(1)=O, and C(2)=S, bonds have a positive Laplacian ($\nabla^2\rho(r) > 0$). Therefore, in contrast to the bonds mentioned above, bond critical points of these bonds are electron depleted regions. Depletion of the electron charge on the bond critical points of the C(1)=O and C(2)=S bonds implies concentration of the electron density elsewhere in the neighbouring region. As these bonds consist of a C atom and either O or S atoms the electron density is more likely to be concentrated on the relatively more electronegative O and S atoms. Such a concentration of the electric charge around the O and S atoms enables them to behave as nucleophilic centres, a finding which is in good agreement with the nucleophilic character of the O & S atoms in these molecules that has been previously proved (Plutin, A.M., 2000).

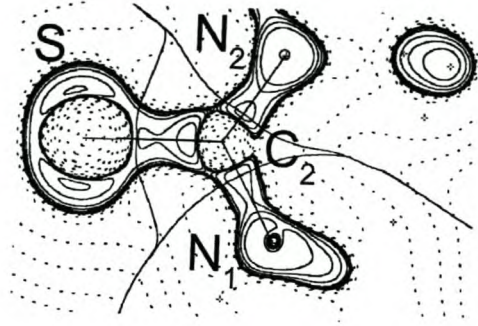
The other important property studied using the AIM method is the formation of hydrogen bonding. As the analysis shows, some of the substituted acylthioureas form hydrogen bonds. The bonds are formed between the proton of one of the substituent groups (**R, R' or R''**), and the heavy atoms such as O, S and N. According to the proposal by Koch and Popelier (Popelier, P. 2000) one of the criteria for a bond to be accepted as a hydrogen bond are an electron density $\rho(r)$ value of 0.002 to 0.04au and a Laplacian $\nabla^2\rho(r)$ of -0.15 to -0.02au at its bond critical point. Therefore the results obtained in this study indicate that compounds C, D, E, J, K and L have hydrogen bonds in their stable structures. As the tabulated data show, the compounds under investigation can have one to three hydrogen bonds and these bonds play significant role in their stabilization.

The electron density distribution that exists in the different bonds can be demonstrated using various plots, such as a contour plot of the Laplacian of the electron density as shown in **fig. 5.5** below.

(A)

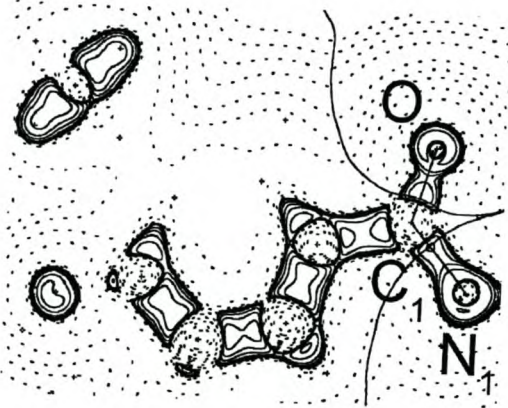


(I)

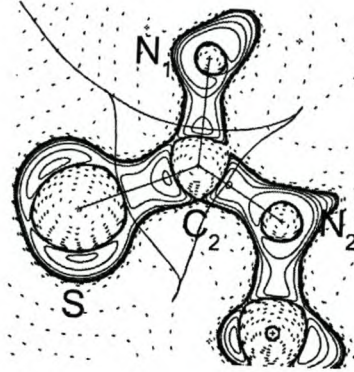


(II)

(B)

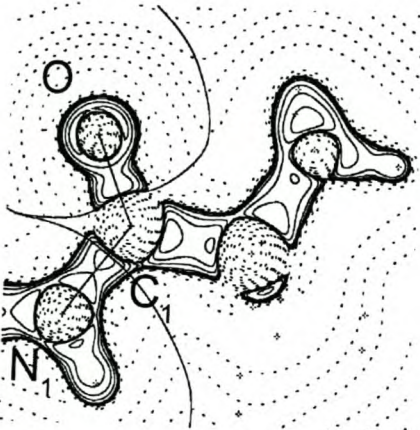


(I)

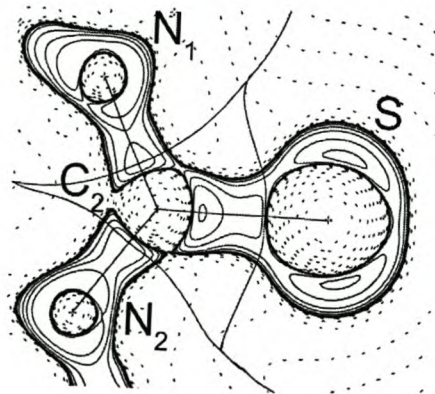


(II)

(C)

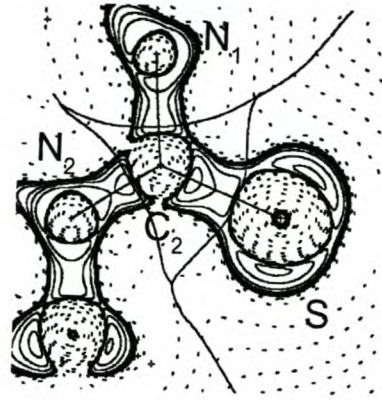
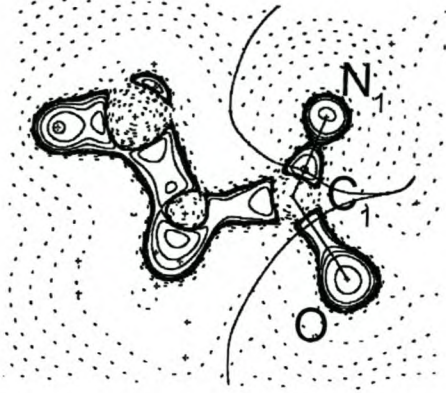


(I)



(II)

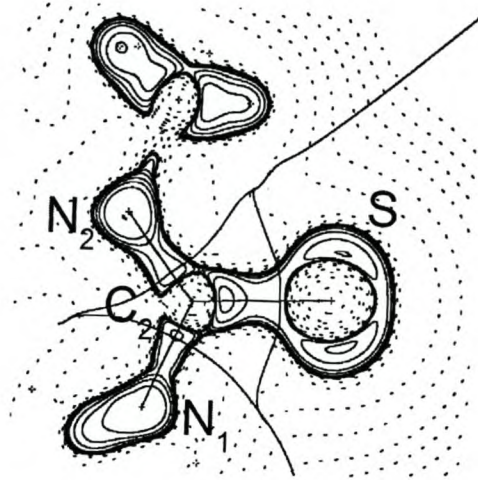
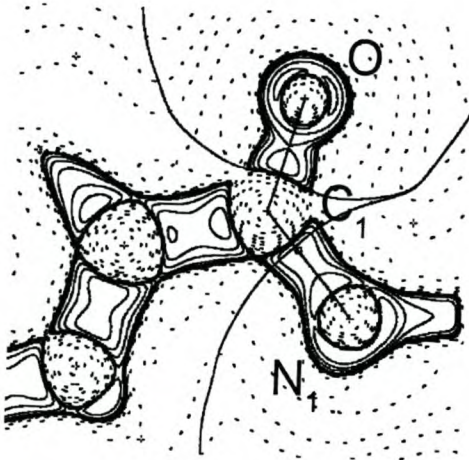
(D)



(I)

(II)

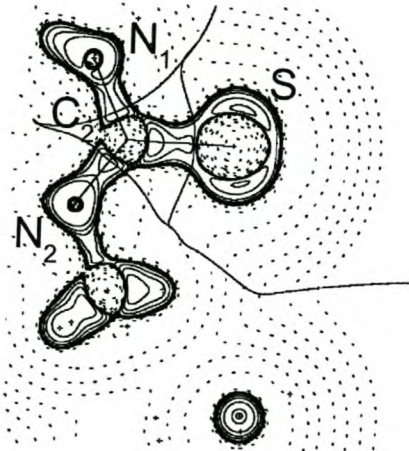
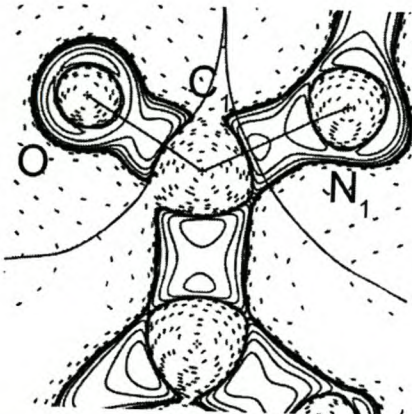
(E)



(I)

(II)

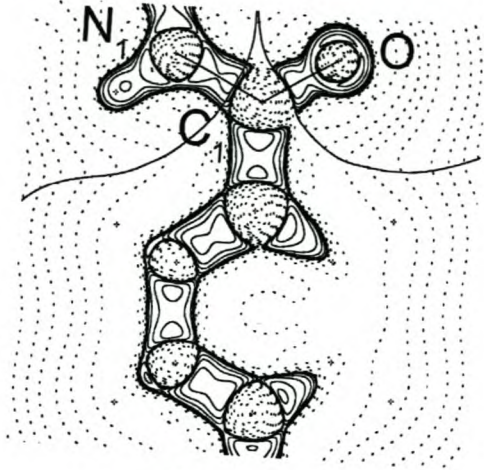
(F)



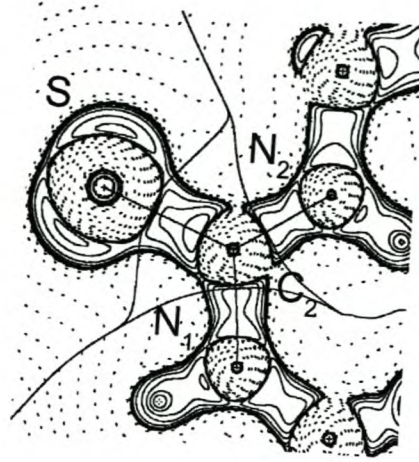
(I)

(II)

(G)

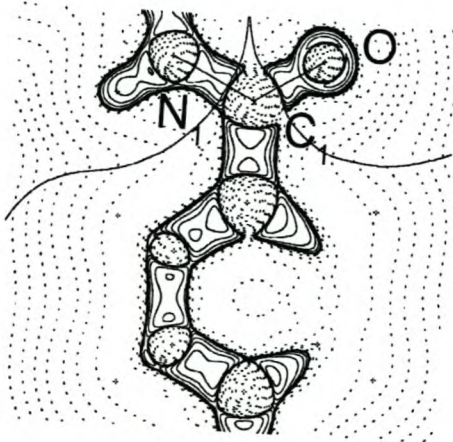


(I)

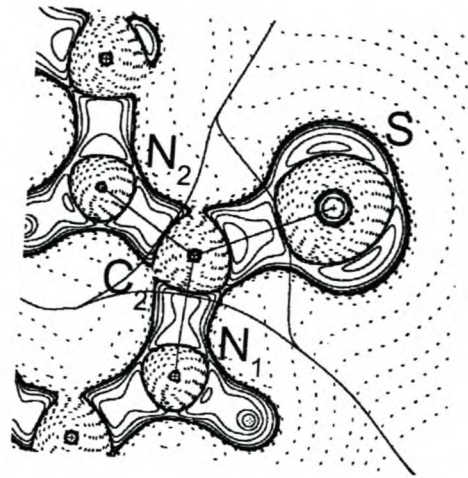


(II)

(H)

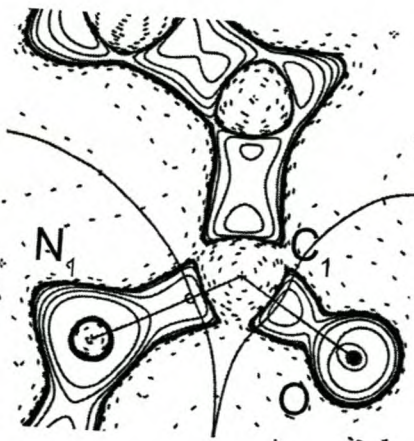


(I)

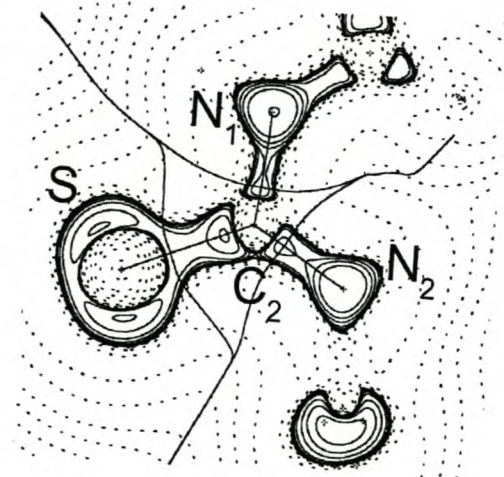


(II)

(I)

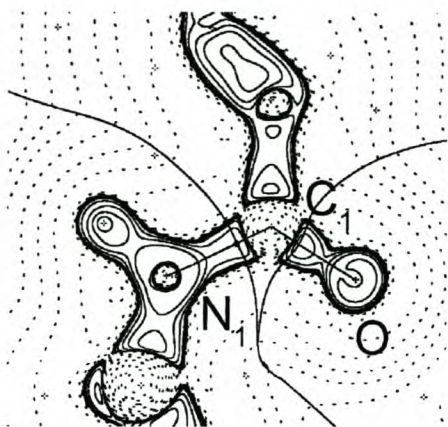


(I)

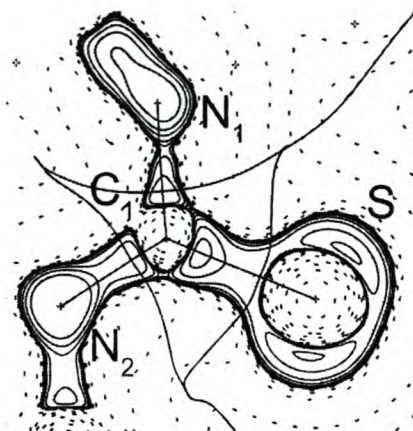


(II)

(J)

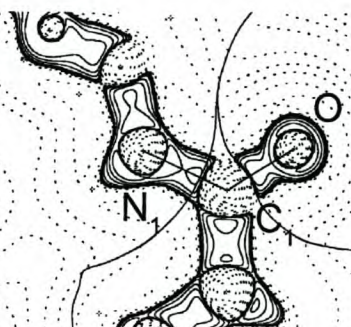


(I)

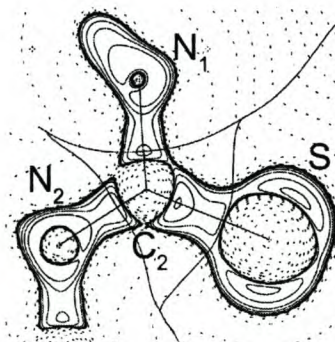


(II)

(K)

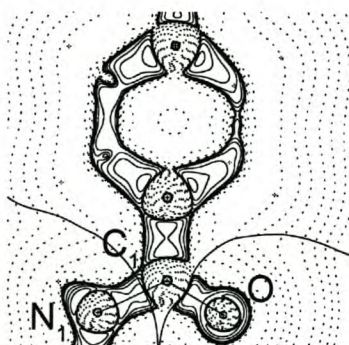


(I)

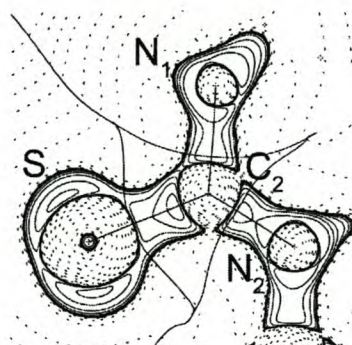


(II)

(L)



(I)



(II)

Fig.5.5 Contour plots of the Laplacian of the electron density, $\nabla^2\rho(r)$, for substituted acylthioureas A to L. (I) Plot in the plane defined by O-C(1)-N(1), which contains bonds C(1)=O and C(1)-N(1) and their bond critical points. (II) Plot in the plane defined by N(1)-C(2)-S-N(2),

which contains bonds $C(2)-N(1)$, $C(2)=S$ and $C(2)-N(2)$ and their bond critical points. The solid lines indicate areas of charge concentration and the dotted lines those of charge depletion. The straight lines connecting the nuclei are bond paths and those, which bisect them at the bond critical point, are gradient paths (zero flux lines).

As can be seen from the contour plots above, the bond critical points are located at the junction between the bond path and gradient path (zero flux line). In all diagrams the electron density is clearly visible, regions with solid contour lines indicate areas of local charge concentration, and those with dotted lines indicate areas of charge depletion.

Besides giving a clear picture of the electron distribution, the AIM analysis is also useful for bond characterisation. Therefore bonds which have negative Laplacian, $\nabla^2\rho(r) < 0$, have high charge concentration on their bond critical points, and they are known as *sharing interaction* bonds; these bonds encompass covalent and polar bonds. Bonds with positive Laplacian, $\nabla^2\rho(r) > 0$, on the other hand, are known as *closed-shell interaction* bonds (Dillen, J.L., 2003); bonds such as ionic, hydrogen, Van der Waals complexes and noble gas clusters fall under this category. Therefore, according to this systematic bond characterisation, the $C(1)=O$, $C(2)=S$, and all the hydrogen bonds fall within the *closed-shell interaction* group and the remaining bonds fall in the *sharing interaction* bond type.

The AIM analysis technique has thus been successfully used to determine the electronic charge distribution, to detect the presence of hydrogen bonding and to characterise bonds in the various substituted acylthioureas under investigation.

5.5 Natural bond orbital analysis

As discussed earlier (section 2.7.2), the natural bond orbital method is a very important tool for the analysis of chemical bonds. It consists of a set of different analysis techniques, of which natural population analysis is one that is very useful for the determination of the occupancy and charge distribution in molecular orbitals. Besides this, it can also be used for the study of donor-acceptor interactions in molecular orbitals. In this work, NBO analysis was conducted on the twelve substituted acylthioureas using the **NBO-5** program (Glendening, E.D. et al., 2001); molecular structure diagrams were drawn using the **NBOView** program.

5.5.1 Natural Population Analysis

With the aim of analysing the charge distribution, NBO based population analysis was carried out on the twelve substituted acylthioureas under consideration. In order to supplement the

analysis Mulliken based charge calculations were also conducted. Results of both are recorded in Table 5.7 below.

Table 5.7 Atomic charges (*e*) of selected atoms in substituted acylthioureas (A-L) calculated using NBO and Mulliken methods.

Method	Atom	Compounds					
		A	B	C	D	E	F
N B O	C(3)	-0.1446	-0.1662	-0.1446	-0.1447	-0.1838	-0.1834
	C(1)	0.8635	0.8511	0.8640	0.8652	0.8499	0.8502
	O	-0.6885	-0.6899	-0.6918	-0.6933	-0.6864	-0.6884
	N(1)	-0.7697	-0.7761	-0.7738	-0.7740	-0.7739	-0.7730
	H(1)	0.4402	0.4480	0.4408	0.4411	0.4480	0.4482
	C(2)	0.4366	0.4346	0.4365	0.4382	0.4342	0.4360
	S	-0.3317	0.3189	-0.3309	-0.3354	-0.3247	-0.3290
	N(2)	-0.5104	-0.5148	-0.5081	-0.4965	-0.5067	-0.4978
M U L L I K E N							
	C(3)	-0.1711	-0.1199	-0.1732	-0.1739	-0.1225	-0.1229
	C(1)	0.7913	0.7757	0.7871	0.7886	0.7727	0.7736
	O	-0.5787	-0.5757	-0.5775	-0.5779	-0.5726	-0.5741
	N(1)	-0.8243	-0.8331	-0.8220	-0.8248	-0.8362	-0.8369
	H(1)	0.4247	0.4252	0.4254	0.4261	0.4253	0.4256
	C(2)	0.4622	0.4630	0.4588	0.4619	0.4678	0.4687
	S	-0.3485	-0.3360	-0.3451	-0.3496	-0.3393	-0.3434
N(2)	-0.6038	-0.6187	-0.5701	-0.5901	-0.5723	-0.5905	
N B O							
		G	H	I	J	K	L
	C(3)	-0.1813	-0.1814	-0.2353	-0.1444	-0.1772	-0.1347
	C(1)	0.8578	0.8578	0.8598	-0.8509	0.8523	0.8450
	O	-0.7117	-0.7117	-0.7202	-0.6857	-0.6442	-0.6754
	N(1)	-0.7407	-0.7407	-0.7420	-0.7680	-0.7831	-0.7704
	H(1)	0.4518	0.4519	0.4502	0.4506	0.4541	0.4487
	C(2)	0.4282	0.4280	0.4287	0.4350	0.4213	0.4260
S	-0.3395	-0.3390	-0.3169	-0.3299	-0.2540	-0.3096	

	N(2)	-0.6784	-0.6792	-0.6895	-0.4981	-0.5531	-0.5077
M							
U	C(3)	-0.1112	-0.1111	-0.1507	-0.0767	-0.1328	-0.1008
L	C(1)	0.8253	0.8252	0.8413	0.7215	0.8184	0.7798
L	O	-0.6158	-0.6159	-0.6260	-0.5678	-0.5337	-0.5617
I	N(1)	-0.8674	-0.8671	-0.8732	-0.8114	-0.9194	-0.8335
K	H(1)	0.4366	0.4366	0.4371	0.4325	0.4751	0.4265
E	C(2)	0.5070	0.5065	0.5004	0.4544	0.4956	0.4595
N	S	-0.3517	-0.3511	-0.3343	-0.3436	-0.2803	-0.3238
	N(2)	-0.7888	-0.7870	-0.8376	-0.5864	-0.6361	-0.5705

5.5.1.1 Result and discussion

As the charges tabulated above show, the assignment of charge was made on selected atoms. The atoms, which were taken into consideration, were those which are close to the carbonyl and thio-carbonyl moieties, and hence located on the chemically active parts of the molecules.

Analysis shows that all the O, S, and N atoms in each compound are assigned negative charges. As these atoms are electronegative by nature, the calculated charges are reasonable. The charge on the C atoms varies depending on its environment. For example, both the carbonyl and thio-carbonyl carbons possess positive charges. As these carbon atoms are attached to the relatively more electronegative O and S atoms this is to be expected. On the other hand, carbon atoms attached to the R substituent group are assigned negative charges, which are probably because these carbons are relatively more electronegative than the atoms in the substituent groups. The charge of the acidic proton H(1), is found to be positive in all compounds. This is reasonable because it is attached to the relatively more electronegative nitrogen atom.

A comparison made between charges on the atoms in different compounds shows the existence of very little but inconsistent variation. Therefore it is impossible to make any generalization on the trend of charge variation with change of substituents in substituted acylthioureas.

All the observations and general remarks made above on atomic charges on different atoms of substituted acylthioureas hold true for both the NBO and Mulliken based calculated charges. The NBO method of analysis is believed to be robust toward the variation of basis sets relative to the Mulliken method, (Frenking, G., & Fröhlich, N., 2000), however since only the 6-31G(d) basis set was used for all the calculations, it is not possible to prove this property of the NBO.

5.5.2 Second order Perturbation theory energy analysis

In order to reveal the secret behind the shortening observed for one of the three C-N bonds of substituted acylthioureas, second order perturbation theory was used. The analysis was conducted by examining all possible interactions between donor Lewis type NBOs and acceptor non-Lewis NBOs and estimating their energetic importance by second order perturbation theory. Since these interactions lead to donation of occupancy from the localized NBOs of the idealized Lewis structure into the empty non-Lewis orbital, they are considered as corrections to the zeroth-order natural Lewis structure delocalization. For each donor NBO (i) and acceptor NBO (j), the stabilization energy $E(2)$ associated with delocalization ($2e^-$ stabilization) is given as:

$$E(2) = \Delta E_{ij} = q_i \frac{F(i,j)^2}{\varepsilon_j - \varepsilon_i} \quad (5.1)$$

where q_i is the donor orbital occupancy, ε_i , and ε_j are orbital energies and $F(i,j)$ is the off-diagonal NBO Fock matrix element.

5.5.2.1 Results and Discussion

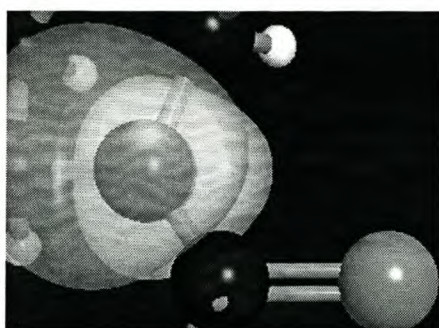
Once the second order perturbation energy analysis had been carried out on all the compounds under consideration, comparisons were made between energies of the donor-acceptor interactions involved in the region of the carbonyl and thio-carbonyl moieties and among them those, which have the largest delocalization energies, are recorded in table 5.8 below.

Table 5.8 Delocalization energies of donor-acceptor interactions in substituted acylthioureas.

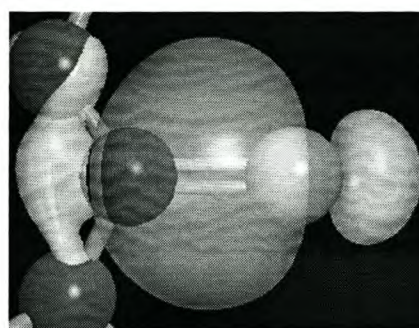
Compound	Donor NBO(i)	Acceptor NBO(j)	Energy (E(2)) (Kcal/mol)	E(j)-E(i) a.u.	Donor occupancy (q _i)	Acceptor occupancy (q _j)
A	$n_{N(2)}$	$\pi^*_{C(2)-S}$	162.21	0.41	1.64	1.98
B	$n_{N(2)}$	$n^*_{C(2)}$	227.08	0.28	1.63	0.76
C	$n_{N(2)}$	$\pi^*_{C(2)-S}$	161.62	0.41	1.63	1.98
D	$n_{N(2)}$	$\pi^*_{C(2)-S}$	164.60	0.40	1.63	1.98
E	$n_{N(2)}$	$n^*_{C(2)}$	216.78	0.28	1.64	0.76

<i>F</i>	$n_{N(2)}$	$n^*_{C(2)}$	221.17	0.28	1.64	0.76
<i>G</i>	$n_{N(2)}$	$n^*_{C(2)}$	210.64	0.29	1.67	0.75
<i>H</i>	$n_{N(2)}$	$n^*_{C(2)}$	210.25	0.29	1.67	0.75
<i>I</i>	$n_{N(2)}$	$n^*_{C(2)}$	192.02	0.30	1.69	0.75
<i>J</i>	$n_{N(2)}$	$n^*_{C(2)}$	219.97	0.28	1.63	0.76
<i>K</i>	$n_{N(2)}$	$\pi^*_{C(2)-S}$	112.32	0.45	1.71	1.98
<i>L</i>	$n_{N(2)}$	$n^*_{C(2)}$	218.82	0.28	1.64	0.76

As the above data show, all the high energy stabilizations take place as a result of donation of lone pairs from the substituent bearing nitrogen atom, N(2) to different sites. Among the many possible sites, two in particular are shown to be favoured by very high delocalization energy. The first one is where the lone pair is donated into the anti-bonding π -orbital of the vicinal C=S bond ($n_{N(2)} \rightarrow \pi^*_{C(2)-S}$), while the second is the non-Lewis lone pair NBO of the geminal thio-carbonyl carbon ($n_{N(2)} \rightarrow n^*_{C(2)}$). These combined donor-acceptor interactions lead to the presence of strong delocalization in the S=C(2)–N(2) region of the acylthioureas. This strong delocalization allows the C(2)-N(2) bond to attain a partial double bond character, and this is the main factor that is responsible for the shortening of this bond relative to the other C-N bonds in acylthiourea compounds.



(A)



(B)

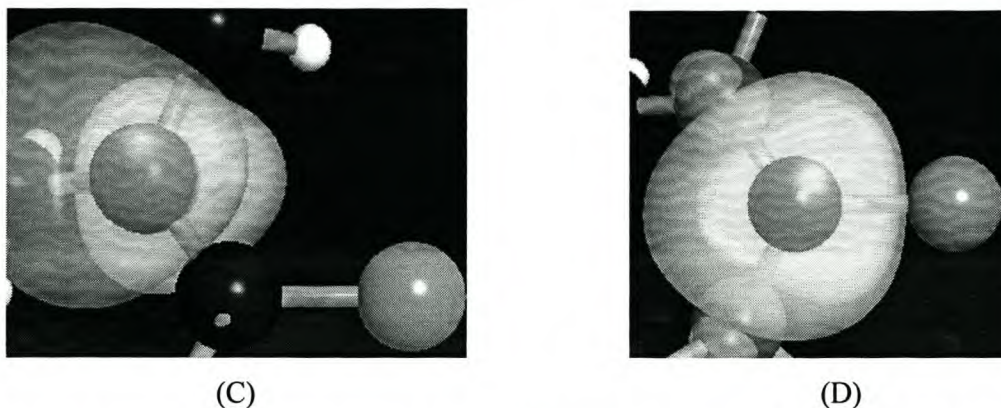


Fig. 5.4 Valence shell NBOs of *N*-pyrrolidine-*N'*-pivaloyl thiourea (HF/6-31G(d)) showing (A) donor orbital $n_{N(2)}$; (B) acceptor orbital $\pi^*_{C(2)-S}$. Similarly for *N*, *N*-diethyl-*N'*-4-nitrobenzoyl thiourea; (C) donor orbital $n_{N(2)}$ and (D) acceptor orbital $n^*_{C(2)}$.

In an effort to identify the possible cause of the strong delocalization in the S=C(2)-N(2) region, further analysis of the proton and methyl substituted compounds was undertaken by exchanging the positions of the O and S atoms. Upon replacement of S by O, the region was no longer delocalized. For instance, the energy of delocalization in the methyl substituted compound before replacement of S with O is 155.38Kcal mol⁻¹, but upon replacement of S with O the energy drops to 16.05Kcal mol⁻¹. Another comparison of the C-N bond lengths in the proton and methyl substituted compounds with exchanged S and O atoms shows that the C(2)-N(2) bond is no longer the shortest one, instead the C(1)-N(1) bond that is located geminal to the newly placed S atom is the shortest. Therefore, these observations lead to the conclusion that the sulphur atom is the main cause of the strong delocalization and hence of the shortening of one of the three C-N bonds in substituted acylthioureas.

5.6 Natural resonance theory analysis

All the theoretical and experimental studies so far have qualitatively proved the existence of a varying degree of delocalization on the substituted acylthioureas. These properties were manifested by the existence of different tautomeric forms, shortening of one of the C-N bonds, etc. Therefore the NRT analysis was carried out to quantitatively determine the extent of delocalization through the study of possible resonance structures.

Substituted acylthioureas have many resonance forms. However as qualitatively predicted by some experimental studies, the most dominant resonance structures are the following four (Dago, A. et al., 1989).

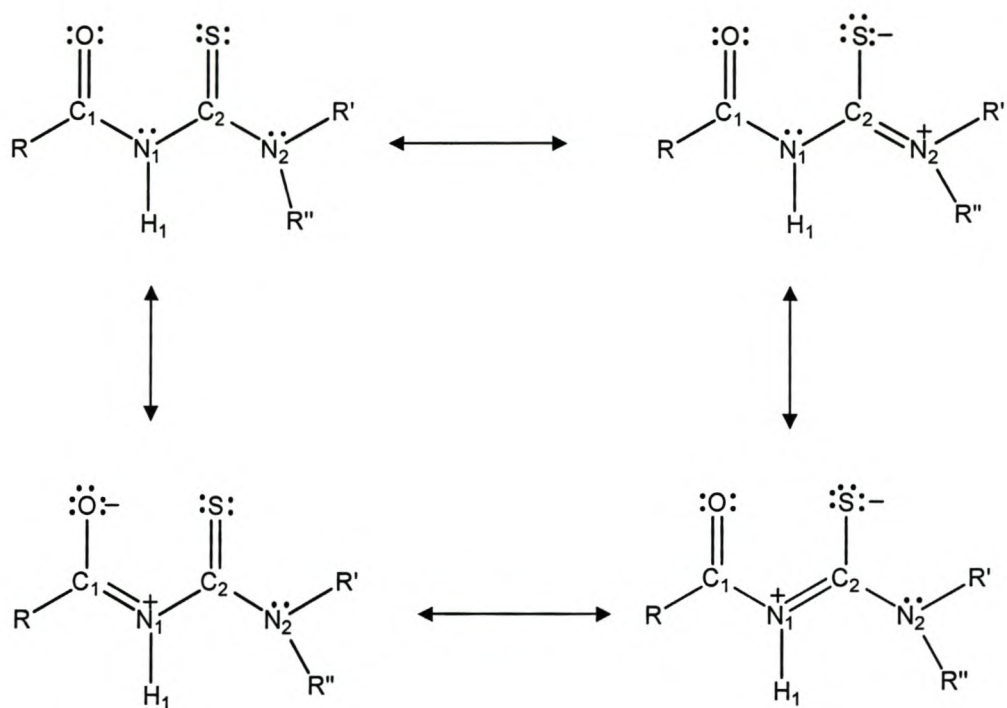


Fig. 5.6 Major resonance structures of substituted acylthioureas.

Therefore, with the aim of determining the contribution of each of the different resonance structures of the substituted acylthioureas quantitatively, and hence identify the dominant resonance structure, NRT analysis was conducted.

5.6.1 Result and discussion:

The analysis was carried out on ten compounds without any difficulty; the only problems raised were by the relatively bulky compounds, N-(2, 6-dimethyl piperidine)-N'-(3, 4, 5-methoxy)-benzoyl thiourea and N-(p-hexoxy) aniline-N'-(p-Methoxy) benzoyl-thiourea. This is due to the existence of too many resonance structures to be handled by NRT. Hence these two were excluded from the analysis. From the large number of resonance structures obtained for the analysed compounds, the top five structures with the highest resonance weight were selected and they are given in table 5.9.

Table 5.9 The five top resonance weight structures of *N*-pyrrolidine-*N'*-pivaloyl thiourea (*A*).

N ^o	Structure	Weight (%)	Interaction
i		30.33	Ref. str.
ii		27.70	$n_{N_2} \rightarrow \sigma^*_{C_2N_2}$
iii		4.0	$n_{N_1} \rightarrow \sigma^*_{C_1N_1}$
iv		3.92	$n_{N_2} \rightarrow \sigma^*_{C_2N_2}$, $n_{N_1} \rightarrow \sigma^*_{C_1N_1}$
v		3.36	$n_{N_1} \rightarrow \sigma^*_{C_2N_1}$

* Ref. str. = Reference structure

Table 5.10 The five top resonance weight structures of *N, N*-diethyl-*N'*-pivaloyl thiourea (*C*).

N ^o	Structure	Weight	Interaction
i		30.59	Ref. str.
ii		28.20	$n_{N_2} \rightarrow \sigma^*_{C_2N_2}$
iii		3.93	$n_{N_1} \rightarrow \sigma^*_{C_1N_1}$, $n_{N_2} \rightarrow \sigma^*_{C_2N_2}$
iv		3.65	$n_{N_1} \rightarrow \sigma^*_{C_1N_1}$
v		3.32	$n_{N_1} \rightarrow \sigma^*_{C_2N_1}$

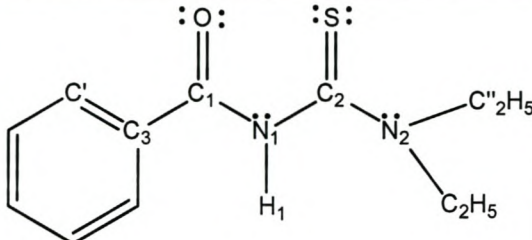
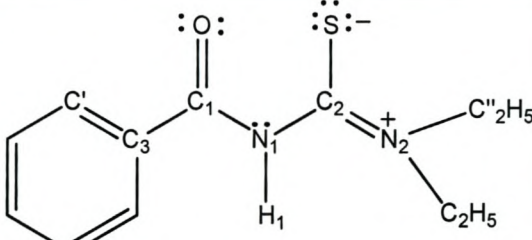
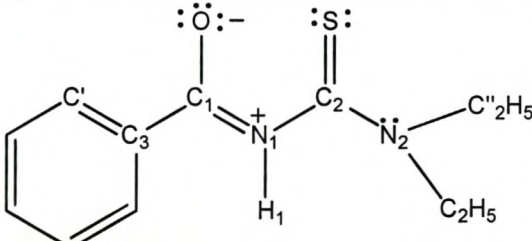
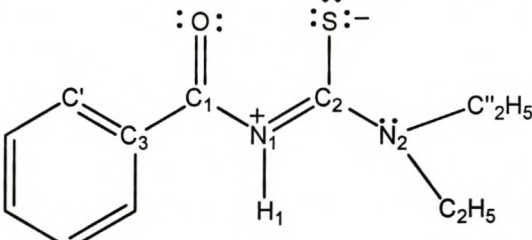
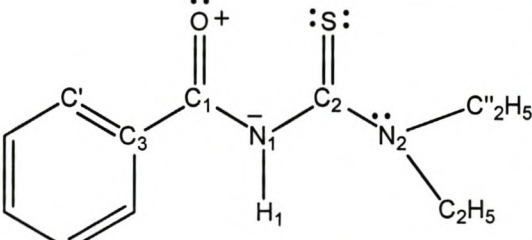
* Ref. str. = Reference structure

Table 5.11 The five top resonance weight structures of *N, N*-dibutyl-*N'*-pivaloyl thiourea (*D*).

N ^o	Structure	Weight	Interaction
i		26.53	Ref. str.
ii		24.57	$n_{N_2} \rightarrow \sigma^*_{C_2N_2}$
iii		3.95	$n_{N_1} \rightarrow \sigma^*_{C_1N_1}$, $n_{N_2} \rightarrow \sigma^*_{C_2N_2}$
iv		3.65	$n_{N_1} \rightarrow \sigma^*_{C_1N_1}$
v		3.43	$n_{N_1} \rightarrow \sigma^*_{C_2N_1}$

* Ref. str. = Reference structure

Table 5.12 The five top resonance weight structures of *N, N*-diethyl-*N'*-benzoyl thiourea (*E*).

N ^o	Structure	Weight	Interaction
i		30.40	Ref. str.
ii		17.16	$n_{N_2} \rightarrow \sigma^*_{C_2N_2}$
iii		6.83	$n_{N_1} \rightarrow \sigma^*_{C_1N_1}$
iv		4.12	$n_{N_1} \rightarrow \sigma^*_{C_2N_1}$
v		3.45	$n_O \rightarrow n_{N_1}$

* Ref. str. = Reference structure

Table 5.13 The five top resonance weight structures of *N, N*-dibutyl-*N'*-benzoyl thiourea (*F*).

N ^o	Structure	Weight	Interaction
i		27.27	Ref. str.
ii		16.75	$n_{N_2} \rightarrow \sigma^*_{C_2N_2}$
iii		6.43	$n_{N_1} \rightarrow \sigma^*_{C_1N_1}$
iv		4.46	$n_{N_1} \rightarrow \sigma^*_{C_2N_1}$
v		3.44	$n_O \rightarrow n_{N_1}$

* Ref. str. = Reference structure

Table 5.14 The five top resonance weight structures of *N*-(*n*-butyl)-*N'*-benzoyl thiourea (*G*).

N ^o	Structure	Weight	Interaction
i		40.92	Ref. str.
ii		30.28	$n_{N_2} \rightarrow \sigma^*_{C_2N_2}$
iii		7.46	$n_{N_1} \rightarrow \sigma^*_{C_2N_1}$
iv		6.78	$n_{N_1} \rightarrow \sigma^*_{C_1N_1}$ $n_{N_2} \rightarrow \sigma^*_{C_2N_2}$
v		5.6	$n_{N_1} \rightarrow \sigma^*_{C_1N_1}$

* Ref. str. = Reference structure

Table 5.15 The five top resonance weight structures of *N*-(*n*-propyl)-*N'*-benzoyl thiourea (*H*).

N ^o	Structure	Weight	Interaction
i		42.06	Ref. str.
ii		31	$n_{N_2} \rightarrow \sigma^*_{C_2N_2}$
iii		7.64	$n_{N_1} \rightarrow \sigma^*_{C_1N_1}$, $n_{N_2} \rightarrow \sigma^*_{C_2N_2}$
iv		6.53	$n_{N_1} \rightarrow \sigma^*_{C_2N_1}$
v		3.41	$n_{N_1} \rightarrow \sigma^*_{C_1N_1}$

* Ref. str. = Reference structure

Table 5.16 The five top resonance weight structures of *N, N*-di (*n*-butyl)-*N'*-naphthoyl thiourea (*J*).

N ^o	Structure	Weight	Interaction
i		37.03	Ref. str.
ii		35.89	$n_{N_2} \rightarrow \sigma^*_{C_2N_2}$
iii		7.21	$n_{N_1} \rightarrow \sigma^*_{C_2N_1}$
iv		2.93	$n_{N_1} \rightarrow \sigma^*_{C_1N_1}$
v		2.54	$n_{N_2} \rightarrow \sigma^*_{C_2N_2}$ $\sigma^*_{OC_1} \rightarrow n_O$

* Ref. str. = Reference structure

Table 5.17 The five top resonance weight structures of *N, N*-di (2-hydroxyethyl)-*N'*-benzoyl thiourea (*K*).

N ^o	Structure	Weight	Interaction
i		46.28	Ref. str.
ii		25.98	$n_{N_2} \rightarrow \sigma^*_{C_2N_2}$
iii		13.14	$n_{N_1} \rightarrow \sigma^*_{C_2N_1}$
iv		5.64	$n_{N_1} \rightarrow \sigma^*_{C_1N_1}$
v		3.96	$n_O \rightarrow n_{N_1}$

* Ref. str. = Reference structure

Table 5.18 The five top resonance weight structures of *N, N*-diethyl-*N'*-4-nitroenzoyl thiourea (*L*).

N ^o	Structure	Weight	Interaction
i		47.29	Ref. str.
ii		38.7	$n_{N_2} \rightarrow \sigma^*_{C_2N_2}$, $n_{N_3} \rightarrow \sigma_{N_3O_3}$
iii		3.48	$n_{N_1} \rightarrow \sigma^*_{C_2N_1}$, $n_{N_3} \rightarrow \sigma_{N_3O_3}$, $n_{O_4} \rightarrow \sigma_{N_3O_4}$
iv		1.24	$n_{N_2} \rightarrow \sigma^*_{C_2N_2}$, $n_{N_3} \rightarrow \sigma_{N_3O_3}$, $n_{O_4} \rightarrow n_{N_3}$, $\pi_{C_3C_1} \rightarrow \sigma^*_{C_3C_1}$, $\pi_{C_1O} \rightarrow n_O$
v		1.12	$\sigma_{C_1O} \rightarrow n_O$, $\pi_{C_3C_1} \rightarrow \sigma^*_{C_3C_1}$, $n_{N_3} \rightarrow \sigma_{N_3O_3}$, $n_{O_4} \rightarrow n_{N_3}$

* Ref. str. = Reference structure

In all the NRT analysis results demonstrated above, the first structure is the reference structure (Ref. str.). This is the leading resonance structure and it contains all the bonds and lone pairs of the compound under consideration. All the other secondary resonance structures are

generated from the reference structure by adding or removing some of the bonds or lone pairs alternatively. Therefore each secondary resonance structure is specified by mentioning the bonds and lone pairs added or removed. For example the first secondary resonance structure in N-pyrrolidine-N'-pivaloyl thiourea, which has a resonance weight of 27.70 %, is formed from the reference structure by removing lone pairs of N(2), adding bond C(2)-N(2), removing bond C(2)-S, and adding a lone pair to S. All these shifts are represented by the NBO interaction $n_{N_2} \rightarrow \sigma^*_{C_2N_2}$, which indicates the removal of a lone pair from N(2), and its transfer to the anti-bonding sigma orbital of bond C(2)-N(2) to form a double bond. The other secondary structures for this compound as well as the other compounds are defined in a similar way and, depending on the number of bonds and lone pairs added and removed, the number of NBO interactions can be more than one.

The NRT analysis made in all substituted acylthioureas under investigation shows that the high weight resonance structure that immediately follows the reference structure is the one in which the C(2)-N(2) bond is the double bond. Comparisons made between resonance weights of the reference structure and the high weighted secondary structures in all compounds show that they have an average difference which is not larger than 10%. For this reason substituted acylthiourea compounds are presumed to exist resonating between these two structures.

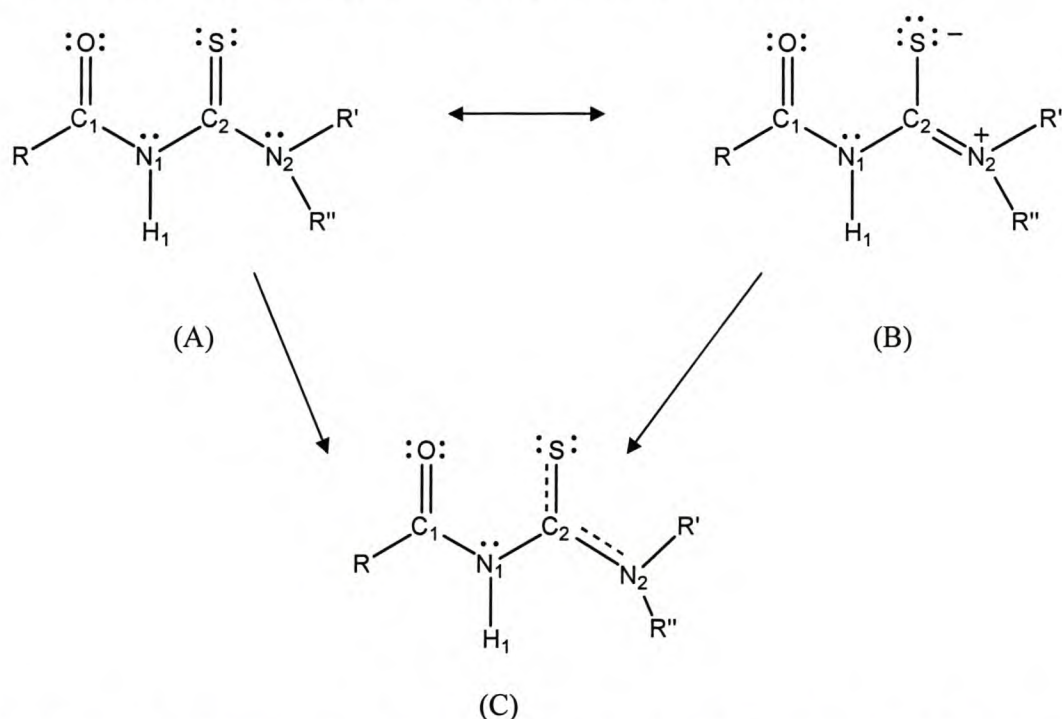


Fig. 5.7 General representation of resonance structures of acylthioureas with dominant weights. (A) The most dominant reference resonance structure. (B) Secondary resonance structure next in weight to the reference structure. (C) Resonance structure intermediate between the two top weighted structures.

Chapter six

Conclusion

6.1 Summary

The comprehensive study of the stability and structural properties of substituted acylthioureas described in this work can be summarized as follows:

6.1.1 Modelling and Stability:

- Due to its better accuracy compared to the other methods, the computational study of the substituted acylthioureas was carried out using *ab initio* quantum mechanical methods. The calculations in this work were carried out using the 6-31G(d) basis set at the Hartree-Fock level of theory. This method was found to be very effective, as expected, as it had been in an earlier study (Albertus, M.S and Piris, M. 2001).
- The search for the preferential tautomeric form of the substituted acylthioureas shows that the one in which the mobile proton is attached to the central nitrogen atom, i.e. N (1) as in **fig. 3.5** is the most stable of the three possible tautomeric forms.
- The quantum mechanical modelling carried out on twelve selected mono and di-alkyl substituted acylthioureas enabled one to find the most stable structure of each compound. According to the analysis, the *trans* orientation of the carbonyl and thio-carbonyl moieties is found to be a general trend in all the compounds studied, and this lead to the conclusion that this is a common trend in the stable structures of all substituted acylthioureas.

6.1.2 Infra-red Studies:

- Comparison of the experimental wavenumbers and their theoretical counterparts showed that they have a considerable agreement. This enabled the exact assignment of the infra-red stretching bands for all bonds in the substituted acylthioureas in general and for the most ambiguous and difficult C=S bond in particular. The bending vibrational modes of all the compounds were also assigned.
- Furthermore, the effect of the variation of substituents, **R**, **R'**, and **R''** on the infra-red absorption frequencies of the chemically active C=O and C=S bonds was studied. This analysis was done by taking the C=O and C=S absorption wavenumbers of the proton substituted acylthioureas, which are 1780 cm⁻¹ and 665 cm⁻¹ respectively as references. It was shown that the substituents of the twelve compounds studied lowered the C=O frequency and raised the C=S frequency. The extent of frequency lowering or raising however varied from one substituent to another with the general trends described in **Section**

In the intermediate structure shown in **fig. 5.7(C)** above, the C(2)-N(2) bond has a partial double bond character. This prediction by the NRT analysis is in good agreement with all theoretical as well as experimental studies made so far. Therefore, it can be concluded that the resonating of substituted acylthioureas between the two top weight resonance structures is the main cause of the shortening of one of their three C-N bonds.

4.4. The greatest effect on the C=O frequency was obtained when the **R** group was substituted with the strongly conjugating methoxy phenyl group in mono-alkyl substituted compounds, and with the tri-methoxy phenyl group in di-alkyl substituted compounds. On the other hand, substitution of the **R'** and **R''** groups by weak electron withdrawing groups such as hexoxy phenyl and piperidine groups in the mono and di-alkyl substituted compounds respectively caused the least rise in the stretching frequency of the thio-carbonyl groups. Therefore these substituent groups due to their relatively better electron enriching potential; enhance the nucleophilic character of the O and S atoms and can make the compounds prone toward coordination to a metal centre when used as ligands.

6.1.3 Electronic Structure Studies (X-ray diffraction, AIM, NBO, NRT):

- In order to confirm the accuracy of the calculated stable structures, single crystal X-ray diffraction analysis was carried out on N-pivaloyl-N'-pyrrolidine thiourea, N-(2, 6-dimethyl piperidine)-N'-(3, 4, 5-methoxy)-benzoyl thiourea and N, N-dibutyl-N'-pivaloyl thiourea. In addition, to obtain comparative experimental crystal structure data CCSD and literature searches were also undertaken. Comparison between the internal coordinates of the calculated and experimentally obtained crystal structures show reasonable agreement. For instance, in all cases the C-N bonds of all the compounds show that the C(1)-N(1) bond lengths have an intermediate length, N(1)-C(2) are the longest and C(2)-N(2) are the shortest. The valence angles also agree. However, small differences were observed between the dihedral angle values, which are to be expected, because the calculations were carried out on isolated molecules, which are free from any interactions with other molecules that could affect their dihedral angles to some extent.
- The atoms in molecules (AIM) analysis carried out on the selected acylthioureas enabled one to see a clear picture of their electron densities. Analysis of the electron density, $\rho(r)$, and Laplacian of the electron density, $\nabla^2\rho(r)$, at the bond critical points gave a large amount of valuable information. For instance, the analysis of the bond critical points of the C-N bonds showed that the C(1)-N(1) bond had an intermediate electron density, the C(2)-N(1) bond had the lowest and the C(2)-N(2) bond had the highest electron densities. This trend shows the inverse proportional relationship that exists between bond length and electron density. Analysis of the Laplacian of the electron density, $\nabla^2\rho(r)$, on the other hand, enables one to categorize bonds into those that have concentrated or depleted bond critical point electron density. According to this N(1)-H(1), all the C-N bonds, and all the hydrogen bonds, were found to have a negative Laplacian of the electron density values

($\nabla^2\rho(r) < 0$), and hence had a high electron charge concentration on their bond critical points. On the other hand C (1)-O, and C (2)-S, were found to have positive Laplacians ($\nabla^2\rho(r) > 0$), consequently they had depleted bond critical points. Since depletion of the electron density on the bond critical points of the C=O and C=S bonds implies a concentration of density around the more electronegative O and S atoms, this finding is in agreement with the nucleophilic character of the O and S atoms which has been proven in many experimental studies (Plutin, A.M., et al., 2000).

- Other information that was extracted from the electron density, $\rho(r)$, and its Laplacian, $\nabla^2\rho(r)$, is a confirmation of the presence of hydrogen bonding in the stable structure of the acylthioureas. According to the analysis, formation of hydrogen bonding between protons on the extended arms of either of the **R**, **R'**, or **R''** substituent groups and heavy atoms such as N, O, and S was observed. Among the candidates analyzed, compounds such as C, D, E, J, K, and L were found to exhibit hydrogen bonding, and these bonds play a significant role in the stabilization of their structures.
- The NBO based population analysis of the acylthioureas enables one to assign charges to all their constituent atoms. According to this assignment, the relatively more electronegative N, O and S atoms were found to have negative charges, the carbonyl and thio-carbonyl carbon atoms also had negative charges, whereas the remaining carbon atoms had either negative or positive charges depending on the environment in which they exist. The mobile proton H(1) was found to have a positive charge. For the sake of comparison a Mulliken based charge analysis was also performed, and was found to give a trend that agree with that observed in the NBO based population analysis discussed above.
- Another important task performed in the NBO study was the second order perturbation theory energy analysis. This analysis yielded stabilization energies involved during donor-acceptor interactions in the compounds. According to the analysis lone pairs of the terminal nitrogen atom, i.e. N (2), in each compound undergo two major delocalizations with high stabilization energies. The first is to the anti-bonding π -orbital of the vicinal thio-carbonyl bond ($n_{N(2)} \longrightarrow \pi^*_{C(2)-S}$), and the second is to the non-Lewis NBO lone pair of the geminal thio-carbonyl carbon, ($n_{N(2)} \longrightarrow n^*_{C(2)}$). These two donor-acceptor interactions cause strong delocalization in the S=C(2)-N(2) region. This enables the C(2)-N(2) bond to attain a double bond character. Therefore, this clearly explains why one of the C-N bonds of substituted acylthioureas is always shorter than the other two. Further analysis showed that the sulphur

atom is responsible for the strong delocalization observed in the region and hence shortening of the C(2)-N(2) bond.

- The NRT analysis carried out on the acylthioureas allowed quantitative determination of all possible resonance structures. This analysis shows that the leading reference resonance structure for the entire investigated compounds is the same. This leading structure which is called reference structure (Ref. str.) has double bonded carbonyl and thio-carbonyl groups as in **fig. 5.7**. The secondary resonance structure that has the highest resonance weight next to the reference structure is the one which has a single bonded thio-carbonyl group and a double bonded carbon nitrogen bond i.e. C(2)=N(2), **fig. 5.7**. Comparison between the resonance weight of the reference resonance structure and the top weighted secondary resonance structure in all compounds showed an average difference of not more than 10%. For this reason, substituted acylthioureas are presumed to exist in a resonant form between these two high resonance weight structures. This resonance gives the C(2)-N(2) bonds a partial double bond character. This further explains the main cause of the shortening of one C-N bond observed in substituted acylthioureas.

6.1.4 Generalizations:

- This work, besides successfully filling the theoretical data gap that existed in substituted acylthioureas, also contributes to explaining experimentally unexplored properties of the compounds such as: detection of the presence of hydrogen bonding, identification of the transition state structures, description of the nature of electron distributions, and the assignment of charges to each of the constituent atoms in the compounds.
- All in all, the considerable agreement observed between the geometries of the calculated and experimentally obtained stable structures, as well as the similarity in the wavenumbers obtained through the experimental infra-red study and their calculated counterparts, proved the accuracy of the quantum mechanical calculations undertaken. These observations thus show the strong link between the theoretical and experimental methods of studies, and that both methods can work hand-in-glove harmoniously in solving chemical problems facing the scientific community today.

6.2 Future Works:

The abundant theoretical and supplementary experimental data collected in this study, clearly define structural properties of substituted acylthioureas. Therefore, this information can be used as a spring board for further studies on the coordination of these compounds to transition metals, or for their use for other applications.

References:

- Albertus, M.S.; Piris, M. *J. Mol. Struct.* 2001, **598**, 261-265.
- Allen, H. H.; Kennard, O. *Chemical Design Automation News*, 1993, **8**, 31.
- Allinger, N. L.; Yuh, Y. H.; Lii, J-H. *J. Am. Chem. Soc.* 1989, **111**, 5851.
- Allinger, N.L. *J. Am. Chem. Soc.* 1977, **99**, 88127.
- Allinger, N.L.; Chen, K.; Lii, J-H. *J. Comput. Chem.* 1996, **17**, 642.
- Atkins, P.; Paula, J.D.; *Atkins's Physical Chemistry, Seventh edition*, Oxford university press: Oxford 2002.
- Bader, R.F.W. *Encyclopaedia of Computational Chemistry* John Wiley: Chichester, 1998, Vol.1, 64.
- Bader, R.F.W. *Atom in molecules, A quantum theory*, Oxford: Oxford, 1990.
- Bailey, B.A.; Rothaupt, K.L.; Kullnig, R.K.; *Inorg. Chem. Acta* 1988, **147**, 233-236.
- Barbour, L. J. *J. Supramol. Chem.* 2001, **1**, 189-191
- Biegler-König, F. W.; Bader, R.F.W.; Ting-Hau, T. *J. Comput. Chem.* 1982, **3**, 317.
- Bourne, S.; Koch, K.R. *J. Chem. Soc., Dalton Trans* 1993, 2071-2072.
- Brooks, R.; Bruccoleri, R.E.; Olafson, B. D.; States, D. J.; Swaminathan, S.; Karplus, M. *J. Comput. Chem.* 1983, **4**, 187.
- Cao, Y.; Zhao, B.; Zhang, Y.-Q.; Zhang, D.-C.; *Acta Crystallogr.C* 1996, **52**, 1772-1774.
- Carpenter, J.E.; Weinhold, F. *J. Am. Chem. Soc.* 1988, **110**, 368-372.
- Cason, C.J. *Pov-Ray for windows, Version 3.5*, 2002.

- Che, D.-J.; Li, G.; Yao, X.-L.; Wu, Q.-J.; Wang, W.-L.; Zhu, Y. *J. Organometallic Chem.* 1999, **584**, 190-196.
- Cook, D.B. *Handbook of Computational Quantum Chemistry* Oxford (1998).
- Cornell, W.D.; Cieplak, P.; Bayly, C.I.; Gould, I. R.; Merz Jr., K.M. ; Ferguson, D. M.; Spellmeyer, D. C.; Fox, T.; Caldwell, J.W.; Kollman, P.A. *J. Am. Chem. Soc.* 1995, **117**, 5179.
- Cross, A.D. *An introduction to practical IR- spectroscopy.* Butterworths scientific, London, 1960.
- Dago, A.; Shepelev, Y.; Fajardo, F.; Alvarez, F.; Pomes, R. *Acta Crystallogr. C*, 1989, **45**, 1192-1194.
- Dago, A.; Simonov, M. A.; Pobedinskaya, E.A.; Martin, A.; Masias, A. *Sov. Phys. Crystallogr.* 1988, **33**(4), 604-606.
- Dago, A.; Simonov, M.A.; Pobedinskaya, E.A.; Martin, A.; Masias, A. *Sov. Phys. Crystallogr* 1987, **32**(4) , 602-603.
- Dewar, M.J.S.; Thiel, W., *J. Am. Chem. Soc.* 1977, **99**, 4899-4907.
- Dewar, M.J.S.; Zoebisch, E.G.; Healy, E.F.; Stewart, J.J.P. *J. Am. Chem. Soc.* 1985, **107**, 3902.
- Dewar, M.J.S.; Jie, C.; Yu, J. *Tetrahedron*, 1993, **49**, 5003-5038.
- Dillen, J.L.M. *Understanding Chemistry with theoretical and molecular models: An introduction to some classical and quantum techniques of molecular modelling (Note book)* Stellenbosch, 2003.
- Ditchfield, R.; Hehre, W.J.; Pople, J.A. *J. Chem. Phys.* 1971, **54**, 724.
- Dubis, A.T.; Grabowski, S. J. *J Phys. Chem. A* 2003, **107**, 8723-8729.

Eliel, E.L. *Encyclopaedia of Computational Chemistry*, John Wiley: Chichester, 1998, Vol.1, 531.

Farrugia, L. J. *J. Appl. Cryst.* 1997, **30**, 565.

Foresman, J.B.; Frisch, Á. *Exploring Chemistry with Electronic Structure Methods, Second edition*, Gaussian: Pittsburgh, 1996.

Foster, J.P.; Weinhold, F. *J.Am.Chem. Soc.* 1980,**102**, 7211-7218.

Frenking, G.; Fröhlich, N. *Chem. Rev.* 2000, **100**(2), 727.

Frenking, G.; *J.Comput. Chem.* 2000, 21(16).

Frisch, M. J.; Trucks, G. W.; Schlegel, H. B.; Scuseria;G. E.; Robb, M.A.; Cheeseman, J.R.; Zakrzewski,V.G.; Montgomery, J.A.; Stratmann, Jr.R. E.; Burant, J.C.; Dapprich, S.; Millam, J.M.; Daniels, A.D.; Kudin, K.N.; Strain, M.C.; Farkas, O.; Tomasi, J.; Barone,V.; Cossi, M.; Cammi, R.; Mennucci, B.; Pomelli, C.; Adamo, C.; Clifford, S.; Ochterski, J.; Petersson, G. A.; Ayala, P.Y.; Cui, Q.; Morokuma, K.; Rega, N.; Salvador, P.; Dannenberg, J.J.; Malick, D.K.; Rabuck, A.D.; Raghavachari, K.; Foresman, J.B.; Cioslowski, J.; Ortiz J.V.; Baboul, A.G.; Stefanov, B.B.; Liu, G.; Liashenko, A.; Piskorz, P.; Komaromi, I.; Gomperts, R.; Martin, R.L.; Fox, D. J.; Keith, T.; Al-Laham, M. A.; Peng, C.Y.; Nanayakkara, A.; Challacombe, M.; Gill, P.M.W.; Johnson, B.; Chen, W.; Wong, M.W.; Andres, J.L.; Gonzalez, C.; Head-Gordon, M.; Replogle, E.S.; and Pople, J.A.; Gaussian 98, Revision A.11.3., Gaussian, Inc., Pittsburgh PA, 2002.

Gabino, D.; Kermer, E.; Baran, E.J; Mombro, A.; Suescun, L.; Mariezcurrena, R.; Kieninger, M.; Ventura, O. *Z. Anorg. Allg. Chem.* 1999, **625**, 813-1819.

Gambino, D.; Kremer, E.; Baran, E. J. *Spectrochimica Acta A*, 2002, **58**, 3085-3092.

Gillespie, R.J.; Popelier, P.L.A. *Chemical Bonding and Molecular Geometry: From Lewis to electron densities*, Oxford University Press: New York, 2001.

Glendening, E. D.; Badenhop, J.K.; Reed A. E.; Carpenter, J. E.; Bohmann, J.A.; Morales, C. M.; Weinhold, F.; NBO 5.0.; Theoretical Chemistry Institute, University of Wisconsin, Madison, WI, (2001).

Glendening, E.D.; Badenhop, J.K.; Weinhold, F. *J.Comput.Chem.* 1998, **19**(6), 628-646.

Glendening, E.D.; Weinhold, F. *J. Comput.Chem.* 1998, **19**(6), 593-609.

Glendening, E.D.; Weinhold, F. *J.Comput.Chem.* 1998, **19**(6), 610-627.

Gordon, M.S. *Chem. Phys. Lett.* 1980, **76**, 163.

Hariharan, P.C.; Pople, J.A. *Mol. Phys.* 1974, **27**, 209.

Hariharan, P.C.; Pople, J.A. *Theor. Chim. Acta*, 1973, **28**, 213.

Hehre, W.J.; DitchHartree-Fockield, R.; Pople, J.A. *J. Chem. Phys.* 1972, **56**, 2257.

Hehre, W.J.; Radom, L.; Schleyer, P.V.R.; Pople, J.A. *Ab initio molecular orbital theory.* John Wiley & Sons: New York 1986.

Hinchliffe, A. *Computational Quantum Chemistry*, John Wiley & Sons: Chichester 1988.

Irving, A.; Koch, K.R.; Matoetoe, M. *Inorg. Chem. Acta*, 1993, **206**, 193-199.

James, D. I. Jr.; Stanley, R.C. *Spectrochemical Analysis*, Prentice-Hall: New Jersey, 1988.

Jensen, F. *Introduction to Computational Chemistry*, John Wiley & Sons: New York, 1999.

Jug, K.; Neumann, F. *Encyclopaedia of Computational Chemistry* John wiley: Chichester, 1998, Vol.1, 507.

Kemp, G.; Roodt, A.; Purcell, W.; Koch, K.R. *J.Chem. Soc., Dalton Trans.*, 1977, 4481-4483.

Knuuttila, P.; Knuuttila, H.; Hennig, H.; Beyer, L. *Acta Chem. Scand.* 1982, **A36**, 541-545.

Koch, K.R.; Grimmbacher, T.; Sacht, C. *Polyhedron* 1998, **17**(2-3), 267-274.

Koch, K.R.; Matoetoe, M.; Mangaka, C. *Magnetic Resonance in chemistry*, 1991, **29**, 11.

Koch, K.R.; Sacht, C.; Bourne, S. *Inorg. Chem. Acta*, 1995, **232**, 109-115.

Koch, K.R.; Sacht, C.; Grimmbacher, T.; Bourne, S. *S.Afr.J.Chem* 1995, **48**, 71-77.

Koch, K.R.; Toit, J.D.; Caira, M.R.; Sacht, C. *J. Chem. Soc., Dalton.Trans.* 1994, 785-786.

Koch, K.R.; Wang, Y.; Coetzee, A. *J.Chem. Soc., Dalton Trans.*, 1999, 1013-1016.

Leach, A.R. *Molecular Modelling-Principles and applications*, second edition, Prentice Hall: Harlow (2001).

Lipkowitz, K.B.; Lipkowitz, K.B.; Boyd, D.B. *Rev.Comput.Chem* 1994,

March, J. *Advanced organic chemistry- Reactions, mechanisms, and structure. Fourth edition*, John Wiley & Sons: New York, 1992.

Mohamadou, A.; Déchamps-Oliver, I.; Barbier, J.P. *Polyhedron* 1994, **13**(9), 1363-1370.

Morales, A.D.; De Armas, H.N.; Blaton, N.M.; Peeters, O.M.; De Ranter, C.J.; Márquez, H.; Hernández, R.P. *Acta Crystallogr.C*, 2000 **56**, 503-504.

Nakamoto, K. *Infrared and Raman Spectra of Inorganic and Coordination Compounds, Fifth edition*, Wiley: New York, 1986.

Pavia, D.L.; Lampman, G.M.; Kriz, G.S. *Introduction to Spectroscopy, Third edition*, Harcourt: New York, 2001.

Perry, W.O.; Beynon, J.H.; Baitinger, W.E.; Amy, J.W.; Caprioli, R.M.; Renaud, R.N.; Leitch, L.C.; Meyerson, S. *J.Am.Chem. Soc*, 1970, **92**, 24.

Plutin, A.M.; Márquez, H.; Ochoa, E.; Morales, M.; Morán, L.; Rodríguez, Y.; Suárez, M.; Martín, N.; Seoane, C.; *Tetrahedron* 2000, **56**, 1533-1539.

Popelier, P. Atom in molecule -An introduction, Pearson Education Ltd: Singapore, 2000.

Raj, S.S.S.; Puviarasan, K.; Velmurugan, D.; Jayanthi, G.; Fun, H.K. *Acta Cryst.C*, 1999, **55**, 1318-1320.

Rappé, A. K.; Casewit, C.J.; Colwell, K.S.; Goddard III, W.A.; Skiff, W.M. *J.Am. Chem. Soc.* 1992, **114**, 10024.

Reed, A.E.; Curtiss, L.A.; Weinhold; *Chem. Rev.* 1988, **88**, 899-926.

Reed, A.E.; Weinhold, F. *J. Chem. Phys.* 1985, **83**(4), 1736-1740

Reed, A.E.; Weinstok, R.B.; Weinhold, F. *J. Chem. Phys.* 1985, **83**(2), 735-746

Ribeiro da Silva, M.A.V.; Ribeiro da Silva, M.D.M.C.; Da Silva, L.C.M.; Dietze, F.; Hoyer, E.; Beyer, L.; Schröder, B.; Damas, A.M.; and Liebman, J.F. *J. Chem. Soc., Perkin Trans.* 2001, **2**, 2174-2178.

Robert, L. C. Molecular symmetry and group theory, John Wiley & Sons: New York, 1997.

Rodger, A.; Patel, K.K.; Sanders, K.J.; Datt, M.; Sacht, C.; Hannon, M.J.; *J.Chem.Soc., Dalton Trans.* 2002, 3656-3663.

Rodríguez, Y.; Macías, A.; Suárez, M. *Stud. Org. Chem.* 35 *Chem. Heterocyclic Comp.*, 1988, 508.

Sacht, C.; Datt, M.S. *Polyhedron* 2000, **19**, 1347-1354.

Sacht, C.; Datt, M.S.; Otto, S.; Roodt, A. *J.Chem. Soc., Dalton Trans* 2000, 727-733.

Schaftenaar, G.; Noordik, J.H. *J. Comput.-Aided Mol. Design*, 2000, **14**, 123.

Schuster, M. *Fresenius J. Anal. Chem* 1992, **342**, 791-794.

Schuster, M.; Kugler, B.; König, K.H. *Fresenius. J. Anal. Chem* 1990, **338**, 717-720.

Scott, A.P.; Radom, L. *J. Phys. Chem.* 1996, **100**, 16502-16513.

Sebastian, J.F.; *J. Chem. Edu.* 1971, **48**(2), 97-98.

Shen, X.; Shi, X.; Kang, B.; Liu, Y.; Tong, Y.; Jiang, H.; Chen, K.; *Polyhedron* 1998, **17**(23-24), 4049-4058.

Siemens *SMART Software Reference Manual* 1996b, Siemens Analytical X-Ray Instruments Inc., Madison, Wisconsin, USA.

Springborg, M. *Methods of Electronic Structure Calculations- From molecules to solid*, John Wiley & Sons: Chichester (2000).

Stewart, J.J.P. *J. Comput. Chem.* 1989, **10**, 209.

Vest, P.; Schuster, M.; König, K.H. *Fresenius J. Anal. chem.* 1991, **339** 142-144.

Weinhold, F. *Encyclopaedia of Computational Chemistry*, 1998, Vol.3, 1792.

Weinhold, F.; Landis, C. R. *Chem. Edu.* 2001, **2**(2), 91-104.

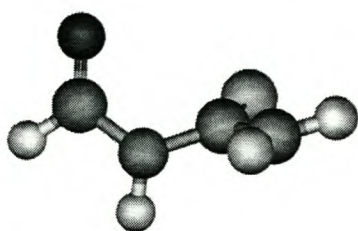
Young, D.C. *Computational chemistry-A practical guide for applying techniques to real-world problems*, John Wiley & Sons: New York 2001.

Yuan, Y.F.; Wang, J.T.; Gimeno, M.C.; Laguna, A.; Jones, P.G. *Inorg. Chem. Acta*, 2001, **324**, 309-317.

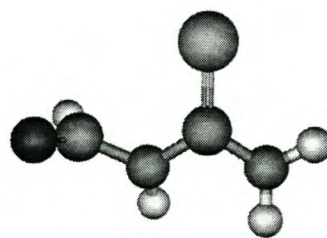
Zerner, M.C. *Rev. Comput. Chem.* 1991, **2**, 313.

Addenda

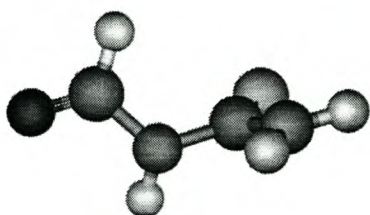
Addendum-A: Molecular geometries:



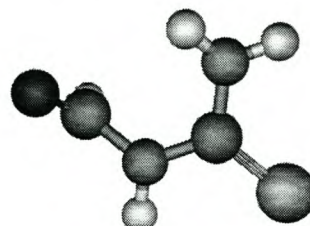
T₁



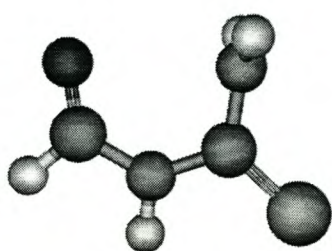
T₂



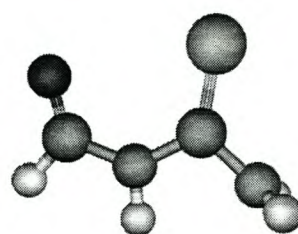
T₃



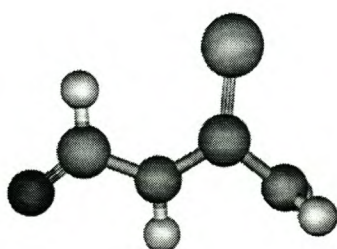
T₄



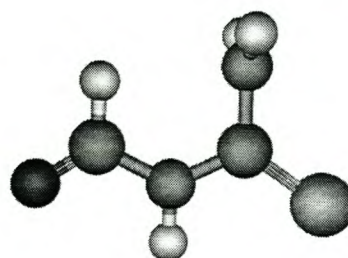
H₁



H₂



H₃



H₄

Fig. A-1. Structures of the transition state (T_n) and hill top (H_n) conformers of proton substituted acylthiourea compound. Oxygen indicated with red, sulphur with yellow, nitrogen with blue, carbon with grey and hydrogen with white.

Addendum-B: Wavenumber analysis.**Table 1** Calculated and scaled* wavenumbers (cm^{-1}) of *N*-pivaloyl -*N'*-pyrrolidine thiourea (*A*).

Description	Calculated	Scaled*	Rel. Intensity
N(1)-H stretching	3869	3454	0.07
CH ₂ assym. stretching	3337	2979	0.03
	3317	2962	0.03
	3285	2933	0.08
CH ₃ assym. stretching	3309	2955	0.04
	3286	2934	0.11
	3273	2923	0.03
	3281	2930	0.07
	3280	2929	0.02
	3274	2923	0.01
CH ₂ symm. stretching	3280	2929	0.08
	3273	2923	0.03
	3256	2907	0.01
	3228	2882	0.05
	3223	2878	0.04
CH ₃ symm. stretching	3222	2877	0.04
	3211	2867	0.03
	3209	2865	0.04
C(1)=O stretching	1988	1775	0.41
N(1)-H in plane bending & C(2)-N(2) stretching	1734	1548	0.80
CH ₂ symm. bending	1679	1499	0.03
	1662	1484	0.01
	1646	1470	0.02
	1638	1463	0.01
CH ₃ assym. bending	1661	1483	0.04
	1654	1477	0.02
	1651	1474	0.01
	1630	1455	0.01
C(2)-N(2) stretching	1605	1433	1.00
CH ₃ symm. bending	1592	1421	0.07

Description	Calculated	Scaled*	Rel. Intensity
	1562	1394	0.01
	1560	1393	0.01
CH ₂ wagging	1527	1363	0.07
	1515	1353	0.01
	1494	1334	0.01
	1131	1010	0.01
C(3)-C(1) stretching	1430	1277	0.02
CH ₂ twisting	1406	1256	0.12
	1375	1228	0.01
	1324	1182	0.03
	1314	1173	0.03
	1015	906	0.01
CH ₃ wagging	1372	1225	0.06
	1145	1023	0.02
	882	789	0.01
N(1)-C(2) stretching	1361	1215	0.27
CH ₃ twisting	1351	1206	0.01
C(1)-N(1) stretching	1290	1152	0.34
C(1)-N(2)-C(2) symm. stretching	1217	1087	0.07
Ring deformation	992	886	0.01
C(2)=S stretching	977	872	0.04
CH ₂ rocking	957	855	0.01
	938	837	0.02
	802	717	0.01
	623	557	0.02
C (3)-C (1)-N (1) oop. bending	845	754	0.04
N (1)-H oop. bending	751	671	0.14
N (2)-C (2)-N (1) oop. & N (1)-H oop. bending	697	622	0.02
N(1)-C(2)-N(2) bending	492	439	0.02
C (1) =O in-plane bend. & CH ₃ wagging	391	349	0.02
CH ₂ rocking & CH ₃ twisting	304	272	0.01
Ring in-plane wagging & CH ₃ rocking	271	242	0.01
C (1) =O oop. bending	102	91	0.01

Table 2 Calculated and scaled* wavenumbers (cm^{-1}) of *N*-(2, 6-dimethyl-piperidine)-*N'*-(3, 4, 5-methoxybenzoyl) thiourea (B).

Description	Calculated	Scaled*	Rel. Intensity
N(1)-H stretching	3842	3430	0.09
Hexane ring C-H stretching	3405	3041	0.04
Methoxy CH ₃ assym.stretching	3332	2975	0.06
	3330	2974	0.09
	3330	2973	0.08
	3305	2951	0.06
	3296	2943	0.09
	3294	2941	0.07
CH ₃ assym. stretching	3331	2974	0.03
	3311	2957	0.03
	3304	2950	0.05
	3280	2928	0.04
	3273	2922	0.09
CH ₂ assym. stretching	3294	2942	0.04
	3262	2913	0.11
	3247	2899	0.10
Methoxy CH ₃ symm. stretching	3228	2883	0.09
	3218	2873	0.12
	3217	2872	0.09
CH ₂ symm. stretching	3221	2876	0.06
	3206	2863	0.02
	3205	2862	0.03
CH ₃ symm. stretching	3220	2875	0.11
	3215	2871	0.05
C(1)=O stretching	1975	1763	0.63
Phenyl C=C stretching	1806	1612	0.01
	1783	1592	0.19
C(1)-H in-plane bending & C(2)-N(2) stretching	1716	1532	0.88
Phenyl C(OMe)-C(OMe)-C(OMe) symm. str.	1680	1500	0.33
CH ₂ scissoring	1662	1484	0.05

Description	Calculated	Scaled*	Rel. Intensity
	1441	1287	0.02
Methoxy CH ₃ assym. bending	1660	1482	0.01
	1654	1477	0.01
	1644	1468	0.01
Methoxy CH ₃ scissoring	1658	1481	0.01
	1645	1469	0.01
CH ₃ assym. bending	1657	1479	0.01
	1638	1463	0.02
	1635	1460	0.04
CH ₃ scissoring	1650	1474	0.01
CH ₃ scissoring & CH ₂ bending	1650	1473	0.01
Methoxy CH ₃ symm. bending	1633	1458	0.01
	1614	1441	0.04
C(2)-N(2) stretching	1597	1426	1.00
Assym. phenyl ring deformation	1577	1408	0.21
CH ₃ symm. bending	1567	1399	0.01
	1565	1397	0.07
Hexane ring C-H oop. bending	1554	1388	0.38
	1541	1376	0.01
	1475	1317	0.01
	1461	1304	0.02
CH ₂ wagging	1533	1369	0.16
	1513	1351	0.03
	1507	1345	0.16
Phenyl symm. breathing	1498	1338	0.82
CH ₂ twisting	1420	1268	0.04
	1350	1205	0.06
	1311	1170	0.25
Phenyl C-H in-plane bending & CH ₂ twisting	1400	1250	0.13
Methoxy O-C (phenyl) stretching	1398	1248	0.25
Phenyl C-H in-plane bending	1379	1231	0.18
	1212	1082	0.05
C(1)-N(1) stretching	1359	1213	0.44

Description	Calculated	Scaled*	Rel. Intensity
Methoxy CH ₃ wagging	1340	1196	0.04
	1331	1188	0.02
	1316	1175	0.14
	1291	1153	0.02
Methoxy CH ₃ twisting	1289	1151	0.01
CH ₂ rocking	1288	1150	0.15
	909	812	0.01
	519	463	0.01
C(2)-N(1) stretching	1259	1124	0.10
CH ₃ wagging	1253	1119	0.10
	1039	928	0.02
Phenyl assym. C=C stretching	1246	1113	0.16
O-C=C symm. stretching	1225	1093	0.27
	1177	1051	0.14
N (2)-C''-CH ₃ assym. stretching	1174	1048	0.05
	1125	1004	0.04
Methoxy O-CH ₃ stretching	1162	1038	0.26
	1141	1019	0.20
Hexane ring symm. C (H ₂)-C (H ₂)-C (H ₂) str.	1134	1012	0.02
C(1)-N(1)-C(2) stretching	1092	975	0.01
CH ₂ & CH ₃ wagging	1078	963	0.01
CH ₂ rocking and CH ₃ wagging	1074	959	0.02
	969	865	0.02
	944	843	0.01
	913	816	0.02
	737	658	0.02
	737	658	0.02
CH ₃ -O-C (Ph) symm. stretching	1059	945	0.02
Phenyl C-H oop. bending	1032	922	0.01
	1019	911	0.07
	1013	904	0.01
C (OMe)-C (OMe)-C (OMe) oop. bending	888	793	0.03

Description	Calculated	Scaled*	Rel. Intensity
C(2)=S bending	858	766	0.03
Symm. phenyl ring deformation	790	705	0.05
N (1)-H oop. bending	765	683	0.15
OCH ₃ oop. wagging	742	663	0.01
Phenyl ring rocking	708	632	0.01
N (1)-H oop. & C (2)-N (2)-C'' oop. bending	691	617	0.06
C (3)-C (1)-N (1) symm. bending	647	578	0.01
Phenyl C-H and N (1)-H oop. bending	635	567	0.02
Methoxy CH ₃ wagging	623	556	0.01
N(2)-C''-CH ₃ bending	602	537	0.03
	526	470	0.01
Phenyl ring oop. bend.& methoxy CH ₃ wagging	485	433	0.02
N(1)-C(2)-N(2) bending	465	415	0.02
CH ₂ -C''-CH ₃ bending	452	403	0.01
CH ₂ rocking & CH ₃ twisting	337	301	0.01
Methoxy wagging	303	270	0.01
C(1)=O in-plane bending	261	233	0.02
CH ₃ twisting	245	219	0.01
CH ₃ twisting and methoxy CH ₃ wagging	221	197	0.01
Methoxy CH ₃ wagging	205	183	0.02
	96	86	0.01
Methoxy CH ₃ rocking	90	81	0.01
	69	61	0.01
	64	57	0.01

Table 3 Calculated and scaled* wavenumbers (cm^{-1}) of *N, N*-diethyl-*N'*-pivaloyl thiourea (C).

Description	Calculated	Scaled*	Rel. Intensity
N(1)-H stretching	3870	3455	0.11
CH ₂ assym. stretching	3392	3028	0.05
CH ₃ assym. stretching	3340	2982	0.03
	3280	2929	0.08
CH ₂ & CH ₃ assym. stretching	3332	2976	0.04
	3312	2958	0.03
	3264	2915	0.10
	3211	2867	0.05
Isobut. CH ₃ assym. stretching	3310	2955	0.06
	3286	2934	0.18
	3282	2930	0.10
	3280	2928	0.10
	3275	2924	0.01
	3274	2923	0.02
CH ₃ assym. and CH ₂ symm. stretching	3273	2922	0.10
Isobut. CH ₃ symm. stretching	3222	2877	0.05
	3211	2867	0.06
	3209	2865	0.06
CH ₃ symm. stretching	3222	2877	0.12
	3217	2873	0.08
C(1)=O stretching	1990	1777	0.65
N(1)-H in-plane bending & C(2)-N(2) str.	1740	1554	1.00
CH ₂ scissoring	1674	1495	0.33
CH ₂ scissoring & CH ₃ assym. bending	1664	1486	0.13
	1648	1471	0.01
Isobut. CH ₃ assym. bending	1660	1483	0.02
Isobut. CH ₃ scissoring	1653	1476	0.01
	1651	1474	0.01
CH ₃ & CH ₂ scissoring	1649	1473	0.01
CH ₃ assym. bending	1637	1462	0.02

Description	Calculated	Scaled*	Rel. Intensity
CH ₃ scissoring	1633	1458	0.04
C(2) – N(2)	1609	1437	0.74
Isobut. CH ₃ symm. bending	1591	1421	0.06
CH ₃ symm. bending & CH ₂ wagging	1574	1405	0.12
	1568	1400	0.04
	1535	1371	0.14
Isobut. CH ₃ symm. stretching	1562	1394	0.01
	1560	1393	0.01
CH ₂ wagging	1519	1356	0.08
CH ₂ twisting	1467	1310	0.12
	1433	1279	0.28
	1428	1275	0.09
C(2)-N(2)-C'' bending	1380	1232	0.43
Isobut. group wagging	1370	1223	0.03
N(1)-C(2) stretching	1315	1174	0.36
C(1)-N(1) stretching	1273	1137	0.42
CH ₂ rocking & CH ₃ wagging	1241	1108	0.12
CH ₃ wagging	1214	1084	0.08
	1207	1078	0.10
C(H ₂)-N(2)-C(H ₂) assym stretching	1177	1051	0.04
Isobut. CH ₃ wagging	1145	1022	0.03
	1029	919	0.01
C (H ₂)-N (2)-C (H ₂) symm. stretching	1115	996	0.01
C(1)-N(1)-C(2) bending	1044	933	0.03
C(2)=S stretching	953	851	0.05
CH ₂ rocking, CH ₃ & isobut. CH ₃ wagging	885	790	0.03
Ethyl rocking	862	770	0.03
C (3)-C (1)-N (1) oop. bending	848	757	0.07
N (1)-H oop. bending	771	688	0.10
	750	670	0.11
N (1)-H oop. & N (1)-C (2)-N (2) oop. bending	703	628	0.02

Description	Calculated	Scaled*	Rel. Intensity
Symm. bending of the 3 CH ₃ groups in Isobut.	622	555	0.04
	388	346	0.05
C''-N(2)-C(2) bending	584	522	0.02
Isobut. and ethyl groups wagging	5021	4483	0.01
C (H ₂)-N (2)-C (H ₂) oop. bending	481	430	0.02
Ethyl rocking	470	420	0.02
	375	335	0.02
Ethyl wagging	364	325	0.01
Assym. bending of the 3 CH ₃ groups in Isobut.	332	297	0.01
CH ₃ & Isobut. CH ₃ twisting	266	237	0.01
C (1) =O oop. bending	94	84	0.01

Table 4 Calculated and scaled* wavenumbers (cm^{-1}) of *N, N*-dibutyl-*N'*-pivaloyl thiourea (*D*).

Description	Calculated	Scaled*	Rel. Intensity
N(1)-H stretching	3872	3457	0.11
CH ₂ assym. stretching	3380	3018	0.04
	3310	2955	0.07
	3347	2989	0.02
	3272	2922	0.05
	3233	2886	0.14
	3224	2878	0.06
	3221	2876	0.03
	3209	2865	0.06
CH ₃ assym. stretching	3310	2955	0.04
	3266	2916	0.13
	3265	2915	0.13
	3262	2912	0.15
	3259	2910	0.11
CH ₂ symm. stretching	3286	2934	0.12
	3187	2846	0.09
	3184	2843	0.09
Isobut. CH ₃ assym. stretching	3286	2934	0.23
	3282	2930	0.10
	3279	2928	0.09
	3274	2924	0.01
	3274	2923	0.02
Isobut. CH ₃ symm. stretching	3222	2877	0.06
	3211	2867	0.05
	3209	2865	0.04
CH ₃ symm. & CH ₂ assym. stretching	3201	2858	0.06
	3196	2854	0.03
CH ₃ symm. stretching	3199	2857	0.08
C(1)=O stretching	1989	1776	0.67
N(1)-H in-plane bending & C(2)-N(2) stretching	1740	1554	1.00

Description	Calculated	Scaled*	Rel. Intensity
CH ₂ scissoring	1671	1492	0.22
	1663	1485	0.15
	1656	1478	0.03
	1640	1464	0.03
CH ₂ & isobut. CH ₃ scissoring	1660	1482	0.01
CH ₂ scissoring & Isobut. CH ₃ assym. bending	1653	1476	0.01
	1650	1473	0.02
Isobut. CH ₃ scissoring	1651	1474	0.01
CH ₂ & CH ₃ scissoring	1646	1470	0.06
CH ₃ scissoring	1644	1468	0.02
	1644	1468	0.01
C(2)-N(2) stretching	1615	1442	0.78
Isobut. CH ₃ symm. bending	1592	1422	0.05
	1562	1395	0.01
	1560	1393	0.01
CH ₂ wagging	1571	1403	0.07
	1570	1402	0.04
	1520	1357	0.01
	1425	1272	0.02
	1423	1271	0.02
CH ₃ symm. bending	1563	1396	0.01
CH ₃ symm. stretching & CH ₂ wagging	1564	1397	0.02
CH ₂ twisting	1472	1315	0.10
	1464	1308	0.05
	1444	1290	0.18
	1406	1256	0.26
CH ₂ wagging & C (3)-C (1)-N (1) assym. str.	1434	1281	0.09
CH ₂ & CH ₃ twisting	1378	1231	0.14
	1254	1120	0.13
	1032	922	0.02
	1022	913	0.01
Isobut. CH ₃ wagging	1369	1222	0.07

Description	Calculated	Scaled*	Rel. Intensity
CH ₂ scissoring	1671	1492	0.22
	1663	1485	0.15
	1656	1478	0.03
	1640	1464	0.03
CH ₂ & Isobut. CH ₃ scissoring	1660	1482	0.01
CH ₂ scissoring & Isobut. CH ₃ assym. bending	1653	1476	0.01
	1650	1473	0.02
Isobut. CH ₃ scissoring	1651	1474	0.01
CH ₂ & CH ₃ scissoring	1646	1470	0.06
CH ₃ scissoring	1644	1468	0.02
	1644	1468	0.01
C(2)-N(2) stretching	1615	1442	0.78
Isobut. CH ₃ symm. bending	1592	1422	0.05
	1562	1395	0.01
	1560	1393	0.01
CH ₂ wagging	1571	1403	0.07
	1570	1402	0.04
	1520	1357	0.01
	1425	1272	0.02
	1423	1271	0.02
CH ₃ symm. bending	1563	1396	0.01
CH ₃ symm. stretching & CH ₂ wagging	1564	1397	0.02
CH ₂ twisting	1472	1315	0.10
	1464	1308	0.05
	1444	1290	0.18
	1406	1256	0.26
CH ₂ wagging & C (3)-C (1)-N (1) assym. str.	1434	1281	0.09
CH ₂ & CH ₃ twisting	1378	1231	0.14
	1254	1120	0.13
	1032	922	0.02
	1022	913	0.01
Isobut. CH ₃ wagging	1369	1222	0.07

Description	Calculated	Scaled*	Rel. Intensity
	3364	300	0.01
Isobutyl wagging	388	346	0.01
Isobut. CH ₃ twisting & butyl wagging	299	267	0.01
Butyl wagging	108	97	0.01
C (1) =O oop. bending	93	83	0.01

Table 5 Calculated and scaled* wavenumbers (cm^{-1}) of *N, N*-diethyl-*N'*-benzoyl thiourea (*E*).

Description	Calculated	Scaled*	Rel. Intensity
N(1)-H stretching	3847	3435	0.12
Ring C-H stretching	3413	3047	0.01
	3395	3031	0.04
	3385	3022	0.07
	3375	3014	0.02
CH ₂ assym. stretching	3376	3014	0.05
	3354	2995	0.02
	3236	2890	0.13
CH ₃ assym. stretching	3347	2988	0.01
	3315	2960	0.06
Assym. CH ₃ & symm. CH ₂ stretching	3290	2938	0.10
CH ₃ & CH ₂ assym. stretching	3269	2919	0.01
	3267	2917	0.13
CH ₃ symm. stretching	3220	2875	0.05
	3212	2868	0.05
C(1)=O stretching	1983	1770	0.78
Ring C=C stretching	1808	1615	0.05
	1783	1592	0.01
N(1)-H in-plane bending & C(2)-N(2) stretching	1736	1550	1.00
CH ₂ scissoring	1674	1495	0.17
CH ₂ scissoring & ring C-H in-plane bending	1669	1490	0.02
CH ₂ scissoring & CH ₃ assym. bending	1661	1484	0.20
	1638	1463	0.06
CH ₃ assym. bending	1651	1474	0.07
CH ₃ scissoring	1636	1461	0.05
C(2)-N(2) stretching	1619	1445	0.83
Ring C-H rocking	1611	1439	0.19
CH ₃ symm. bending & CH ₂ wagging	1572	1403	0.07
	1568	1400	0.02
	1537	1372	0.05

Description	Calculated	Scaled*	Rel. Intensity
	1519	1356	0.05
CH ₂ twisting	1463	1306	0.10
	1429	1276	0.49
C(1)-N(1) stretching	1399	1249	0.41
C(2)-N(2)-C'' bending	1374	1227	0.78
Ring C-H scissoring	1347	1203	0.04
C(2)-N(1) stretching	1306	1167	0.13
Ring C-H in-plane bending	1303	1164	0.01
Ethyl rocking & N (1)-C (2)-N (2) symm. stretching	1250	1116	0.40
CH ₂ rocking & CH ₃ wagging	1232	1100	0.02
Ring C-H in-plane bending & CH ₃ wagging	1228	1097	0.06
	1190	1062	0.02
CH ₃ wagging	1199	1071	0.05
C (1)-N (1)-C (2) symm. stretching	1163	1038	0.09
Ring deformation	1126	1005	0.02
Ring C-H oop. bend & CH ₂ -N (2)-CH ₂ symm. str.	1114	994	0.01
C(1)-N(1)-C(2) bending	1035	924	0.03
CH ₂ & CH ₃ wagging	1006	898	0.01
C(2)=S stretching	925	826	0.08
Ring oop. wagging	898	802	0.02
Ethyl twisting	863	770	0.04
N (1)-H & ring C-H oop. bending	814	727	0.21
	773	690	0.11
C (2)-N (2)-C'' symm. stretching	785	701	0.01
N (1)-H & N (1)-C (2)-N (2) oop. bending	669	598	0.02
N (1)-H oop. stretching	712	636	0.10
	742	663	0.07
Ring assym. breathing	678	605	0.01
Ethyl wagging	591	528	0.01
C(3)-C(1)-N(1) bending	555	496	0.02
C(H ₂)-N(2)-C(H ₂) bending	497	444	0.01
Ring oop. wagging	457	408	0.01

Description	Calculated	Scaled*	Rel. Intensity
C(1)=O in plane bending	455	406	0.02
N(1)-C(2)-N(2) bending	450	402	0.03
Ethyl rocking	405	362	0.01
Ring & ethyl rocking	315	281	0.02
CH ₃ twisting	252	225	0.02
C (1) =O oop. bending & ethyl rocking	125	113	0.01
Ring & ethyl wagging	36	32	0.01

Table 6 Calculated and scaled* wavenumbers (cm^{-1}) of *N, N*-dibutyl-*N'*-benzoyl thiourea (*F*).

Description	Calculated	Scaled*	Rel. Intensity
N(1)-H stretching	3848	3435	0.12
Ring C-H stretching	3412	3047	0.01
	3395	3031	0.04
	3385	3022	0.07
	3375	3014	0.02
CH ₂ assym. stretching	3372	3010	0.05
	3360	3000	0.01
	3223	2878	0.05
	3311	2956	0.05
	3236	2889	0.14
	3225	2879	0.07
CH ₂ symm. stretching	3286	2934	0.17
	3185	2844	0.08
	3184	2843	0.09
CH ₃ assym. stretching	3273	2923	0.07
	3266	2916	0.12
	3265	2915	0.15
	3262	2912	0.15
CH ₂ & CH ₃ assym. stretching	3269	2918	0.04
CH ₃ symm. stretching	3207	2864	0.04
	3199	2857	0.07
CH ₂ & CH ₃ symm. stretching	3204	2861	0.09
C(1)=O stretching	1980	1768	0.81
Symm. ring C=C stretching	1808	1615	0.05
Assym. ring C=C stretching	1783	1592	0.01
N (1)-H in-plane bending & C (2)-N (2) str.	1738	1551	1.00
CH ₂ scissoring	1673	1494	0.15
	1668	1489	0.03
	1659	1481	0.27
CH ₃ & CH ₂ scissoring	1654	1477	0.01

Description	Calculated	Scaled*	Rel. Intensity
	1653	1476	0.01
	1636	1461	0.01
	1650	1473	0.03
	1645	1469	0.05
	1637	1462	0.04
CH ₃ assym. bending	1644	1468	0.01
C(2)-N(2) stretching	1618	1445	0.75
Phenyl ring rocking	1611	1439	0.20
CH ₃ symm. bending	1573	1405	0.01
CH ₂ wagging	1570	1402	0.06
	1524	1361	0.01
	1518	1356	0.02
	1483	1324	0.01
	1431	1278	0.05
CH ₂ wagging & CH ₃ symm. stretching	1568	1400	0.02
	1564	1396	0.03
CH ₂ twisting & ring rocking	1475	1317	0.03
	1473	1315	0.06
CH ₂ twisting	1462	1305	0.05
	1448	1293	0.15
	1419	1267	0.16
	1406	1255	0.06
	1376	1229	0.12
C(1)-N(1) stretching	1393	1244	0.92
Ring C-H scissoring	1347	1203	0.02
CH ₂ & CH ₃ twisting	1335	1192	0.38
	1053	940	0.01
Ring C-H in-plane bending	1304	1165	0.08
	1230	1098	0.04
	1188	1061	0.01
C(1)-N(1) stretching	1302	1162	0.02
CH ₂ rock. & N (1)-C (2)-N (2) symm. str.	1260	1125	0.32

Description	Calculated	Scaled*	Rel. Intensity
CH ₃ wagging & CH ₂ rocking	1242	1109	0.02
	1227	1095	0.03
	1035	924	0.01
	802	716	0.01
Ring C-H rocking	1188	1061	0.01
C (1)-N (1)-C (2) symm. stretching	1165	1040	0.10
Ring deformation	1124	1004	0.03
	679	606	0.01
CH ₂ -N (2)-CH ₂ symm. stretching	1119	999	0.01
Ring C-H oop. bending & CH ₃ wagging	1075	960	0.01
Ring C-H oop. bending	1070	955	0.01
CH ₂ twisting & CH ₃ wagging	1035	924	0.01
	1026	916	0.01
CH ₃ rocking & ring C-H oop. bending	964	861	0.01
C(2)=S stretching	953	851	0.07
C (H ₂)-C (H ₂)-C (H ₃) symm. stretching	945	844	0.01
Ring oop. wagging	899	803	0.02
CH ₂ & CH ₃ rocking	873	780	0.03
	849	758	0.01
	790	705	0.01
N(1)-C(2)-N(2) bending	830	741	0.01
N (1)-H oop. & ring oop bending	814	727	0.21
	772	690	0.10
N (1)-H oop. & N (1)-C (2)-N (2) oop. bending	746	666	0.03
	670	598	0.02
N (1)-H oop. bending	724	646	0.13
C(2)-N(2)-C'' bending	632	565	0.03
CH ₂ -N(2)-CH ₂ & C(3)-C(1)-N(1) bending	573	511	0.01
Ring oop. & butyl wagging	501	447	0.01
Butyl wagging	482	430	0.03
	446	398	0.01

Description	Calculated	Scaled*	Rel. Intensity
C(1)=O in-plane bending	457	408	0.01
Butyl rocking	384	343	0.01
	309	276	0.02
CH ₃ twisting	284	254	0.01
Ring & Butyl groups oop. wagging	167	149	0.01
Ring rocking & butyl wagging	125	111	0.01

Table 7 Calculated and scaled* wavenumbers (cm^{-1}) of *N*-(*n*-butyl)-*N'*-benzoyl thiourea (*G*).

Description	Calculated	Scaled*	Rel. Intensity
N(1)-H stretching	3893	3476	0.08
N(2)-H stretching	3813	3404	0.24
Ring C-H stretching	3395	3032	0.02
	3385	3022	0.03
	3374	3012	0.01
CH ₂ assym. stretching	3291	2938	0.05
CH ₃ assym. stretching	3267	2918	0.07
	3264	2914	0.09
CH ₂ symm. stretching	3246	2898	0.02
	3197	2855	0.07
	3189	2847	0.01
CH ₂ & CH ₃ assym. stretching	3233	2886	0.02
CH ₃ symm. stretching	3201	2858	0.04
C(1)=O stretching	1948	1740	0.45
Ring symm. C=C stretching	1808	1615	0.03
N(2)-H in-plane bending	1759	1570	0.65
N (1)-H in-plane bending & C (2)-N (2) str.	1731	1546	1.00
Ring C-H in-plane bending	1670	1491	0.01
CH ₂ scissoring	1666	1488	0.03
CH ₃ twisting	1644	1468	0.01
CH ₂ wagging	1580	1410	0.05
	1496	1336	0.25
	1427	1274	0.05
Ring C-H rocking	1613	1441	0.02
	1477	1318	0.01
	1232	1100	0.02
CH ₃ scissoring	1569	1401	0.01
C(2)-N(2) stretching	1539	1374	0.20
C(1)-N(1) stretching	1398	1248	0.26
Ring C-H scissoring	1347	1202	0.02

Description	Calculated	Scaled*	Rel. Intensity
	1308	1168	0.12
N(1)-C(2) stretching	1303	1163	0.32
N(2)-C'' stretching	1263	1128	0.01
N(1)-C(2)-N(2) bending	1196	1068	0.02
C (1)-N (1)-C (2) symm. stretching	1181	1054	0.02
CH ₃ wagging	968	864	0.02
C(2)=S stretching	846	755	0.05
Ring oop. wagging	815	727	0.19
	474	423	0.01
	189	169	0.01
N (2)-H & ring C-H oop. bending	771	688	0.01
N (2)-H oop. bending	753	672	0.05
	663	592	0.05
N (1)-H oop. bending	730	652	0.07
	725	648	0.06
C(3)-C(1)-N(1) bending	553	494	0.01
C(1)=O in plane bending	373	333	0.01
Ring rocking	298	266	0.01
C(2)=S in-plane bending & n-butyl wagging	228	203	0.01

Table 8 Calculated and scaled* wavenumbers (cm^{-1}) of *N*-(*n*-propyl) *N'*-benzoyl thiourea (*H*).

Description	Calculated	Scaled*	Rel. Intensity
N(1)-H stretching	3893	3476	0.08
N(2)-H stretching	3812	3404	0.25
Ring C-H stretching	3395	3032	0.02
	3385	3022	0.03
	3374	3012	0.01
CH ₂ assym. stretching	3291	2939	0.06
	3227	2882	0.1
CH ₃ assym. stretching	3275	2924	0.06
	3267	2917	0.04
CH ₂ symm. stretching	3245	2898	0.02
	3199	2856	0.04
CH ₃ symm. stretching	3206	2862	0.03
C(1)=O stretching	1948	1740	0.45
Ring C=C stretching	1808	1615	0.03
N(2)-H in-plane bending	1759	1571	0.63
N (1)-H in-plane bending & C (2)-N (2) str.	1731	1546	1.00
Ring C-H in-plane bending	1670	1491	0.01
	1232	1100	0.02
CH ₂ scissoring	1666	1488	0.03
CH ₃ assym. bending	1644	1468	0.01
CH ₂ scissoring & CH ₃ assym. bending	1639	1464	0.01
Ring C-H rocking	1613	1441	0.02
CH ₂ & CH ₃ wagging	1576	1408	0.08
CH ₃ symm. bending	1567	1399	0.03
C(2)-N(2) stretching	1517	1354	0.32
CH ₂ wagging	1458	1302	0.12
C(1)-N(1) stretching	1399	1249	0.25
Ring C-H scissoring	1347	1202	0.02
N(1)-C(2) stretching	1309	1169	0.28

Description	Calculated	Scaled*	Rel. Intensity
Ring C-H scissoring & N(1)-C(2) stretching	1306	1166	0.15
N(2)-C'' stretching	1267	1131	0.03
N(1)-C(2)-N(2) bending	1185	1058	0.05
C (1)-N (1)-C (2) symm. stretching	1178	1052	0.02
Ring C=C symm. stretching	1127	1006	0.01
C(1)-N(1)-C(2) bending	991	884	0.02
C(2)=S stretching	848	757	0.05
CH ₂ rocking	818	731	0.05
Ring C-H oop. bending & CH ₂ rocking	813	726	0.15
N (2)-H oop & ring C-H oop. bending	770	688	0.01
N (2)-H oop. bending	752	672	0.05
N (1)-H oop. bending	730	652	0.07
	725	648	0.06
N(2)-H & N(1)-H oop bending	663	592	0.05
C(3)-C(1)-N(1) bending	552	493	0.01
Phenyl ring wagging	479	428	0.01
C(1)=O in-plane bending	382	341	0.01
n-propyl wagging	329	294	0.01
C(2)=S in-plane bending & n-propyl wagging	277	247	0.01
n-propyl wagging	227	203	0.01

Table 9 Calculated and scaled* wavenumbers (cm^{-1}) of *N*-(*p*-hexyloxy) aniline-*N'*-(*p*-methyloxy) benzoyl-thiourea (I).

Description	Calculated	Scaled*	Rel. Intensity
N(1)-H stretching	3899	3482	0.06
N(2)-H stretching	3787	3381	0.30
Ring-1 C-H stretching	3419	3053	0.01
	3375	3013	0.01
Ring-2 C-H stretching	3413	3047	0.01
	3400	3036	0.01
	3885	3469	0.01
	3380	3018	0.01
Methoxy CH ₃ assym. stretching	3339	2981	0.04
	3284	2932	0.05
Hexoxy CH ₂ assym. stretching	3264	2914	0.17
Hexoxy CH ₃ assym. stretching	3262	2913	0.06
	3260	2911	0.03
Hexoxy CH ₂ & CH ₃ assym. stretching	3229	2883	0.04
Methoxy CH ₃ symm. stretching	3217	2872	0.05
Hexoxy CH ₂ symm. stretching	3214	2870	0.05
	3191	2849	0.06
Hexoxy CH ₂ & CH ₃ symm. stretching	3199	2856	0.03
Hexoxy CH ₃ symm. stretching	3198	2856	0.04
C(1)=O stretching	1940	1732	0.38
Ring-2 C=C stretching	1823	1628	0.04
Ring-1 C=C stretching	1809	1615	0.23
	1767	1578	0.02
N(2)-H in-plane bending	1750	1563	0.73
N(1)-H in-plane bending & C(2)-N(2) stretching	1731	1546	0.56
Ring-2 C-H in-plane bending	1698	1516	0.15
Ring-1 C-H in-plane bending	1695	1514	0.20
Hexoxy CH ₂ scissoring	1676	1496	0.06
Methoxy CH ₃ assym. bending	1659	1481	0.04
Methoxy CH ₃ symm. bending	1631	1457	0.03

Description	Calculated	Scaled*	Rel. Intensity
Hexoxy CH ₂ wagging	1592	1421	0.04
	1525	1362	0.01
Hexoxy CH ₂ wagging & CH ₃ symm. bending	1564	1397	0.01
C(2)-N(2)stretching	1505	1344	0.49
Methoxy C-O stretching	1445	1291	0.24
Hexoxy C-O stretching	1424	1272	1.00
C(1)-N(1) stretching	1406	1256	0.13
N(2)-C'' stretching	1369	1222	0.03
Methoxy CH ₃ wagging	1337	1193	0.06
Ring-1 C-H scissoring	1304	1165	0.18
	1224	1093	0.01
N(1)-C(2) stretching	1299	1160	0.57
Ring-1 C=C=C assym. stretching	1295	1156	0.02
Ring-2 C-H scissoring	1292	1154	0.05
	1200	1072	0.01
Ring-2 C=C=C assym. stretching	1277	1140	0.02
Hexoxy CH ₃ wagging	1242	1109	0.01
C (1)-N (1)-C (2) symm. stretching	1195	1067	0.03
Hexoxy O-C ₆ H ₁₃ stretching	1182	1055	0.07
Methoxy O-CH ₃ stretching	1173	1047	0.05
C(1)-N(1)-C(2) bending	1040	929	0.01
Ring-2 C-H oop. bending	960	858	0.03
	933	833	0.01
Ring-1 C-H oop. bending	954	852	0.04
Ring-2 breathing	901	805	0.02
Ring-1 breathing	869	776	0.01
C (3)-C (1)-N (1) oop. bending	859	767	0.09
C(2)=S stretching	815	728	0.06
N (2)-H oop. bending	793	708	0.04
Ring-2 oop. wagging	777	694	0.01
Ring-1 C-H & N2-H oop. bending	759	678	0.01
N1-H oop. bending	729	651	0.05

Description	Calculated	Scaled*	Rel. Intensity
Ring-2 assym. breathing	704	628	0.01
C(2)-N(2)-C'' bending	699	624	0.05
N (1)-H & N (2)-H oop. bending	664	593	0.04
Ph-O-CH ₃ bending	656	585	0.03
Ph-O-C ₆ H ₁₃ bending	601	537	0.02
Ring-1 & Ring-2 C-H oop. bending	579	517	0.01
Ring-2 C-H oop. bend. & Ph-O-C ₆ H ₁₃ bending	565	505	0.01
Ph-O-CH ₃ bending & hexyl wagging	535	477	0.02
C(1)-O in-plane bending	393	351	0.01
Ring-2 & Hexoxy wagging	248	221	0.01
Methoxy CH ₃ rocking	217	194	0.01
C (1) =O oop. bending & Ph-O-CH ₃ rocking	126	112	0.01

Table 10 Calculated and scaled* wavenumbers (cm^{-1}) of *N, N*-di (*n*-butyl)-*N'*-naphthoyl-thiourea (*J*).

Description	Calculated	Scaled*	Rel. Intensity
N(1)-H stretching	3858	3444	0.16
Naphthalene C-H stretching	3401	3037	0.02
	3397	3033	0.04
	3388	3025	0.07
	3382	3020	0.06
	3374	3013	0.03
CH ₂ assym. stretching	3324	2968	0.04
	3386	3024	0.05
	3307	2953	0.05
	3279	2928	0.15
	3214	2870	0.02
	3221	2876	0.12
	3210	2866	0.02
	3206	2862	0.90
CH ₃ assym. stretching	3266	2916	0.14
	3265	2915	0.10
	3262	2912	0.12
CH ₂ symm. & CH ₃ assym. stretching	3262	2913	0.16
	3259	2910	0.09
CH ₂ symm. stretching	3226	2881	0.07
	3185	2844	0.08
	3184	2843	0.09
CH ₃ symm. stretching	3200	2857	0.1
	3199	2857	0.06
C(1)=O stretching	1981	1768	1.00
Naphthalene deformation	1836	1639	0.01
Naphthalene C=C stretching	1786	1594	0.03
N (1)-H in-plane bending & C (2)-N (2) str.	1733	1547	0.88
Naphthalene C-H in-plane bending	1684	1504	0.06
	1149	1026	0.04

Description	Calculated	Scaled*	Rel. Intensity
CH ₂ scissoring	1670	1491	0.34
	1663	1485	0.15
CH ₂ scissoring & CH ₃ assym. bending	1654	1477	0.03
	1651	1475	0.02
	1644	1468	0.01
	1644	1468	0.03
	1643	1467	0.08
CH ₃ assym. bending	1644	1468	0.02
Naphthalene ring rocking	1628	1454	0.01
C(2)-N(2) stretching	1610	1438	0.84
Naphthalene C-H in-plane bending	1603	1431	0.03
CH ₂ wagging	1572	14.04	0.24
	1529	1366	0.02
	1519	1356	0.03
	1432	1279	0.05
	1421	1269	0.08
CH ₂ wagging & CH ₃ symm. bending	1568	1400	0.02
	1563	1396	0.07
CH ₃ symm. bending	1567	1399	0.05
Naphthalene C-H rocking	1548	1382	0.01
CH ₂ twisting	1476	1218	0.02
	1474	1316	0.05
	1461	1305	0.06
	1456	1300	0.01
	1446	1291	0.25
Naphthalene ring wagging	1462	1305	0.07
C (3)-C (1)-N (1) assym. stretching	1417	1265	0.06
CH ₂ -N (2)-CH ₂ assym. stretching	1407	1256	0.25
CH ₂ & CH ₃ twisting	1378	1231	0.32
	1028	918	0.01
	1022	912	0.01
Butyl twisting & naphthalene C-H rocking	1376	1228	0.06

Description	Calculated	Scaled*	Rel. Intensity
N(1)-C(2)-N(2) bending & butyl twisting	1348	1204	0.28
C(1)-N(1) stretching	1322	1181	0.21
Naphthalene C-H scissoring	1311	1170	0.05
	1288	1150	0.04
Naphthalene C-H scissoring & butyl rocking	1301	1162	0.05
C (1)-N (1)-C (2) assym. stretching	1269	1133	0.26
CH ₂ rocking	1253	1119	0.07
	392	350	0.03
	789	705	0.01
	797	712	0.02
CH ₃ rocking	1231	1099	0.04
	1228	1096	0.02
	990	884	0.02
	978	873	0.01
Naphthalene C-H rocking	1225	1094	0.01
N(1)-C(2) stretching	1195	1067	0.10
Naphthalene C-H oop. bending	1119	999	0.01
	916	818	0.04
	878	784	0.25
	834	745	0.03
C (3)-C (1)-N (1) symm. stretching	1112	993	0.02
C(1)-N(1)-C(2) bending	1062	949	0.03
C(2)=S stretching	959	856	0.05
Naphthalene ring symm. breathing	902	805	0.04
Butyl rocking	872	778	0.01
	797	712	0.02
	789	705	0.01
Naphthalene ring assym. breathing	861	769	0.01
C (3)-C (1)-N (1) oop. bending	838	748	0.04
N (1)-C (2)-N (2) symm. stretching	810	724	0.01
N (1)-H oop. bending	773	690	0.24

Description	Calculated	Scaled*	Rel. Intensity
N (1)-C (2)-N (2) oop. bend. & naphthalene breathing	730	652	0.01
N (1)-H oop. & naphthalene C-H oop. bending	700	625	0.01
N (1)-H oop. bend. & naphthalene ring deform.	678	605	0.01
C(3)-C(1)-N(1) bending & CH ₂ rocking	636	568	0.02
C(2)-N(2)-C'' bending	597	533	0.04
Naphthalene ring deformation	572	511	0.01
Naphthalene ring C-H oop. twisting	522	466	0.01
C(2)-N(2)- CH ₂ (not C'') bending	513	458	0.02
CH ₂ -N (2)-CH ₂ oop. bending	504	450	0.01
CH ₂ -N(2)-CH ₂ bending	482	430	0.01
C (1)-N (1)-C (2) oop. bending	416	372	0.01
C(1)=O in-plane bending	375	335	0.01
Butyl groups twisting	351	313	0.01
	309	276	0.01
Naphthalene ring oop. bending	286	255	0.01
Butyl wagging	214	191	0.01
	154	138	0.01
	87	78	0.01
C (1) =O oop. bending	110	98	0.02

Table 11 Calculated and scaled* wavenumbers (cm^{-1}) of *N, N*-di (2-hydroxyethyl)-*N'*-benzoyl thiourea (*K*).

Description	Calculated	Scaled*	Rel. Intensity
O(2)-H stretching	4125	3684	0.14
O(3)-H stretching	4120	3679	0.15
N(1)-H stretching	3847	3435	0.12
Ring C-H stretching	3413	3047	0.01
	3395	3032	0.04
	3385	3023	0.07
	3375	3014	0.02
CH ₂ assym. stretching	3384	3022	0.04
	3367	3006	0.02
	3196	2854	0.17
	3313	2958	0.06
	3270	2920	0.09
	3246	2899	0.06
CH ₂ symm. stretching	3306	2952	0.02
	3220	2876	0.11
C(1)=O stretching	1974	1763	0.81
Ring C=C stretching	1808	1614	0.05
	1783	1592	0.02
N (1)-H in-plane bending & C (2)-N (2) str.	1734	1548	1.00
CH ₂ scissoring	1679	1500	0.30
	1676	1496	0.30
	1647	1471	0.10
Ring C-H in-plane bending & CH ₂ scissoring	1671	1492	0.10
N(1)-H in-plane bending & CH ₂ scissoring	1661	1483	0.39
CH ₂ wagging	1621	1448	0.04
	1611	1439	0.07
	1536	1372	0.10
	1510	1348	0.05
Ring C-H rocking	1614	1441	0.12

Description	Calculated	Scaled*	Rel. Intensity
C(2)-N(2) stretching	1598	1427	0.81
CH ₂ twisting	1464	1308	0.07
	1444	1290	0.18
	1416	1265	0.06
	1397	1247	0.08
C(1)-N(1) stretching	1397	1248	0.76
C-O-H bending & CH ₂ wagging	1373	1226	0.50
C-O-H bending	1354	1209	0.32
Ring C-H in-plane bending	1345	1201	0.06
	1304	1165	0.04
	1230	1098	0.07
	1188	1061	0.01
CH ₂ twisting & C-O-H bending	1322	1181	0.21
N(1)-C(2) stretching	1255	1121	0.06
CH ₂ rocking	1245	1112	0.34
	864	772	0.01
	522	466	0.06
C-O(2) stretching	1212	1082	0.25
C-O(3) stretching	1194	1066	0.19
CH ₂ rocking & C-O(2)-H bending	1177	1051	0.04
C (1)-N (1)-C (2) symm. stretching	1169	1044	0.09
Ring deformation	1126	1005	0.01
Hydroxyethyl C-C stretching	1112	993	0.05
CH ₂ -N (2)-CH ₂ symm. stretching	1097	980	0.09
Ring C-H oop. bending	1068	954	0.01
CH ₂ -N (2)-CH ₂ assym. stretching	1029	919	0.04
C(1)-N(1)-C(2) bending & CH ₂ rocking	991	885	0.06
C(2)=S stretching	917	818	0.06
Ring oop. wagging	900	804	0.02
	815	728	0.21
N (1)-C (2)-N (2) symm. stretching	832	743	0.04
N (1)-H oop. bending & ring wagging	774	691	0.12

Description	Calculated	Scaled*	Rel. Intensity
N (1)-C (2)-N (2) oop. bend. & ring deformation	753	672	0.02
N (1)-H oop. bending	732	653	0.12
N (1)-H oop. bending & ring deformation	680	607	0.04
	673	601	0.02
CH ₂ -N(2)-CH ₂ bending	599	535	0.01
N(1)-C(2)-N(2) bending & ring wagging	555	496	0.05
CH ₂ rocking & ring oop. bending	480	428	0.03
Hydroxyethyl groups wagging	460	411	0.06
Ring C-H oop. twisting	455	407	0.01
C (1)-N (1)-C (2) oop. bending	425	380	0.01
Hydroxyl groups rocking	370	331	0.02
	151	135	0.02
	111	99	0.01
	89	79	0.01
C(1)=O in-plane bending & hydroxyl rocking	334	299	0.02
O-H oop. bending	291	260	0.24
	211	189	0.26
Hydroxyethyl rocking & O-H oop. bending	305	272	0.02
	276	246	0.05
	138	123	0.08
C (1) =O oop. bending & hydroxyethyl rocking	113	101	0.02

Table 12 Calculated and scaled* wavenumbers (cm^{-1}) of *N, N*-diethyl-*N'*-4-nitrobenzoylthiourea (L).

Description	Calculated	Scaled*	Rel. Intensity
N(1)-H stretching	3841	3429	0.11
Ring C-H stretching	3395	3031	0.01
CH ₂ assym. stretching	3382	3019	0.05
CH ₃ assym. stretching	3338	2980	0.02
CH ₂ & CH ₃ assym. stretching	3333	2976	0.03
	3313	2959	0.03
	3282	2931	0.06
CH ₂ symm. & CH ₃ assym. stretching	3276	2925	0.09
	3266	2916	0.08
CH ₂ assym. & CH ₃ symm. stretching	3225	2879	0.09
	3216	2872	0.03
CH ₃ symm. stretching	3219	2875	0.08
C(1)=O stretching	1989	1776	0.65
O-N (3)-O assym. stretching	1873	1673	0.87
Ring C=C stretching	1814	1619	0.02
	1774	1584	0.17
N (1)-H in-plane bending & C (2)-N (2) str.	1739	1553	0.88
Ring C-H in-plane bend. & CH ₂ scissoring	1679	1499	0.15
CH ₂ scissoring	1673	1494	0.1
	1663	1485	0.12
Assym. CH ₃ & symm. CH ₂ bending	1648	1471	0.01
O-N (3)-O symm. str. & CH ₃ assym. bending	1645	1469	0.57
CH ₃ assym. bending	1637	1462	0.09
CH ₃ scissoring	1633	1458	0.09
C(2)-N(2) stretching	1611	1439	1
CH ₃ symm. stretching	1574	1406	0.1
	1569	1401	0.04
CH ₂ wagging	1535	1370	0.13
	1518	1356	0.07

Description	Calculated	Scaled*	Rel. Intensity
CH ₂ twisting	1466	1309	0.09
	1430	1277	0.4
C(1)-N(1) stretching	1402	1252	0.41
C(2)-N(1) stretching	1374	1227	0.65
Ring symm. deformation	1326	1184	0.16
Ring C-H in-plane bending	1308	1168	0.02
CH ₂ & CH ₃ rocking	1305	1165	0.04
CH ₂ & CH ₃ rock. & C(1)-N(1)-C(2) assym. str.	1254	1119	0.34
N(3)-C(ph) stretching	1244	1111	0.05
Ethyl twisting	1232	1100	0.04
CH ₃ wagging	1210	1081	0.05
	1186	1059	0.01
Ring C-H in-plane bending	1196	1068	0.01
C (1)-N (1)-C (2) symm. stretching	1164	1039	0.1
Ring C-H oop. bending	1115	996	0.02
Ring assym. deformation	1113	994	0.01
C(1)-N(1)-C(2) bending	1043	931	0.03
CH ₂ -CH ₃ stretching	1009	901	0.01
Ring C-H oop. bending	993	887	0.04
O-N(3)-O bending	967	863	0.12
C(2)=S stretching	925	826	0.12
Ring wagging & C (3)-C (1)-N (1) oop. bend.	883	789	0.02
Ethyl rocking	864	772	0.04
Ring C-H oop. & O-N (3)-O oop. bending	829	740	0.2
Ring assym. breathing	805	719	0.01
N (1)-H oop. bending	779	696	0.12
	719	642	0.09
C (2)-N (2)-C'' symm. stretching	756	675	0.01
N (1)-H oop. bending & ring deform.	693	618	0.01
	683	610	0.01
Ring rocking	600	536	0.01

Description	Calculated	Scaled*	Rel. Intensity
CH ₂ -N(2)-CH ₂ bending	577	515	0.02
	471	421	0.02
O-N(3)-C(ph) bending	562	502	0.03
Ring wagging	511	456	0.03
	282	252	0.01
N(2)-CH ₂ -CH ₃ bending	490	438	0.02
C(1)-C(3)=C(Ph) bending	434	388	0.01
Ethyl wagging	362	324	0.01
	354	316	0.02
NO ₂ rocking	237	211	0.01
Ethyl groups twisting	178	159	0.01
C (1) =O oop. bending	99	88	0.02
C (2) =S oop. bending	84	75	0.01

*scaling factor=0.8929 *assym.* = asymmetric, *bend.* = bending, *deform.* = deformation,
Isobut. = isobutyl, *oop.* = out of plane *str.* = stretching,
symm. = symmetric

Addendum-C: Crystal structure Data.**Compound-A:****Table 1** Crystal structure data for N-pivaloyl-N'-pyrrolidine thiourea (compound-A).

Empirical formula	C ₁₀ H ₁₈ N ₂ O S	
Formula weight	214.32	
Temperature	173 (2) K ⁰	
Wavelength	0.71073 Å	
Crystal system, space group	Orthorhombic, Pca2 ₁	
Unit cell dimensions	a = 12.243 (4) Å	alpha = 90 ⁰
	b = 9.924 (3) Å	beta = 90 ⁰
	c = 10.002 (3) Å	gamma = 90 ⁰
Volume	1215.1 (7) Å ³	
Z, Calculated density	4, 1.172 Mg/m ³	
Absorption coefficient	0.240 mm ⁻¹	
F(000)	464	
Theta range for data collection	2.05 ⁰ to 28.31 ⁰	
Limiting indices	-16 ≤ h ≤ 15, -12 ≤ k ≤ 13, -13 ≤ l ≤ 12	
Reflections collected / unique	13163 / 2882 [R(int) = 0.0487]	
Completeness to theta = 28.31	97.6 %	
Refinement method	Full-matrix least-squares on F ²	
Data / restraints / parameters	2882 / 1 / 130	
Goodness-of-fit on F ²	1.047	

Final R indices [$I > 2 \sigma(I)$]	$R_1 = 0.0402$, $wR_2 = 0.0917$
R indices (all data)	$R_1 = 0.0441$, $wR_2 = 0.0936$
Absolute structure parameter	0.05(8)
Largest diff. peak and hole	0.399 and -0.168 e. \AA^{-3}

Table 2 Atomic coordinates ($\times 10^4$) and equivalent isotropic displacement parameters ($\text{\AA}^2 \times 10^3$) for Compound A.

$U(\text{eq})$ is defined as one third of the trace of the orthogonalized U_{ij} tensor.

	x	y	z	$U(\text{eq})$
S	364(1)	6546(1)	5197(1)	27(1)
C(2)	1606(2)	6488(2)	5900(2)	18(1)
N(1)	2377(1)	7490(1)	5595(1)	18(1)
N(2)	1941(1)	5520(2)	6709(2)	19(1)
C(8)	1926(2)	3625(2)	8131(2)	34(1)
C(1)	2852(1)	8281(2)	6565(2)	18(1)
C(9)	3066(2)	3803(2)	7563(2)	30(1)
C(7)	1207(2)	4439(2)	7173(2)	29(1)
C(10)	3081(1)	5272(2)	7133(2)	21(1)
O	2630(1)	8138(1)	7746(1)	23(1)
C(6)	4522(2)	8633(2)	5166(4)	39(1)
C(5)	3070(2)	10415(2)	5271(2)	35(1)
C(3)	3669(2)	9322(2)	6063(2)	24(1)
C(4)	4232(2)	9975(2)	7273(2)	37(1)

Table 3 Bond lengths [\AA] and angles [$^\circ$] for compound A.

S-C(2)	1.6763(19)
C(2)-N(2)	1.321(2)
C(2)-N(1)	1.405(2)

N(1)-C(1)	1.377(2)
N(2)-C(7)	1.475(2)
N(2)-C(10)	1.479(2)
C(8)-C(9)	1.518(3)
C(8)-C(7)	1.531(3)
C(1)-O	1.220(2)
C(1)-C(3)	1.523(3)
C(9)-C(10)	1.521(3)
C(6)-C(3)	1.537(3)
C(5)-C(3)	1.530(3)
C(3)-C(4)	1.536(3)
N(2)-C(2)-N(1)	115.99(15)
N(2)-C(2)-S	124.33(13)
N(1)-C(2)-S	119.64(13)
C(1)-N(1)-C(2)	122.33(14)
C(2)-N(2)-C(7)	122.18(16)
C(2)-N(2)-C(10)	126.14(15)
C(7)-N(2)-C(10)	111.32(14)
C(9)-C(8)-C(7)	103.51(17)
O-C(1)-N(1)	121.42(16)
O-C(1)-C(3)	122.97(16)
N(1)-C(1)-C(3)	115.60(15)
C(8)-C(9)-C(10)	103.18(16)
N(2)-C(7)-C(8)	103.34(16)
N(2)-C(10)-C(9)	103.25(14)
C(1)-C(3)-C(5)	109.64(16)
C(1)-C(3)-C(4)	108.73(15)
C(5)-C(3)-C(4)	108.90(17)
C(1)-C(3)-C(6)	109.67(16)
C(5)-C(3)-C(6)	109.83(18)
C(4)-C(3)-C(6)	110.1(2)

Table 4 Anisotropic displacement parameters ($\text{\AA}^2 \times 10^3$) for compound A.

The anisotropic displacement factor exponent takes the form:

$$-2 \pi^2 [h^2 a^{*2} U_{11} + \dots + 2 h k a^* b^* U_{12}]$$

	U_{11}	U_{22}	U_{33}	U_{23}	U_{13}	U_{12}
S	17(1)	39(1)	24(1)	2(1)	-3(1)	-1(1)
C(2)	18(1)	26(1)	10(1)	-3(1)	2(1)	-1(1)
N(1)	20(1)	25(1)	10(1)	0(1)	0(1)	-3(1)
N(2)	16(1)	21(1)	19(1)	1(1)	1(1)	-3(1)
C(8)	33(1)	31(1)	39(1)	12(1)	11(1)	3(1)
C(1)	21(1)	19(1)	14(1)	0(1)	-1(1)	3(1)
C(9)	30(1)	24(1)	36(1)	5(1)	5(1)	4(1)
C(7)	26(1)	28(1)	32(1)	7(1)	4(1)	-10(1)
C(10)	19(1)	22(1)	21(1)	0(1)	-2(1)	1(1)
O	36(1)	22(1)	12(1)	1(1)	1(1)	-2(1)
C(6)	30(1)	44(1)	44(1)	8(1)	11(1)	-8(1)
C(5)	51(1)	22(1)	31(1)	6(1)	-15(1)	-9(1)
C(3)	32(1)	23(1)	17(1)	3(1)	-3(1)	-7(1)
C(4)	44(1)	40(1)	26(1)	6(1)	-10(1)	-21(1)

Table 5 Hydrogen coordinates ($\times 10^4$) and isotropic displacement parameters ($\text{\AA}^2 \times 10^3$) for compound A.

	x	y	z	U(eq)
H(1)	2564	7616	4755	22
H(8A)	1879	3985	9052	41
H(8B)	1711	2664	8137	41
H(9A)	3189	3197	6791	36
H(9B)	3630	3624	8251	36
H(7A)	955	3876	6417	34
H(7B)	564	4815	7642	34
H(10A)	3287	5868	7886	25
H(10B)	3596	5417	6384	25

H (6A)	5096	9280	4935	58
H (6B)	4169	8311	4347	58
H (6C)	4844	7869	5645	58
H (5A)	2481	10792	5820	52
H (5B)	2760	10021	4456	52
H (5C)	3584	11132	5031	52
H (4A)	4619	9283	7786	55
H (4B)	3681	10405	7843	55
H (4C)	4754	10655	6962	55

Table 6 Torsion angles [$^{\circ}$] for compound A.

N (2) - C (2) - N (1) - C (1)	-59.8 (2)
S - C (2) - N (1) - C (1)	122.49 (15)
N (1) - C (2) - N (2) - C (7)	176.77 (16)
S - C (2) - N (2) - C (7)	-5.7 (2)
N (1) - C (2) - N (2) - C (10)	-10.8 (3)
S - C (2) - N (2) - C (10)	166.80 (14)
C (2) - N (1) - C (1) - O	0.8 (3)
C (2) - N (1) - C (1) - C (3)	-179.79 (16)
C (7) - C (8) - C (9) - C (10)	39.6 (2)
C (2) - N (2) - C (7) - C (8)	-176.78 (17)
C (10) - N (2) - C (7) - C (8)	9.8 (2)
C (9) - C (8) - C (7) - N (2)	-30.3 (2)
C (2) - N (2) - C (10) - C (9)	-158.56 (17)
C (7) - N (2) - C (10) - C (9)	14.6 (2)
C (8) - C (9) - C (10) - N (2)	-33.13 (19)
O - C (1) - C (3) - C (5)	-111.8 (2)
N (1) - C (1) - C (3) - C (5)	68.7 (2)
O - C (1) - C (3) - C (4)	7.1 (3)
N (1) - C (1) - C (3) - C (4)	-172.31 (16)
O - C (1) - C (3) - C (6)	127.5 (2)
N (1) - C (1) - C (3) - C (6)	-51.9 (2)

Compound – B**Table 1** Crystal structure data for *N*-(2, 6-dimethyl-piperidine)-*N'*-(3, 4, 5-methoxybenzoyl) thiourea (compound-B).

Empirical formula	C ₁₈ H ₂₆ N ₂ O ₄ S
Formula weight	366.47
Temperature	173(2) K ⁰
Wavelength	0.71073 Å
Crystal system, space group	triclinic, Pī
Unit cell dimensions	a = 12.427(2) Å alpha = 96.486(2) ⁰ b = 12.666(2) Å beta = 91.758(3) ⁰ c = 13.894(2) Å gamma = 118.402(2) ⁰
Volume	1902.5(5) Å ³
Z, Calculated density	4, 1.279 Mg/m ³
Absorption coefficient	0.194 mm ⁻¹
F (000)	784
Theta range for data collection	1.85 ⁰ to 25.00 ⁰
Limiting indices	-14 ≤ h ≤ 14, -15 ≤ k ≤ 15, -16 ≤ l ≤ 16
Reflections collected / unique	18232 / 6672 [R (int) = 0.0325]
Completeness to theta = 25.00	99.6 %
Refinement method	Full-matrix least-squares on F ²
Data / restraints / parameters	6672 / 0 / 444
Goodness-of-fit on F ²	1.036
Final R indices [I > 2σ (I)]	R ₁ = 0.0482, wR ₂ = 0.1119

R indices (all data) $R_1 = 0.0595$, $wR_2 = 0.1175$ Largest diff. peak and hole 0.787 and $-0.410 \text{ e} \cdot \text{Å}^{-3}$

Table 2 Atomic coordinates ($\times 10^4$) and equivalent isotropic displacement parameters ($\text{Å}^2 \times 10^3$) for compound B. $U(\text{eq})$ is defined as one third of the trace of the Orthogonalized U_{ij} tensor.

	X	Y	Z	U(eq)
S(1A)	3323(1)	5058(1)	604(1)	23(1)
O(1A)	1322(1)	1875(1)	1613(1)	20(1)
N(1A)	1141(2)	3258(2)	809(1)	18(1)
C(1A)	796(2)	2454(2)	1482(2)	17(1)
S(1B)	-9122(1)	-3980(1)	1066(1)	24(1)
O(1B)	-8780(2)	-4091(2)	3795(1)	27(1)
N(1B)	-7748(2)	-4106(2)	2493(1)	19(1)
C(1B)	-8190(2)	-4493(2)	3352(2)	19(1)
O(2A)	-1813(2)	862(2)	4094(1)	28(1)
N(2A)	2343(2)	2750(2)	-222(1)	18(1)
C(2A)	2239(2)	3595(2)	359(2)	17(1)
O(2B)	-8366(2)	-6899(2)	5911(1)	35(1)
N(2B)	-7469(2)	-2167(2)	2399(1)	18(1)
C(2B)	-8073(2)	-3338(2)	2035(2)	19(1)
O(3A)	-3331(1)	1637(2)	3499(1)	25(1)
C(3A)	-278(2)	2323(2)	2015(2)	18(1)
O(3B)	-6825(2)	-7544(2)	5084(1)	30(1)
C(3B)	-7854(2)	-5359(2)	3741(2)	19(1)
O(4A)	-2914(2)	2898(2)	2007(1)	30(1)
C(4A)	-495(2)	1690(2)	2808(2)	20(1)
O(4B)	-5948(2)	-6856(2)	3415(1)	27(1)
C(4B)	-8326(2)	-5751(2)	4602(2)	21(1)
C(5A)	-1506(2)	1481(2)	3311(2)	21(1)
C(5B)	-7983(2)	-6481(2)	5054(2)	23(1)
C(6A)	-2300(2)	1904(2)	3027(2)	20(1)
C(6B)	-7176(2)	-6830(2)	4629(2)	22(1)
C(7A)	-2072(2)	2537(2)	2231(2)	21(1)

C (7B)	-6728 (2)	-6460 (2)	3753 (2)	20 (1)
C (8A)	-1065 (2)	2746 (2)	1721 (2)	20 (1)
C (8B)	-7057 (2)	-5715 (2)	3306 (2)	19 (1)
C (9A)	-1049 (3)	383 (3)	4394 (2)	33 (1)
C (9B)	-9236 (3)	-6596 (3)	6333 (2)	55 (1)
C (10A)	-3246 (2)	2640 (2)	4151 (2)	30 (1)
C (10B)	-5677 (3)	-6832 (3)	5668 (2)	41 (1)
C (11A)	-2668 (3)	3641 (3)	1254 (2)	33 (1)
C (11B)	-5577 (2)	-6650 (2)	2463 (2)	29 (1)
C (12A)	3540 (2)	3060 (2)	-616 (2)	18 (1)
C (12B)	-7701 (2)	-1301 (2)	1905 (2)	25 (1)
C (13A)	3886 (2)	2071 (2)	-511 (2)	23 (1)
C (13B)	-7660 (2)	-290 (2)	2643 (2)	28 (1)
C (14A)	2855 (2)	815 (2)	-969 (2)	31 (1)
C (14B)	-6515 (2)	309 (2)	3355 (2)	31 (1)
C (15A)	1677 (3)	558 (2)	-466 (2)	32 (1)
C (15B)	-6473 (2)	-662 (2)	3884 (2)	27 (1)
C (16A)	1292 (2)	1523 (2)	-564 (2)	26 (1)
C (16B)	-6449 (2)	-1673 (2)	3199 (2)	21 (1)
C (17A)	732 (3)	1421 (3)	-1573 (2)	38 (1)
C (17B)	-5213 (2)	-1301 (2)	2796 (2)	29 (1)
C (18A)	3554 (2)	3354 (2)	-1655 (2)	29 (1)
C (18B)	-6835 (3)	-831 (3)	1115 (2)	41 (1)

Table 3 Bond lengths [Å] and angles [°] for compound B.

S (1A)-C (2A)	1.679 (2)
O (1A)-C (1A)	1.215 (3)
N (1A)-C (1A)	1.386 (3)
N (1A)-C (2A)	1.412 (3)
C (1A)-C (3A)	1.495 (3)
S (1B)-C (2B)	1.676 (2)
O (1B)-C (1B)	1.220 (3)
N (1B)-C (1B)	1.372 (3)
N (1B)-C (2B)	1.418 (3)
C (1B)-C (3B)	1.491 (3)
O (2A)-C (5A)	1.370 (3)
O (2A)-C (9A)	1.424 (3)
N (2A)-C (2A)	1.325 (3)

N (2A) -C (12A)	1.486 (3)
N (2A) -C (16A)	1.487 (3)
O (2B) -C (5B)	1.365 (3)
O (2B) -C (9B)	1.429 (3)
N (2B) -C (2B)	1.329 (3)
N (2B) -C (12B)	1.489 (3)
N (2B) -C (16B)	1.495 (3)
O (3A) -C (6A)	1.369 (3)
O (3A) -C (10A)	1.433 (3)
C (3A) -C (8A)	1.390 (3)
C (3A) -C (4A)	1.394 (3)
O (3B) -C (6B)	1.377 (3)
O (3B) -C (10B)	1.431 (3)
C (3B) -C (4B)	1.386 (3)
C (3B) -C (8B)	1.397 (3)
O (4A) -C (7A)	1.367 (3)
O (4A) -C (11A)	1.430 (3)
C (4A) -C (5A)	1.385 (3)
O (4B) -C (7B)	1.360 (3)
O (4B) -C (11B)	1.426 (3)
C (4B) -C (5B)	1.385 (3)
C (5A) -C (6A)	1.392 (3)
C (5B) -C (6B)	1.396 (3)
C (6A) -C (7A)	1.396 (3)
C (6B) -C (7B)	1.391 (3)
C (7A) -C (8A)	1.385 (3)
C (7B) -C (8B)	1.388 (3)
C (12A) -C (13A)	1.524 (3)
C (12A) -C (18A)	1.530 (3)
C (12B) -C (18B)	1.525 (4)
C (12B) -C (13B)	1.526 (3)
C (13A) -C (14A)	1.536 (3)
C (13B) -C (14B)	1.516 (3)
C (14A) -C (15A)	1.548 (4)
C (14B) -C (15B)	1.522 (4)
C (15A) -C (16A)	1.527 (4)
C (15B) -C (16B)	1.520 (3)
C (16A) -C (17A)	1.510 (4)
C (16B) -C (17B)	1.522 (3)
C (1A) -N (1A) -C (2A)	121.36 (18)
O (1A) -C (1A) -N (1A)	121.8 (2)

O (1A) -C (1A) -C (3A)	122.3 (2)
N (1A) -C (1A) -C (3A)	115.84 (19)
C (1B) -N (1B) -C (2B)	121.58 (19)
O (1B) -C (1B) -N (1B)	120.6 (2)
O (1B) -C (1B) -C (3B)	122.0 (2)
N (1B) -C (1B) -C (3B)	117.28 (19)
C (5A) -O (2A) -C (9A)	117.36 (18)
C (2A) -N (2A) -C (12A)	119.03 (18)
C (2A) -N (2A) -C (16A)	123.21 (19)
C (12A) -N (2A) -C (16A)	117.60 (17)
N (2A) -C (2A) -N (1A)	118.49 (19)
N (2A) -C (2A) -S (1A)	124.80 (17)
N (1A) -C (2A) -S (1A)	116.71 (16)
C (5B) -O (2B) -C (9B)	115.99 (19)
C (2B) -N (2B) -C (12B)	118.61 (19)
C (2B) -N (2B) -C (16B)	122.16 (18)
C (12B) -N (2B) -C (16B)	118.69 (18)
N (2B) -C (2B) -N (1B)	115.98 (19)
N (2B) -C (2B) -S (1B)	126.71 (17)
N (1B) -C (2B) -S (1B)	117.24 (16)
C (6A) -O (3A) -C (10A)	113.90 (18)
C (8A) -C (3A) -C (4A)	120.8 (2)
C (8A) -C (3A) -C (1A)	123.0 (2)
C (4A) -C (3A) -C (1A)	116.1 (2)
C (6B) -O (3B) -C (10B)	111.66 (19)
C (4B) -C (3B) -C (8B)	120.8 (2)
C (4B) -C (3B) -C (1B)	116.2 (2)
C (8B) -C (3B) -C (1B)	122.9 (2)
C (7A) -O (4A) -C (11A)	117.27 (18)
C (5A) -C (4A) -C (3A)	119.6 (2)
C (7B) -O (4B) -C (11B)	118.06 (18)
C (5B) -C (4B) -C (3B)	120.0 (2)
O (2A) -C (5A) -C (4A)	124.5 (2)
O (2A) -C (5A) -C (6A)	115.3 (2)
C (4A) -C (5A) -C (6A)	120.2 (2)
O (2B) -C (5B) -C (4B)	125.2 (2)
O (2B) -C (5B) -C (6B)	115.3 (2)
C (4B) -C (5B) -C (6B)	119.6 (2)
O (3A) -C (6A) -C (5A)	119.6 (2)
O (3A) -C (6A) -C (7A)	120.6 (2)
C (5A) -C (6A) -C (7A)	119.7 (2)
O (3B) -C (6B) -C (7B)	120.1 (2)

O(3B)-C(6B)-C(5B)	119.5(2)
C(7B)-C(6B)-C(5B)	120.4(2)
O(4A)-C(7A)-C(8A)	124.5(2)
O(4A)-C(7A)-C(6A)	114.94(19)
C(8A)-C(7A)-C(6A)	120.5(2)
O(4B)-C(7B)-C(8B)	125.0(2)
O(4B)-C(7B)-C(6B)	114.80(19)
C(8B)-C(7B)-C(6B)	120.2(2)
C(7A)-C(8A)-C(3A)	119.2(2)
C(7B)-C(8B)-C(3B)	119.1(2)
N(2A)-C(12A)-C(13A)	110.42(17)
N(2A)-C(12A)-C(18A)	111.95(18)
C(13A)-C(12A)-C(18A)	113.40(19)
N(2B)-C(12B)-C(18B)	110.9(2)
N(2B)-C(12B)-C(13B)	111.08(19)
C(18B)-C(12B)-C(13B)	113.3(2)
C(12A)-C(13A)-C(14A)	111.6(2)
C(14B)-C(13B)-C(12B)	112.8(2)
C(13A)-C(14A)-C(15A)	108.2(2)
C(13B)-C(14B)-C(15B)	108.2(2)
C(16A)-C(15A)-C(14A)	112.0(2)
C(16B)-C(15B)-C(14B)	112.9(2)
N(2A)-C(16A)-C(17A)	112.5(2)
N(2A)-C(16A)-C(15A)	109.98(19)
C(17A)-C(16A)-C(15A)	113.2(2)
N(2B)-C(16B)-C(15B)	110.46(18)
N(2B)-C(16B)-C(17B)	111.36(19)
C(15B)-C(16B)-C(17B)	113.4(2)

Table 4 Anisotropic displacement parameters ($\text{\AA}^2 \times 10^3$) for compound B.

The anisotropic displacement factor exponent takes the form:

$$-2 \pi^2 [h^2 a^{*2} U_{11} + \dots + 2 h k a^* b^* U_{12}]$$

	U_{11}	U_{22}	U_{33}	U_{23}	U_{13}	U_{12}
S(1A)	22(1)	16(1)	28(1)	2(1)	10(1)	6(1)
O(1A)	21(1)	22(1)	20(1)	4(1)	5(1)	12(1)

C (1A)	17 (1)	14 (1)	15 (1)	-3 (1)	1 (1)	5 (1)
S (1B)	28 (1)	25 (1)	19 (1)	-1 (1)	-5 (1)	14 (1)
O (1B)	36 (1)	34 (1)	24 (1)	9 (1)	10 (1)	26 (1)
C (1B)	22 (1)	18 (1)	18 (1)	1 (1)	1 (1)	10 (1)
O (2A)	33 (1)	34 (1)	23 (1)	14 (1)	14 (1)	19 (1)
C (2A)	18 (1)	23 (1)	14 (1)	6 (1)	4 (1)	12 (1)
O (2B)	49 (1)	47 (1)	33 (1)	25 (1)	26 (1)	37 (1)
C (2B)	24 (1)	24 (1)	16 (1)	5 (1)	6 (1)	16 (1)
O (3A)	22 (1)	27 (1)	25 (1)	3 (1)	13 (1)	11 (1)
C (3A)	19 (1)	14 (1)	16 (1)	-3 (1)	2 (1)	6 (1)
O (3B)	41 (1)	32 (1)	32 (1)	17 (1)	14 (1)	26 (1)
C (3B)	21 (1)	15 (1)	19 (1)	-1 (1)	-1 (1)	8 (1)
O (4A)	29 (1)	45 (1)	28 (1)	15 (1)	14 (1)	25 (1)
C (4A)	21 (1)	20 (1)	17 (1)	-1 (1)	2 (1)	9 (1)
O (4B)	38 (1)	33 (1)	26 (1)	13 (1)	14 (1)	27 (1)
C (4B)	23 (1)	21 (1)	24 (1)	4 (1)	6 (1)	14 (1)
C (5A)	24 (1)	17 (1)	16 (1)	2 (1)	5 (1)	7 (1)
C (5B)	27 (1)	22 (1)	23 (1)	9 (1)	8 (1)	13 (1)
C (6A)	19 (1)	19 (1)	20 (1)	-1 (1)	7 (1)	7 (1)
C (6B)	24 (1)	17 (1)	25 (1)	7 (1)	5 (1)	11 (1)
C (7A)	21 (1)	22 (1)	20 (1)	2 (1)	4 (1)	11 (1)
C (7B)	20 (1)	17 (1)	24 (1)	3 (1)	3 (1)	10 (1)
C (8A)	23 (1)	20 (1)	17 (1)	4 (1)	6 (1)	10 (1)
C (8B)	22 (1)	18 (1)	19 (1)	3 (1)	3 (1)	10 (1)
C (9A)	44 (2)	39 (2)	27 (1)	18 (1)	15 (1)	25 (1)
C (9B)	78 (2)	74 (2)	57 (2)	45 (2)	50 (2)	63 (2)
C (10A)	36 (2)	38 (2)	20 (1)	1 (1)	11 (1)	21 (1)
C (10B)	51 (2)	62 (2)	30 (2)	14 (1)	4 (1)	42 (2)
C (11A)	38 (2)	50 (2)	28 (1)	19 (1)	15 (1)	31 (1)
C (11B)	36 (2)	35 (1)	27 (1)	12 (1)	16 (1)	25 (1)
C (12A)	15 (1)	19 (1)	19 (1)	2 (1)	5 (1)	6 (1)
C (12B)	33 (1)	24 (1)	24 (1)	4 (1)	-4 (1)	19 (1)
C (13A)	22 (1)	28 (1)	23 (1)	8 (1)	9 (1)	15 (1)
C (13B)	32 (1)	21 (1)	35 (1)	3 (1)	-1 (1)	17 (1)
C (14A)	36 (2)	30 (1)	29 (1)	5 (1)	8 (1)	17 (1)
C (14B)	34 (2)	23 (1)	37 (2)	-5 (1)	-1 (1)	17 (1)
C (15A)	43 (2)	20 (1)	23 (1)	2 (1)	7 (1)	7 (1)
C (15B)	32 (1)	27 (1)	22 (1)	-5 (1)	-4 (1)	15 (1)
C (16A)	17 (1)	27 (2)	23 (1)	-2 (1)	6 (1)	3 (1)
C (16B)	26 (1)	21 (1)	18 (1)	3 (1)	-1 (1)	14 (1)
C (17A)	33 (2)	44 (2)	36 (2)	-5 (1)	-7 (1)	21 (1)
C (17B)	28 (1)	29 (1)	35 (2)	4 (1)	3 (1)	17 (1)

C(18A)	29(1)	34(2)	25(1)	11(1)	12(1)	15(1)
C(18B)	66(2)	42(2)	29(2)	18(1)	10(1)	34(2)

Table 5 Hydrogen coordinates ($\times 10^4$) and isotropic displacement parameters ($\text{\AA}^2 \times 10^3$) for compound B.

	x	y	z	U(eq)
H(1A)	665	3566	658	22
H(1B)	-7251	-4339	2220	23
H(2A)	47	1404	3002	23
H(12B)	-8884	-5520	4882	26
H(12A)	-915	3172	1178	24
H(2B)	-6744	-5451	2712	23
H(4A)	-1022	-166	3851	49
H(5A)	-1382	-64	4940	49
H(3A)	-217	1049	4599	49
H(11B)	-8860	-5713	6501	82
H(9B)	-9485	-6976	6922	82
H(10B)	-9959	-6890	5865	82
H(7A)	-2550	2924	4645	44
H(6A)	-4007	2381	4470	44
H(8A)	-3124	3300	3785	44
H(6B)	-5045	-6349	5261	61
H(7B)	-5438	-7370	5958	61
H(8B)	-5760	-6290	6186	61
H(11A)	-1869	4372	1421	50
H(9A)	-3312	3873	1185	50
H(10A)	-2655	3187	638	50
H(4B)	-6306	-6994	1993	43
H(5B)	-5076	-7039	2292	43
H(3B)	-5094	-5776	2448	43
H(13A)	4176	3815	-201	22
H(13B)	-8555	-1764	1573	30
H(18A)	4057	2063	188	28
H(17A)	4644	2255	-830	28
H(17B)	-7695	331	2290	33

H(18B)	-8393	-631	3009	33
H(20A)	3093	187	-876	38
H(19A)	2706	798	-1675	38
H(20B)	-6536	943	3828	37
H(19B)	-5774	696	3003	37
H(22A)	1000	-246	-760	38
H(21A)	1823	529	232	38
H(21B)	-5733	-280	4357	33
H(22B)	-7202	-1015	4254	33
H(23A)	641	1390	-113	31
H(23B)	-6607	-2345	3584	25
H(26A)	513	2067	-1593	57
H(24A)	-8	630	-1737	57
H(25A)	1327	1500	-2044	57
H(24B)	-5256	-1990	2364	44
H(25B)	-4575	-1050	3335	44
H(26B)	-5013	-624	2430	44
H(14A)	3044	2606	-2104	43
H(15A)	4400	3727	-1835	43
H(16A)	3229	3919	-1692	43
H(16B)	-6024	-201	1416	62
H(15B)	-7165	-490	666	62
H(14B)	-6759	-1502	758	62

Table 6 Torsion angles [$^{\circ}$] for compound B.

C(2A)-N(1A)-C(1A)-O(1A)	-10.6(3)
C(2A)-N(1A)-C(1A)-C(3A)	170.88(19)
C(2B)-N(1B)-C(1B)-O(1B)	-7.3(3)
C(2B)-N(1B)-C(1B)-C(3B)	176.30(19)
C(12A)-N(2A)-C(2A)-N(1A)	-173.57(18)
C(16A)-N(2A)-C(2A)-N(1A)	11.1(3)
C(12A)-N(2A)-C(2A)-S(1A)	6.8(3)
C(16A)-N(2A)-C(2A)-S(1A)	-168.56(17)
C(1A)-N(1A)-C(2A)-N(2A)	64.9(3)
C(1A)-N(1A)-C(2A)-S(1A)	-115.45(19)
C(12B)-N(2B)-C(2B)-N(1B)	175.54(19)
C(16B)-N(2B)-C(2B)-N(1B)	4.1(3)
C(12B)-N(2B)-C(2B)-S(1B)	-1.5(3)

C (16B) -N (2B) -C (2B) -S (1B)	-172.93 (17)
C (1B) -N (1B) -C (2B) -N (2B)	79.5 (3)
C (1B) -N (1B) -C (2B) -S (1B)	-103.2 (2)
O (1A) -C (1A) -C (3A) -C (8A)	-164.3 (2)
N (1A) -C (1A) -C (3A) -C (8A)	14.2 (3)
O (1A) -C (1A) -C (3A) -C (4A)	12.5 (3)
N (1A) -C (1A) -C (3A) -C (4A)	-169.00 (19)
O (1B) -C (1B) -C (3B) -C (4B)	4.5 (3)
N (1B) -C (1B) -C (3B) -C (4B)	-179.1 (2)
O (1B) -C (1B) -C (3B) -C (8B)	-172.0 (2)
N (1B) -C (1B) -C (3B) -C (8B)	4.4 (3)
C (8A) -C (3A) -C (4A) -C (5A)	-0.1 (3)
C (1A) -C (3A) -C (4A) -C (5A)	-177.0 (2)
C (8B) -C (3B) -C (4B) -C (5B)	1.6 (3)
C (1B) -C (3B) -C (4B) -C (5B)	-175.0 (2)
C (9A) -O (2A) -C (5A) -C (4A)	-1.3 (3)
C (9A) -O (2A) -C (5A) -C (6A)	178.3 (2)
C (3A) -C (4A) -C (5A) -O (2A)	179.4 (2)
C (3A) -C (4A) -C (5A) -C (6A)	-0.2 (3)
C (9B) -O (2B) -C (5B) -C (4B)	3.3 (4)
C (9B) -O (2B) -C (5B) -C (6B)	-177.3 (3)
C (3B) -C (4B) -C (5B) -O (2B)	178.5 (2)
C (3B) -C (4B) -C (5B) -C (6B)	-0.9 (4)
C (10A) -O (3A) -C (6A) -C (5A)	105.3 (2)
C (10A) -O (3A) -C (6A) -C (7A)	-78.3 (3)
O (2A) -C (5A) -C (6A) -O (3A)	-3.0 (3)
C (4A) -C (5A) -C (6A) -O (3A)	176.6 (2)
O (2A) -C (5A) -C (6A) -C (7A)	-179.5 (2)
C (4A) -C (5A) -C (6A) -C (7A)	0.2 (3)
C (10B) -O (3B) -C (6B) -C (7B)	84.2 (3)
C (10B) -O (3B) -C (6B) -C (5B)	-95.8 (3)
O (2B) -C (5B) -C (6B) -O (3B)	-0.2 (3)
C (4B) -C (5B) -C (6B) -O (3B)	179.3 (2)
O (2B) -C (5B) -C (6B) -C (7B)	179.8 (2)
C (4B) -C (5B) -C (6B) -C (7B)	-0.7 (4)
C (11A) -O (4A) -C (7A) -C (8A)	-6.2 (3)
C (11A) -O (4A) -C (7A) -C (6A)	174.7 (2)
O (3A) -C (6A) -C (7A) -O (4A)	2.8 (3)
C (5A) -C (6A) -C (7A) -O (4A)	179.2 (2)
O (3A) -C (6A) -C (7A) -C (8A)	-176.3 (2)
C (5A) -C (6A) -C (7A) -C (8A)	0.1 (3)
C (11B) -O (4B) -C (7B) -C (8B)	-9.9 (3)

C (11B) -O (4B) -C (7B) -C (6B)	171.9 (2)
O (3B) -C (6B) -C (7B) -O (4B)	-0.1 (3)
C (5B) -C (6B) -C (7B) -O (4B)	179.8 (2)
O (3B) -C (6B) -C (7B) -C (8B)	-178.4 (2)
C (5B) -C (6B) -C (7B) -C (8B)	1.6 (4)
O (4A) -C (7A) -C (8A) -C (3A)	-179.4 (2)
C (6A) -C (7A) -C (8A) -C (3A)	-0.4 (3)
C (4A) -C (3A) -C (8A) -C (7A)	0.4 (3)
C (1A) -C (3A) -C (8A) -C (7A)	177.0 (2)
O (4B) -C (7B) -C (8B) -C (3B)	-179.0 (2)
C (6B) -C (7B) -C (8B) -C (3B)	-0.9 (3)
C (4B) -C (3B) -C (8B) -C (7B)	-0.7 (3)
C (1B) -C (3B) -C (8B) -C (7B)	175.6 (2)
C (2A) -N (2A) -C (12A) -C (13A)	133.7 (2)
C (16A) -N (2A) -C (12A) -C (13A)	-50.7 (3)
C (2A) -N (2A) -C (12A) -C (18A)	-98.9 (2)
C (16A) -N (2A) -C (12A) -C (18A)	76.7 (2)
C (2B) -N (2B) -C (12B) -C (18B)	-89.1 (3)
C (16B) -N (2B) -C (12B) -C (18B)	82.7 (3)
C (2B) -N (2B) -C (12B) -C (13B)	144.0 (2)
C (16B) -N (2B) -C (12B) -C (13B)	-44.3 (3)
N (2A) -C (12A) -C (13A) -C (14A)	53.9 (2)
C (18A) -C (12A) -C (13A) -C (14A)	-72.7 (2)
N (2B) -C (12B) -C (13B) -C (14B)	50.5 (3)
C (18B) -C (12B) -C (13B) -C (14B)	-75.1 (3)
C (12A) -C (13A) -C (14A) -C (15A)	-58.3 (3)
C (12B) -C (13B) -C (14B) -C (15B)	-58.3 (3)
C (13A) -C (14A) -C (15A) -C (16A)	58.1 (3)
C (13B) -C (14B) -C (15B) -C (16B)	59.2 (3)
C (2A) -N (2A) -C (16A) -C (17A)	98.2 (3)
C (12A) -N (2A) -C (16A) -C (17A)	-77.2 (3)
C (2A) -N (2A) -C (16A) -C (15A)	-134.5 (2)
C (12A) -N (2A) -C (16A) -C (15A)	50.1 (3)
C (14A) -C (15A) -C (16A) -N (2A)	-52.9 (3)
C (14A) -C (15A) -C (16A) -C (17A)	73.9 (3)
C (2B) -N (2B) -C (16B) -C (15B)	-143.8 (2)
C (12B) -N (2B) -C (16B) -C (15B)	44.8 (3)
C (2B) -N (2B) -C (16B) -C (17B)	89.2 (2)
C (12B) -N (2B) -C (16B) -C (17B)	-82.2 (2)
C (14B) -C (15B) -C (16B) -N (2B)	-51.6 (3)
C (14B) -C (15B) -C (16B) -C (17B)	74.2 (3)

Compound-D**Table 1** Crystal structure data for *N,N*-dibutyl-*N'*-pivaloylthiourea (compound-D).

Empirical formula	C ₁₄ H ₂₈ N ₂ O S
Formula weight	272.44
Temperature	103(2) K ⁰
Wavelength	0.71073 Å
Crystal system, space group	Orthorhombic, Pna2 ₁
Unit cell dimensions	a = 10.0259(8) Å alpha = 90 ⁰ b = 13.2126(10) Å beta = 90 ⁰ c = 12.1805(10) Å gamma = 90 ⁰
Volume	1613.5(2) Å ³
Z, Calculated density	4, 1.122 Mg/m ³
Absorption coefficient	0.194 mm ⁻¹
F(000)	600
Crystal size	0.20 x 0.20 x 0.10 mm
Theta range for data collection	2.27 ⁰ to 28.29 ⁰
Limiting indices	-13 ≤ h ≤ 12, -17 ≤ k ≤ 16, -16 ≤ l ≤ 8
Reflections collected / unique	9342 / 2926 [R(int) = 0.0312]
Completeness to theta = 28.29	95.9 %
Max. and min. transmission	0.9809 and 0.9622
Refinement method	Full-matrix least-squares on F ²
Data / restraints / parameters	2926 / 1 / 168

Goodness-of-fit on F^2	1.085
Final R indices [$I > 2\sigma(I)$]	$R_1 = 0.0411$, $wR_2 = 0.0938$
R indices (all data)	$R_1 = 0.0440$, $wR_2 = 0.0953$
Absolute structure parameter	-0.05(8)
Largest diff. peak and hole	0.334 and -0.181 e. \AA^{-3}

Table 2 Atomic coordinates ($\times 10^4$) and equivalent isotropic displacement parameters ($\text{\AA}^2 \times 10^3$) for compound D. $U(\text{eq})$ is defined as one third of the trace of the Orthogonalized U_{ij} tensor.

	x	y	z	U(eq)
S	1203(1)	9451(1)	8384(1)	21(1)
O	-877(1)	7298(1)	9587(2)	29(1)
N(1)	1280(1)	7752(1)	9561(2)	15(1)
N(2)	559(2)	9191(1)	10491(2)	15(1)
C(1)	293(2)	7054(1)	9497(2)	17(1)
C(2)	982(2)	8811(1)	9550(2)	14(1)
C(3)	161(2)	10262(1)	10562(2)	17(1)
C(4)	1291(2)	10958(1)	10920(2)	20(1)
C(5)	888(2)	12066(1)	10874(2)	22(1)
C(6)	2023(2)	12775(2)	11187(2)	26(1)
C(7)	579(2)	8609(1)	11525(2)	19(1)
C(8)	1980(2)	8487(2)	11999(2)	24(1)
C(9)	1987(2)	7913(2)	13087(2)	29(1)
C(10)	1548(3)	6823(2)	12988(3)	42(1)
C(11)	692(2)	5945(1)	9289(2)	16(1)
C(12)	2179(2)	5736(1)	9451(2)	26(1)
C(13)	-133(2)	5292(2)	10076(2)	25(1)
C(14)	294(2)	5713(2)	8099(2)	24(1)

Table 3 Bond lengths [Å] and angles [°] for compound D.

S-C(2)	1.668 (2)
O-C(1)	1.222 (2)
N(1)-C(1)	1.355 (2)
N(1)-C(2)	1.431 (2)
N(2)-C(2)	1.321 (3)
N(2)-C(3)	1.472 (2)
N(2)-C(7)	1.476 (3)
C(1)-C(11)	1.540 (2)
C(3)-C(4)	1.523 (3)
C(4)-C(5)	1.519 (3)
C(5)-C(6)	1.522 (3)
C(7)-C(8)	1.527 (3)
C(8)-C(9)	1.528 (3)
C(9)-C(10)	1.511 (3)
C(11)-C(12)	1.529 (3)
C(11)-C(13)	1.533 (3)
C(11)-C(14)	1.533 (3)
C(1)-N(1)-C(2)	120.84 (14)
C(2)-N(2)-C(3)	120.23 (17)
C(2)-N(2)-C(7)	122.55 (15)
C(3)-N(2)-C(7)	116.98 (16)
O-C(1)-N(1)	121.07 (17)
O-C(1)-C(11)	121.03 (16)
N(1)-C(1)-C(11)	117.90 (16)
N(2)-C(2)-N(1)	115.49 (17)
N(2)-C(2)-S	126.07 (14)
N(1)-C(2)-S	118.44 (15)
N(2)-C(3)-C(4)	113.34 (15)
C(5)-C(4)-C(3)	111.98 (15)
C(4)-C(5)-C(6)	112.67 (16)
N(2)-C(7)-C(8)	112.92 (17)
C(7)-C(8)-C(9)	112.61 (18)
C(10)-C(9)-C(8)	113.7 (2)
C(12)-C(11)-C(13)	110.10 (17)
C(12)-C(11)-C(14)	109.87 (18)
C(13)-C(11)-C(14)	109.75 (16)
C(12)-C(11)-C(1)	113.79 (15)

C(13)-C(11)-C(1)	107.03(16)
C(14)-C(11)-C(1)	106.16(16)

Table 4 Anisotropic displacement parameters ($\text{\AA}^2 \times 10^3$) for compound D.
The anisotropic displacement factor exponent takes the form:

$$-2 \pi^2 [h^2 a^{*2} U_{11} + \dots + 2 h k a^* b^* U_{12}]$$

	U_{11}	U_{22}	U_{33}	U_{23}	U_{13}	U_{12}
S	27(1)	21(1)	16(1)	3(1)	1(1)	4(1)
O	12(1)	18(1)	57(1)	-7(1)	0(1)	1(1)
N(1)	9(1)	14(1)	21(1)	-1(1)	-1(1)	1(1)
N(2)	13(1)	15(1)	18(1)	1(1)	-1(1)	-1(1)
C(1)	14(1)	16(1)	22(1)	-1(1)	-1(1)	-1(1)
C(2)	8(1)	16(1)	18(1)	-1(1)	-3(1)	-2(1)
C(3)	15(1)	14(1)	22(1)	-2(1)	-1(1)	1(1)
C(4)	16(1)	16(1)	26(1)	-1(1)	-5(1)	0(1)
C(5)	17(1)	17(1)	32(1)	-3(1)	-4(1)	1(1)
C(6)	23(1)	17(1)	37(1)	-5(1)	-6(1)	-2(1)
C(7)	24(1)	17(1)	15(1)	-1(1)	3(1)	1(1)
C(8)	30(1)	23(1)	20(1)	5(1)	-5(1)	-5(1)
C(9)	34(1)	32(1)	21(1)	6(1)	-5(1)	-1(1)
C(10)	49(2)	29(1)	47(2)	17(1)	-11(1)	-4(1)
C(11)	12(1)	13(1)	25(1)	-2(1)	1(1)	1(1)
C(12)	16(1)	15(1)	49(2)	-8(1)	-4(1)	4(1)
C(13)	28(1)	19(1)	29(1)	3(1)	2(1)	-1(1)
C(14)	27(1)	20(1)	26(1)	-4(1)	1(1)	0(1)

Table 5 Hydrogen coordinates ($\times 10^4$) and isotropic displacement parameters ($\text{\AA}^2 \times 10^3$) for compound D.

	X	Y	Z	U(eq)
H(1)	2115	7552	9610	18
H(3A)	-584	10325	11091	20

H(3B)	-169	10485	9836	20
H(4A)	1559	10785	11679	23
H(4B)	2071	10849	10436	23
H(5A)	129	12179	11379	26
H(5B)	585	12230	10121	26
H(6A)	2316	12625	11937	39
H(6B)	1713	13478	11146	39
H(6C)	2770	12679	10678	39
H(7A)	194	7930	11390	22
H(7B)	9	8955	12072	22
H(8A)	2376	9166	12112	29
H(8B)	2543	8120	11462	29
H(9A)	2900	7931	13396	35
H(9B)	1389	8265	13610	35
H(10A)	598	6799	12799	63
H(10B)	1693	6476	13688	63
H(10C)	2067	6488	12411	63
H(12A)	2450	5961	10185	40
H(12B)	2693	6106	8896	40
H(12C)	2348	5009	9377	40
H(13A)	64	4575	9946	38
H(13B)	-1085	5416	9951	38
H(13C)	93	5466	10836	38
H(14A)	775	6168	7602	36
H(14B)	-668	5813	8011	36
H(14C)	522	5009	7926	36

Table 6 Selected torsion angles [$^{\circ}$] for compound D.

-10.67 (0.33)	C2 - N1 - C1 - O
168.42 (0.18)	C2 - N1 - C1 - C11
-177.07 (0.15)	C3 - N2 - C2 - N1
8.68 (0.24)	C7 - N2 - C2 - N1
3.52 (0.24)	C3 - N2 - C2 - S
-170.72 (0.14)	C7 - N2 - C2 - S
79.14 (0.24)	C1 - N1 - C2 - N2
-101.41 (0.20)	C1 - N1 - C2 - S
-92.88 (0.22)	C2 - N2 - C3 - C4
81.68 (0.22)	C7 - N2 - C3 - C4
174.21 (0.18)	N2 - C3 - C4 - C5

-177.80 (0.20) C3 - C4 - C5 - C6
73.80 (0.22) C2 - N2 - C7 - C8
-100.62 (0.19) C3 - N2 - C7 - C8
178.16 (0.17) N2 - C7 - C8 - C9
65.33 (0.26) C7 - C8 - C9 - C10
-167.09 (0.23) O - C1 - C11 - C12
13.82 (0.29) N1 - C1 - C11 - C12
-45.23 (0.28) O - C1 - C11 - C13
135.68 (0.20) N1 - C1 - C11 - C13
71.95 (0.26) O - C1 - C11 - C14
-107.14 (0.21) N1 - C1 - C11 - C14
